DIFFERENTIAL PULSE CODE MODULATION OF COLOUR TELEVISION SIGNALS USING VARIOUS PREDICTION METHODS

by

HAMID GHARAVI

B.Sc. (Tehran Polytechnic, Iran).

M.Sc. (Loughborough University of Technology, England).

A Doctoral Thesis

Submitted in partial fulfilment of the requirements

for the award of

Doctor of Philosophy

of the Loughborough University of Technology

ACKNOWLEDGEMENTS

It gives me great pleasure to express my deep gratitude to my former supervisor, Dr. Raymond Steele, for his guidance, encouragement and inspiration throughout this work. His invaluable suggestions and comments helped considerably to initiate and develop the work presented here.

My thanks to Mr. R.J. Clarke for his guidance in the manuscript of this thesis. I express my special thanks to Dr. C. Xydeas for his friendly enthusiasm and his support and useful comments during the preparation of this work. I also wish to thank all my colleagues, particularly Mr. C.C. Evci and Mr. A. Hessami for their help and the many useful discussions we have had.

Many thanks are due to the British Post Office with whom I have had many fruitful communications.

I would like to thank Professor J.W.R. Griffiths, Head of the Electronic and Electrical Engineering Department of Loughborough University of Technology for providing all the research facilities.

I wish to express my sincere gratitude to my parents for their moral and financial support. I am also indebted to my wife, Kirsty, for her constant encouragement which enabled me to continue under extreme pressure. Without her assistance , it would not have been possible to see this work through to completion.

To her I dedicate this thesis.

LIST OF PRINCIPAL SYMBOLS

$\{a_i\}$	:	coefficients of a linear predictor
a_p	:	predictor coefficient in the P^{th} block
b_i	:	unweighted predictor coefficients
C_1	:	average bits per sample excluding overhead information
C_2	:	average bits per sample of overhead information
D_B	:	blue SECAM chrominance signal
D_R	:	red SECAM chrominance signal
$\{e_i\}$	:	sequence of error samples
f_L	:	line frequency Hz
f_m	:	highest frequency in baseband signal
f_N	:	Nyquist rate
f_o	:	sub-carrier frequency for a specific coloured area
f_{oc}	:	central frequency of the sub-carrier
f_{sc}	:	sub-carrier frequency
k	:	number of quantizers
L	:	number of quantization levels
L_a	:	number of quantization levels required to quantize predictor coefficient
L_k	:	number of quantization levels of the k^{th} quantizer
L_K	:	leak factor
Lu	:	luminance
n	:	sampling to sub-carrier frequency ratios
N	:	block length
P(e)	:	probability density function of error signal
P_K	:	selection probability of k^{th} quantizer

Q	:	quantizer
$Q(e)$	:	quantizer output function
r_{jl}	:	normalized autocorrelation coefficients of input samples
$S(t)$	:	composite colour television signal
$\{S_i\}$	:	sequence of input samples
$\{\hat{\hat{S}}_i\}$	:	sequence of unweighted predicted samples
$\{\hat{S}_i\}$	:	sequence of weighted predicted samples
t	:	threshold
$T(e)$	:	visibility function
T_S	:	sampling period
$Y_1, Y_2 \ldots$	:	quantizer output decision level
$Z_1, Z_2 \ldots$	:	quantizer input decision level
φ	:	hue
ψ_{sa}	:	sample phase shift
φ_{sc}	:	sub-carrier phase shift
$\sigma^2_{\hat{e}}$	:	variance of the error signal
σ^2_S	:	variance of the input signal
σ^2_η	:	variance of the white Gaussian noise
η_i	:	sequence of the white Gaussian noise

CONTENTS

SYNOPSIS

Predictive coding, which is often associated with differential pulse code modulation (DPCM), can offer an attractive means of data compression of television signals.

This thesis describes investigations of various adaptive and non-adaptive DPCM schemes in order to reduce the high bit-rate required for the transmission of broadcast quality colour television signals.

Initially, a predictor based on three previous samples along a scan line is examined for DPCM encoding of composite PAL signals. The predictor coefficients are described in terms of the ratio of sampling frequency f_s to colour sub-carrier f_{sc}. The prediction can be improved by using a simple adaptive algorithm which uses previous sample prediction for three consecutive samples when there is a rapid change in the luminance level. For a colour bar signal it is shown that the SNR of the DPCM system using $f_s/f_{sc} = 2.5$ is a close approximation to that for $f_s/f_{sc} = 3.0$. In order to obtain a significant improvement in SNR, prediction based on samples on the second previous and previous line are derived for the case of $f_s/f_{sc} = 2.5$. Simple two dimensional predictors are then formed and used in the DPCM encoding of a PAL colour bar signal. The bit-rate of 5 and 6 bit DPCM for $f_s/f_{sc} = 2.5$ is 55 and 66 Mb/s which is still relatively high compared with 5.5MHz

bandwidth of the analogue signal. Thus, for further reduction of bit-rate, block adaptive DPCM is then investigated. The technique involves block adaptive predictors and block adaptive variable length and fixed length quantizers. The adaptation algorithm had been extended to work at any desired sampling frequency. As a result, a lower bit-rate is obtained by exploiting the redundancy of the picture with respect to the statistical variation of each block of incoming samples. A bit-rate of only 28.34 Mb/s is obtained for a PAL colour bar signal yielding a 50dB SNR at a sampling frequency of twice the sub-carrier frequency (sub-Nyquist).

In a further development the composite coding of SECAM signals is considered. To deal with frequency variations of the SECAM sub-carrier, a new block adaptive algorithm is developed which results in a significant improvement in system performance compared with other relevant techniques.

CHAPTER 1

ORGANIZATION OF THE THESIS

1.1. INTRODUCTION.

The problems of digital television transmission were first outlined long before colour television systems became commonplace. The use of digital communication systems now receives serious attention in a growing variety of applications - telephony, television, facsimile, communication between digital computer installations, radar warning networks and transmission of numerical data of various sorts for industrial use. For continuous sources, digital transmission is not required but is recognised as having suitable properties for long-distance transmission such as great reliability and freedom from accumulating distortion and noise. On the other hand, conventional means for encoding continuous signals into binary PCM (pulse code modulation), for example, result in a need for greatly increased channel width. The digital transmission of television would be greatly facilitated, therefore, if improved coding methods could be found to obtain more economical numerical descriptions of picture signals.

In this thesis attention is focussed on one particular kind of communication system for transmitting colour video signals over a digital channel. More specifically, the source encoding aspect of this transmission system is considered.

Since the repertoire of the digital channel is limited to 1's and 0's, the source encoding problem can be stated as requiring the conversion of the given picture into a stream of 1's and 0's so that

a) the distortion in the reconstructed picture is as small as possible

b) the bandwidth occupied by this stream is minimized.

1.2. ARRANGEMENT OF THE THESIS.

Here each of the following chapters in the thesis is briefly outlined.

Chapter II is a further introductory chapter which provides the necessary background knowledge for non-specialized readers. It begins with a brief review of several coding techniques as applied to video signals. Following that, the principle of differential pulse code modulation (DPCM), linear estimation theory and its application in determining the optimum prediction coefficients is described. The essential element of all digitization algorithms-- namely the quantizer-is also discussed in detail. The remainder of this chapter is concerned with the video signal and some important characteristics of NTSC, PAL and SECAM colour television signals.

Chapter III describes various sampling frequency (f_s): sub-carrier frequency (f_{sc}) relations. For one-dimensional prediction of PAL colour signals a three-coefficient predictor is presented, where the predictor coefficient can be determined at non-integral ratios of sampling to sub-carrier frequency. In this chapter computer simulation is used to examine

the performance of this one-dimensional predictor at $f_s = 2.5f_{sc}$ compared with the standard form at $f_s = 3f_{sc}$. Simulation results obtained for these systems when PAL colour bar signals are used as the input signals are presented.

Chapter IV is the extension of one-dimensional prediction into two dimensions. The chapter begins with a brief review of some of the important previous work in two-dimensional prediction of colour television signals. Then, for intra-line prediction a general formula is derived in relation to the selection of sampling frequency. The performance of both inter-line and intra-line methods is illustrated by means of computer simulation and signal to noise ratio (SNR) calculations. SNR results are compared for the relation $f_s = 2.5f_{sc}$.

Whilst the prediction schemes in Chapters III and IV concentrate on less complex techniques, Chapter V deals with more complex methods. Novel block adaptive predictors and quantizers are proposed. A detailed mathematical analysis of the adaptation algorithm for various sampling frequencies is presented. Then a wide range of SNR results for various sampling frequencies , block lengths and block adaptive quantization strategies are considered. It is concluded that with this adaptive strategy at sub-Nyquist sampling rates it is possible to transmit a broadcast quality colour television signal below the internationally agreed hierarchical level of 34.368 Mb/s.

In Chapter V an adaptive algorithm for PAL colour television signals is developed which can also be applied to the NTSC system. In Chapter VI a similar strategy for SECAM signals (where the nature of the chrominance modulation is entirely different from that of PAL and NTSC) is considered. For the frequency modulated chrominance signal of SECAM, a novel algorithm is presented in which the prediction can adapt itself to the frequency variation of the sub-carrier. For a saturated SECAM colour bar signal various adaptive and non-adaptive prediction algorithms are examined with the help of computer simulation.

Finally, in Chapter VII, the main results reported in the thesis are analysed and criticized. The overall arrangement of the thesis is shown schematically in Fig.(1.1)

1.3. SUMMARY OF MAIN RESULTS.

The main results presented in this thesis are outlined as follows:

In Chapter III, for one-dimensional DPCM, it is shown that reducing the sampling frequency from 3 to 2.5 times the sub-carrier frequency causes a reduction in the SNR performance. However, the prediction can be improved by using a simple algorithm which uses previous sample prediction for three consecutive pels when there is a rapid change in the luminance level. The results for both sampling to sub-carrier frequency ratios using this adaptive strategy show a similar SNR.

In Chapter IV a two-dimensional DPCM system at $f_s = 2.5f_{sc}$ is introduced with satisfactory results. The prediction is based on samples along the same and either previous or second previous line. The best result can be obtained when the two-dimensional predictor combines with the one-dimensional adaptive predictor.

In Chapters V and VI the use of block adaptive predictors for NTSC, PAL and SECAM signals is proposed and, since quantizer operation is a vital element in the performance of a DPCM system, a block adaptive quantizer with fixed and variable lengths is developed. Very good results are obtained in terms of SNR and resulting bit-rate. A bit-rate of only 28.34 Mb/s is obtained for a saturated colour bar signal yielding a 50dB SNR at a sampling frequency of twice the sub-carrier frequency.

DPCM coding of composite SECAM colour bar signals is described in Chapter VI. The system comprises a block adaptive predictor and fixed quantizer, and computer simulation results show an SNR advantage of 4.5dB over non-adaptive DPCM.

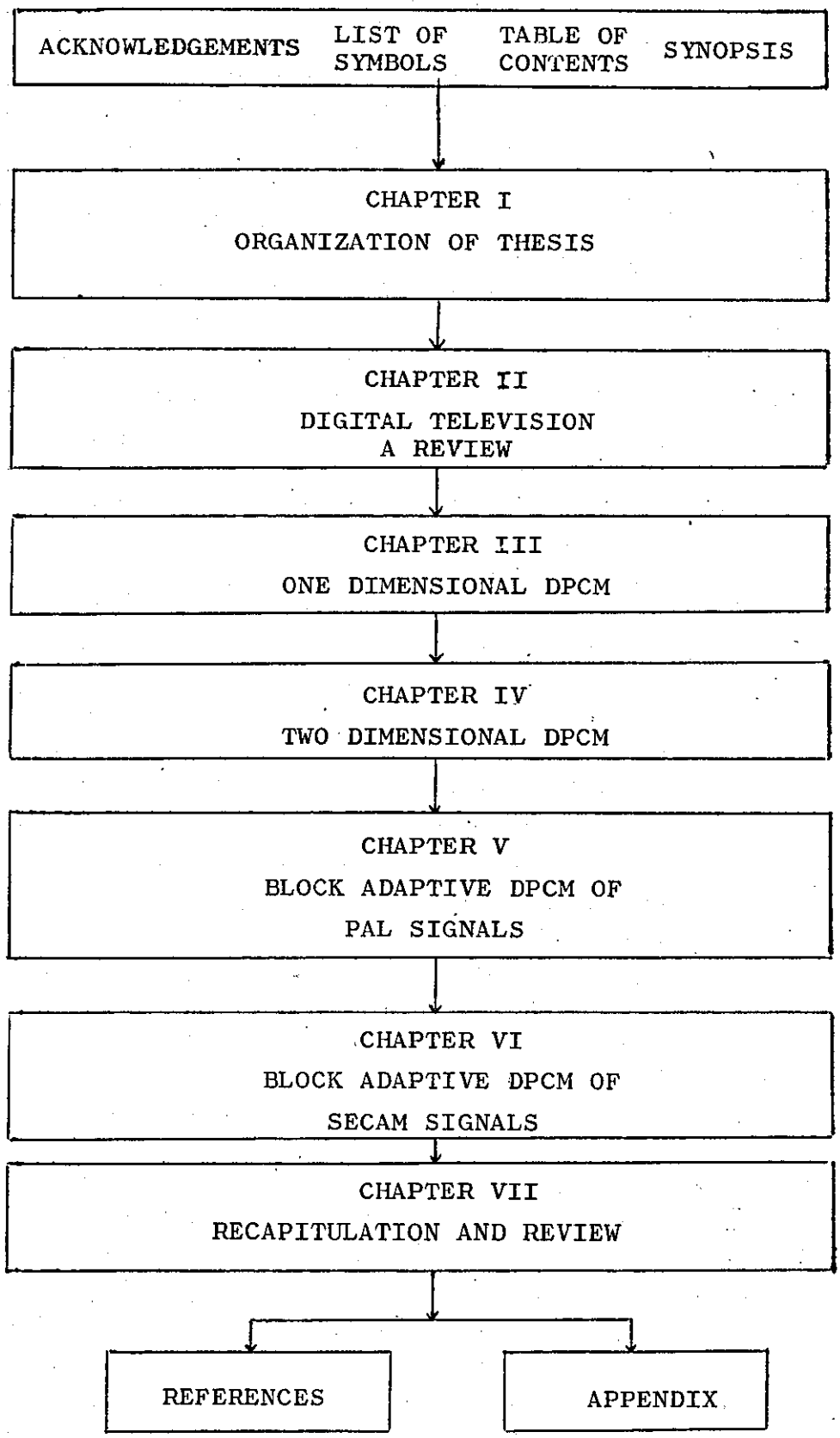

FIGURE 1.1. Thesis Lay-out

CHAPTER II

DIGITAL TELEVISION

2.1. INTRODUCTION.

With the increasing emphasis on the use of digital communications, the area of digital television systems is one in which there is considerable interest in the possibility of reducing channel capacity requirements. Digital methods for coding television signals can be broadly classified into two categories: orthogonal transform coding systems and waveform coding techniques. In orthogonal transform coding the video signal is transformed into a new domain where the correlation between coefficients is much smaller than that between the samples in the original time domain sequence, and it has been extensively studied since 1966. One of the earliest articles was published in 1967 by C.A. Andrews, J.M. Davis and G.R. Swartz[1] considering the use of the Kahunen-Loeve transform and in 1968 Andrews and Pratt [2] reported the application of the Fourier transform to television picture coding. In addition, a number of other transformations have been considered, such as the Hadamard, Cosine and Slant transforms[3,4,5]. The main difficulty regarding orthogonal transformation resides in the fact that it generally requires very complex equipment.

In the video waveform encoding system the objective is to reconstruct the television picture from its time samples. In such a system the video waveform is sampled, encoded

and transmitted. Examples of video waveform coding are pulse code modulation (PCM), delta modulation (DM) and differential pulse code modulation (DPCM). Attention is focussed on the latter system in this thesis.

2.2. PULSE CODE MODULATION.

Pulse code modulation is an encoding scheme which has become widely used over the last twenty years for the transmission of digital signals[7]. Such encoding generally involves the sampling of the analogue waveform at a uniform rate and encoding of the samples into a binary code. Conventional PCM techniques require a high data rate for the transmission of images[8,9,10] because of the large bandwidth of the base-band signal. Therefore, many new digital techniques have been developed in order to reduce the capacity requirements of the digital image communication system, by making use of the statistical and psychovisual properties of images[11].

The principles of PCM have been described in great detail by Cattermole[12] and others[13,14] and can be summarized in the following steps;

1. The band limited input signal is sampled at a rate of at least $2f_m$ Hz, where f_m is the highest frequency contained in the waveform. Such a sampling rate ensures that perfect reconstruction of the analogue signal is possible.

2. The amplitude of each signal sample is quantized into one of L levels. This implies an information of $I = \log_2 L$ bits per sample and an overall bit-rate of $2f_m I$ bits per second.

3. For decoding, the binary words are mapped back into amplitude levels and the amplitude-time pulse sequence is low-pass filtered with a filter whose cut off frequency is f_m.

One of the most important applications of pulse code modulation to digital television is analogue to digital conversion[15,16,17] in which the analogue video signal is converted into a series of 8 bit words prior to encoding.

2.3. DIFFERENTIAL PULSE CODE MODULATION (DPCM).

DPCM systems are primarily based on Cutler's work[18]. Later efforts in predictive quantization are due to Oliver[19], Harrison[20], Elias[21], Graham[22], O'Neal[23], Connor, Pease and Scholes[24], Kummerow[25] and Thoma[26], who proposed and investigated a number of one-dimensional and two dimensional predictors described in more detail subsequently.

The PCM system is inefficient in coding correlated data such as picture samples, since the encoder in the PCM assigns the same number of bits to every sample. The principle of DPCM is to generate a set of uncorrelated values, following classical prediction theory[27]. The block diagram of the DPCM codec (coder/decoder) is illustrated in Fig.(2.1). The transmitter is composed of a predictor and a quantizer. The predictor uses n previous decoded samples to predict the present value of the input signal. The difference between this and the actual value of the signal is quantized and is transmitted over an error-free digital

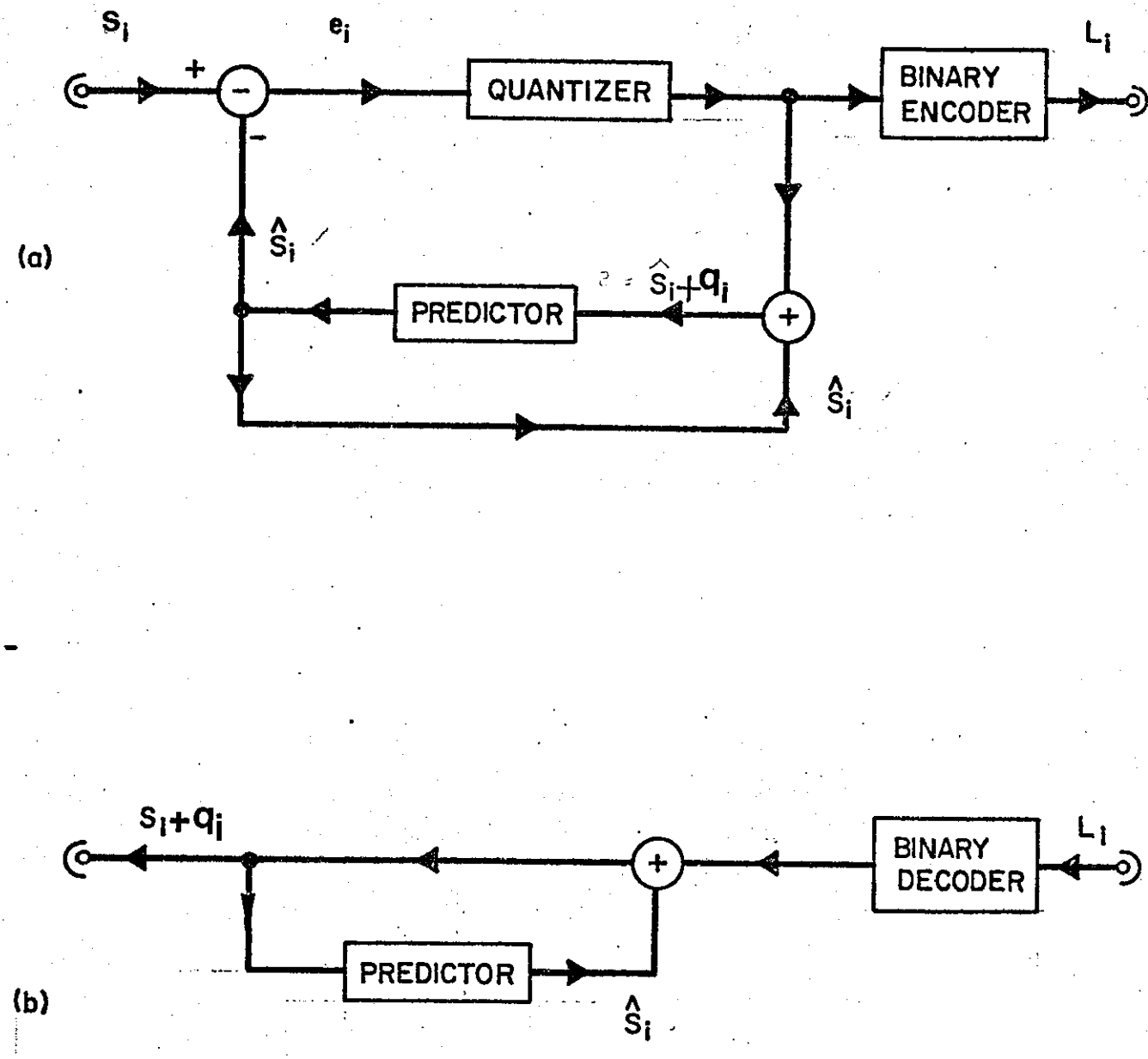

FIGURE 2.1 - DPCM System
a: Encoder
b: Decoder

channel. At the receiver a similar predictor uses n previous transmitted values of the quantized differential signal to reconstruct the facsimile of the signal at the transmitter. Such a system can reduce the variance of the transmitted signal and provide a well-behaved probability density function which would allow for the design of an optimum quantizer.

2.3.1. THE OPTIMUM LINEAR PREDICTOR.

Referring to Fig.(2.1), the input signal s(t) is sampled at a rate f_s to produce a sequence of sample values $\{S_i\}$ $i = 1,2,\ldots$. At the same time, the predictor makes an estimate of each sample value based on n previous reconstructed samples. These estimates are the sequence $\{\hat{S}_i\}$ where

$$\hat{S}_i = \sum_{j=1}^{j=n} a_j \, (S_{i-j} + q_{i-j}) \qquad (2.1)$$

where 'a_j' is the weighting coefficient applied to the appropriate past reconstructed sample $S_{i-j} + q_{i-j}$.

When the number of quantizing levels 'L' is large, equation (2.1) can be written approximately as,

$$\hat{S}_i = \sum_{j=1}^{n} a_j \, S_{i-j} \qquad (2.2)$$

Each estimate is subtracted from the actual sample value producing a difference error sequence $\{e_i\}$ where

$$e_i = S_i - \hat{S}_i \tag{2.3}$$

or

$$e_i = S_i - \sum_{j=1}^{n} a_j S_{i-j} \tag{2.4}$$

If the mean-square values of the sequences $\{S_i\}$ and $\{e_i\}$ are denoted by σ_S^2 and σ_e^2 respectively,

$$\sigma_e^2 = E\left[(S_i - \sum_{j=1}^{n} a_j S_{i-j})^2\right] \tag{2.5}$$

For the interval of N_1 samples this can be shown as,

$$\sigma_e^2 = \frac{1}{N_1} \sum_{i=1}^{N_1} \left[S_i - \sum_{j=1}^{n} a_j S_{i-j}\right]^2 \tag{2.6}$$

expanding equation (2.6) yields

$$\sigma_e^2 = \frac{1}{N_1}\sum_{i=1}^{N_1} S_i^2 - \frac{2}{N_1} \sum_{i=1}^{N1} \sum_{j=1}^{n} a_j S_i S_{i-j} + \frac{1}{N_1} \sum_{i=1}^{N_1} \left[\sum_{j=1}^{n} a_j S_{i-j}\right]\left[\sum_{l=1}^{n} a_l S_{i-l}\right] \tag{2.7}$$

defining σ_S^2 and r_{jl} as

$$\sigma_S^2 = \frac{1}{N_1} \sum_{i=1}^{N_1} S_i^2 \tag{2.8}$$

and

$$r_{jl} = \frac{1}{N_1 \sigma_S^2} \sum_{i=1}^{N_1} S_{i-l} S_{i-j} \tag{2.9}$$

Using the above equations, equation (2.7) can be shown as

$$\sigma_e^2 = \sigma_S^2 \left[1-2 \sum_{j=1}^{n} a_j r_{0j} + \sum_{j=1}^{n} \sum_{l=1}^{n} a_j a_l r_{jl}\right] \quad (2.10)$$

The above equation can be expressed in matrix notation as

$$\sigma_e^2 = \sigma_S^2 \left[1-2A^T G_1 + A^T R_1 A\right] \quad (2.11)$$

where

$$A = \begin{bmatrix} a_1 \\ a_2 \\ . \\ . \\ a_n \end{bmatrix} \quad G_1 = \begin{bmatrix} r_{0,1} \\ r_{0,2} \\ . \\ . \\ r_{0,n} \end{bmatrix} \quad R_1 = \begin{bmatrix} r_{1,1} & r_{1,2} & . & . & r_{1,n} \\ r_{2,1} & r_{2,2} & . & . & r_{2,n} \\ . & . & . & . & . \\ . & . & . & . & . \\ r_{n,1} & r_{n,2} & . & . & r_{n,n} \end{bmatrix}$$

The elements of G_1 and R_1 are values of a normalized auto-correlation function r_{jl} of the input sequence $\{S_i\}$.

The optimum coefficients of A that minimize σ_e^2 are obtained by equating the derivative of equation (2.11) to zero [28,29].

$$\frac{\delta \sigma_e^2}{\delta A} = -2 G_1 + 2 A R_1 = 0$$

or

$$A_{opt} = R_1^{-1} G_1 \quad (2.12)$$

and in this case the minimum value of σ_e^2 is

$$\sigma_e^2(\min) = \sigma_S^2 \left[1 - G_1^T R_1^{-1} G_1\right] \tag{2.13}$$

or

$$\sigma_e^2(\min) = \sigma_S^2 \left[1 - \sum_{j=1}^{n} a_j r_{oj}\right] \tag{2.14}$$

As $n \rightarrow \infty$ the sequence of error samples can be made uncorrelated. However, if the sequence of samples $\{S_i\}$ forms on the n^{th} order auto-gressive process, then, using only n samples in forming the estimate of $\hat{S}_o$, will make the resulting sequence of error terms uncorrelated. In this case a further increase in the number of samples employed in forming the optimum will not improve the quality of the estimate. As an example, the first order Markov model is considered here to design an optimum linear predictor. The one-dimensional Markov model is shown in Fig. (2.2) where the input to the model is white Gaussian noise with variance σ_η^2. The output of the model, which represents the input to the predictor, is given by the following equation (see Fig.2.2);

$$S_i = \eta_i + \alpha S_{i-1} \tag{2.15}$$

If the input sample sequence is first-order Markov, then only the first-order predictor shown in Fig.(2.3) need be considered. The output of the predictor is given by

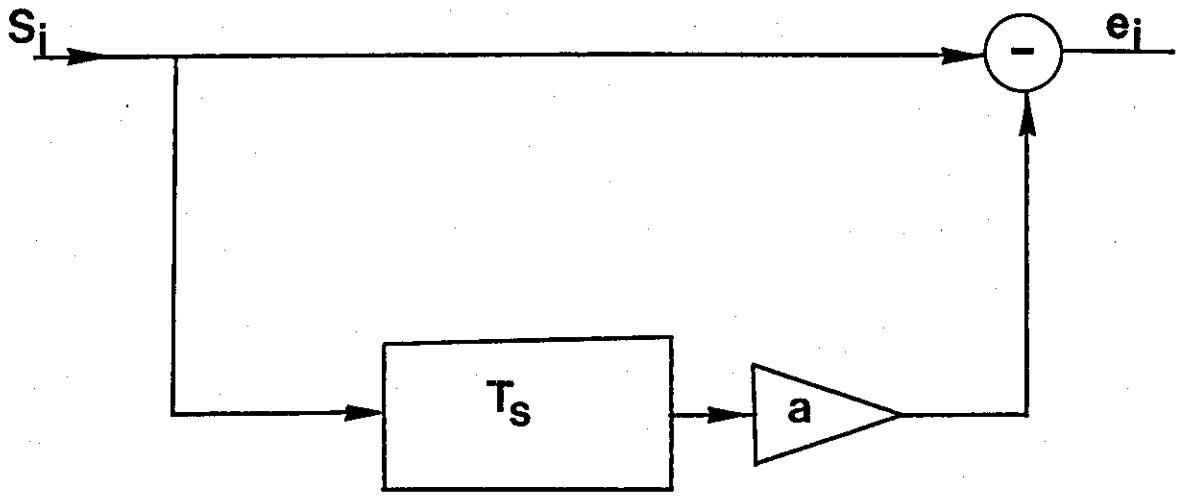

FIGURE 2.3 - First order predictor

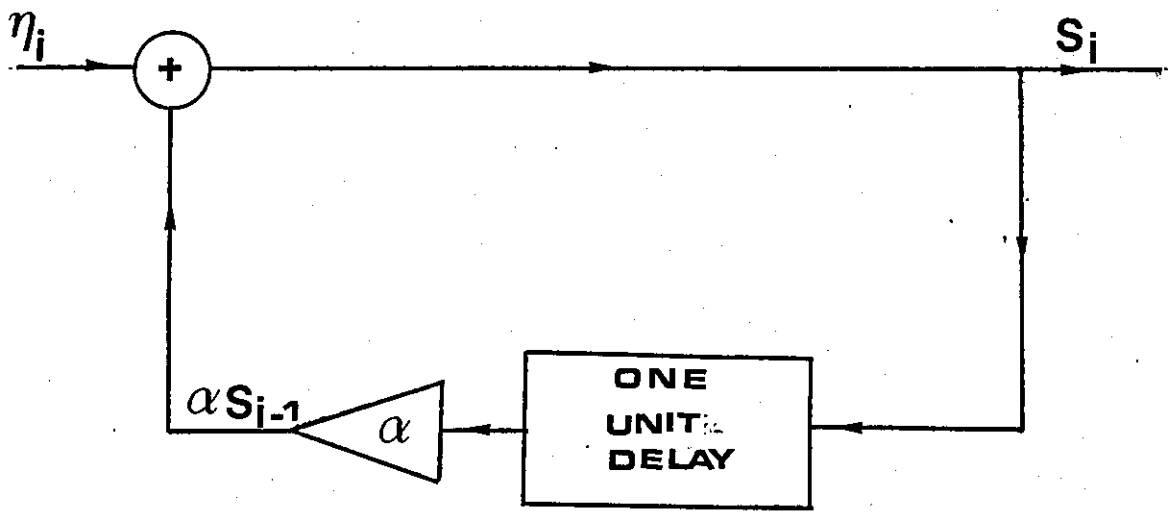

FIGURE 2.2 - One dimensional Markov model

the following difference equation

$$e_i = S_i - aS_{i-1} \tag{2.16}$$

The optimum weighting coefficient of the predictor 'a' can be obtained from equation (2.9) and (2.12) for the first order case (n=1) thus,

$$a = \frac{r_{0,1}}{r_{1,1}} \tag{2.17}$$

where $r_{0,0} = r_{1,1} = 1$ and

$$r_{0,1} = \frac{E\left\{S_i\ S_{i-1}\right\}}{\sigma_S^2} \tag{2.18}$$

Thus, from equations (2.15), (2.17) and (2.18)

$$a\ \sigma_S^2 = E\left\{S_i\ S_{i-1}\right\} = E\left\{\eta_i\ S_{i-1}\right\} + \alpha E\left\{S_{i-1}^2\right\} \tag{2.19}$$

As can be deduced from Fig.(2.2), S_{i-1} is a function of past uncorrelated noise samples thus, $E\left\{\eta_i\ Si\text{-}1\right\}$ is zero. Thus, from equation (2.19)

$$a = \alpha \tag{2.20}$$

From equations (2.15) and (2.20), equation (2.16) can be shown as

$$e_i = \eta_i \tag{2.21}$$

Therefore, the optimum predictor is an exact inverse to the Markov model when the error signal for the first-order predictor is white noise with variance σ_η^2. From equation (2.11) the mean-square prediction error can be represented as

$$\sigma_e^2 = \sigma_\eta^2 = \sigma_S^2 (1 - \alpha^2) \tag{2.22}$$

One possible application of the first order system is in the transmission of television signals[106]. Suppose the power spectrum of the Gaussian signal is the bandlimited function

$$F(\omega) = \frac{1}{(\omega/\omega_c)^2 + 1} \quad -\omega_0 \leqslant \omega \leqslant \omega_c \tag{2.23}$$

$$= 0 \qquad \text{otherwise}$$

where ω_c and ω_0 are the corner and cutoff frequencies of the power spectrum. O'Neal[106] states that this is a good approximation of the envelope of the power spectrum of a television signal where its one line autocorrelation function is similar to $e^{-\omega_c T_S}$. T_S is the sampling period and is equal to π/ω_0, thus,

$$r_{01} = e^{-\omega_c \pi/\omega_0} \tag{2.24}$$

For monochrome television signals the value of $\omega_0/2\pi\omega_c$ changes from 10 to 30, depending on the picture material. O'Neal states that the results for the

predictor were $\omega_0/2\pi\,\omega_c = 25$[106], this yields

$$a = r_{01} = 0.98$$

Equations (2.12) and (2.13) are obtained ignoring quantization noise. If there is an insufficient number of quantizing levels, the noise interacts with the predictor and makes it suboptimum. As a result, the differential signal becomes more correlated and its distribution changes, thus degrading the performance of the quantizer.

2.3.2. OPTIMUM QUANTIZERS.

Quantization is the other important operation which determines encoding performance. In most cases quantizer optimization has been based on a minimum mean-square error criterion. Such quantizers were originally studied by Panter and Dite[30] and an algorithm for their design was presented by Max [31]. Nitadori[32] and O'Neal[23] found that for speech and television, well designed DPCM systems had quantizer input signals whose probability density functions were approximately Laplacian. Quantizers designed using Max's technique minimize the quantizing noise for any given number of quantizing levels and will be discussed briefly.

2.3.2.1. QUANTIZATION BASED ON A MINIMUM MEAN-SQUARE CRITERION.

Let P(e) be the probability density function of the difference signal (e) and L denote the number of quantization levels. Output decision levels are represented by $Y_1, Y_2, \ldots Y_L$. It is temporarily assumed that the input to the quantizer (e) is a continuous variable. Let $Z_1, Z_2, \ldots Z_{L+1}$ be the quantizer input decision levels such that ,(see Fig.2.4)

$$Z_1 \leqslant e \leqslant Z_{L+1} \tag{2.25}$$

where

$$Z_1 < Z_2 < \ldots Z_L < Z_{L+1}$$

and

$$-Z_1 = Z_{L+1} = \infty$$

The error power of the quantizer $E(q^2)$ can be shown

$$E(q^2) = \sum_{k=1}^{L} \int_{Z_k}^{Z_{k+1}} (e - Y_k)^2 P(e)\, de \tag{2.26}$$

The necessary conditions for minimum mean-square quantization noise can be obtained by differentiating $E(q^2)$ with respect to the Z_k's and Y_k's and setting the derivatives equal to zero.

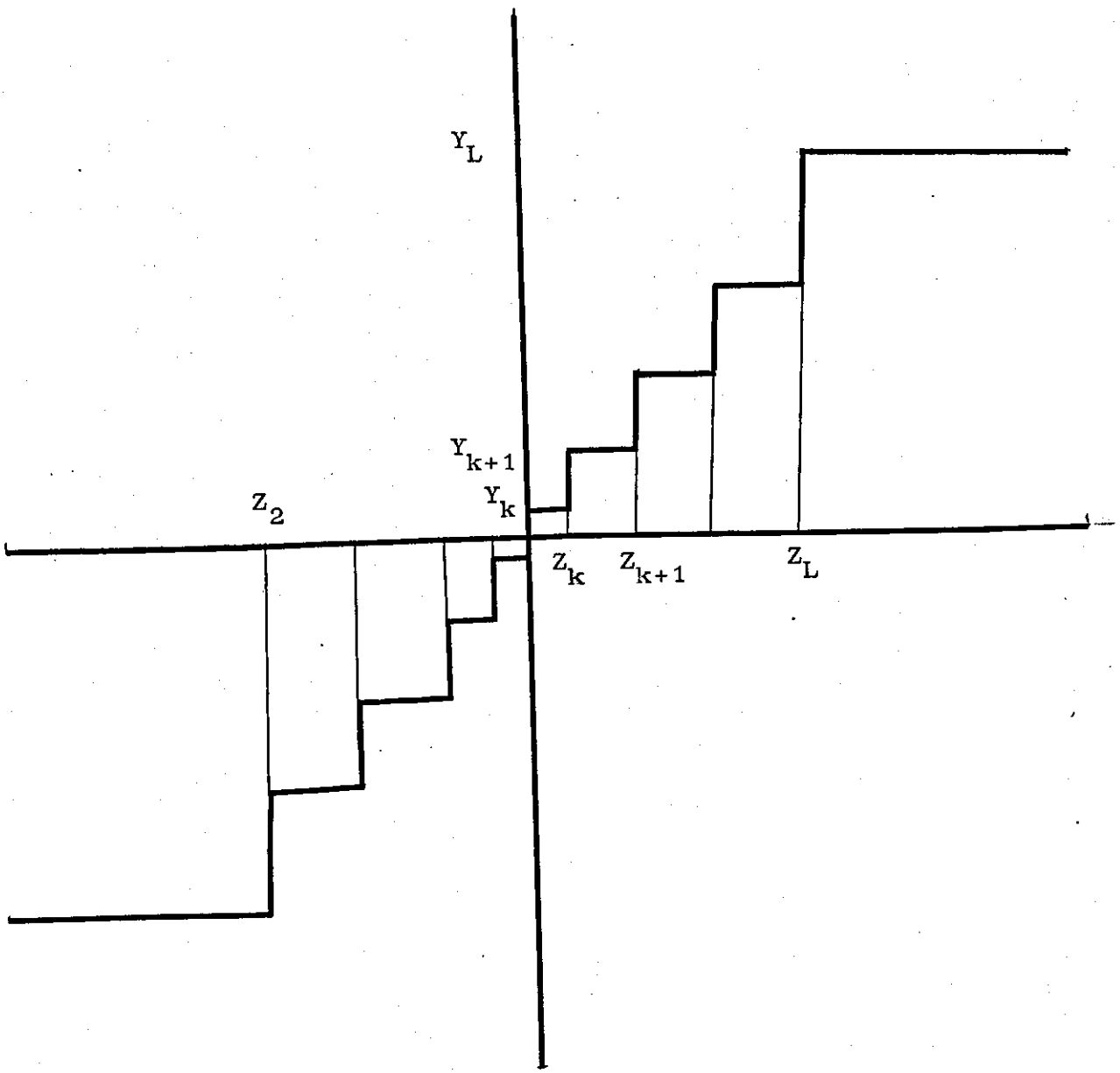

FIGURE 2.4 - Non-uniform quantization

$$\frac{\partial E(q^2)}{\partial e_k} = \frac{\partial}{\partial e_k} \int_{Z_{k-1}}^{Z_k} (e - Y_{k-1})^2 P(e)\, de + \frac{\partial}{\partial e_k} \int_{Z_k}^{Z_{k+1}} (e - Y_k)^2 P(e)\, de$$

Therefore,

$$\frac{\partial E(q^2)}{\partial e_k} = (Z_k - Y_{k-1})^2 P(Z_k) - (Z_k - Y_k)^2 P(Z_k) = 0 \quad (2.27)$$

$$k = 2....L$$

thus,

$$Z_k = \frac{Y_{k-1} + Y_k}{2} \quad (2.28)$$

also

$$\frac{\partial E(q^2)}{\partial Y_k} = 2 \int_{Z_k}^{Z_{k+1}} (e - Y_k) P(e)\, de = 0 \quad (2.29)$$

therefore,

$$\int_{Z_k}^{Z_{k+1}} (e - Y_k) P(e)\, de = 0 \quad (2.30)$$

Equation (2.28) imposes the first condition for minimum mean-square error; that Z_k should lie half way between Y_k and Y_{k-1}. Equation (2.30) shows Y_k to be the centroid of the area of P(e) between Z_k and Z_{k+1}. It is

assumed that the probability function P(e) is unchanged by the use of a quantizer. Equations (2.28) and (2.30) describe the overall relationships of the optimum quantizer.

One method of solving these equations is to apply a search procedure. For example; for a given number of levels (L) with respect to $Z_1=-\infty$ and arbitrary selection of Z_2, the most negative quantizer output (Y_1) can be obtained. If Y_L is the centroid of the area of P(e) between Z_L and ∞, Y_1 was chosen correctly. If the Y_L does not satisfy the equation (2.17) then L_1 must be reselected.

2.3.2.2. QUANTIZER DESIGN BASED ON THE VISIBILITY OF QUANTIZING NOISE.

Consideration of the human visual system in the encoding of picture signals is another criterion for the design of quantizers. Candy and Bosworth[33] and Thoma[34] have studied the visibility of the quantization error and Netravali[35] uses a similar experimental technique (Fig.2.5) to determine the visibility function. By switching between A and B the subject can compare the processed pictures, which are generated by adding different amounts of random noise (simulating quantizing noise) to Pels having slopes with a certain range (say $T - \Delta T/2$, $T + \Delta T/2$), with an unimpaired picture to which can be added an appropriate amount of white noise to obtain a similar picture quality. Given three

different random noise powers (V_{n1}, V_{n2}, and V_{n3}) the equivalent white noise powers are V_{w1}, V_{w2} and V_{w3} respectively.

In this test, by assuming that the visibility of noise is relatively constant in the range $\left[T - (\Delta T/2), T + (\Delta T/2)\right]$ the subject's visibility function f(T) can be defined as

$$f(T) = \frac{1}{\Delta T} \quad \frac{V_{w1} + V_{w2} + V_{w3}}{V_{n1} + V_{n2} + V_{n3}} \tag{2.31}$$

f(T) is the subjective visibility (in terms of equivalent white noise) of unit random noise added to all picture elements having slope values in a small neighbourhood of T.

Using the visibility function, the mean-square subjective distortion (MSSD) is given by

$$MSSD = \sum_{k=1}^{L} \int_{Z_k}^{Z_{k+1}} (e - Y_k)^2 \, f(e) \, de \tag{2.32}$$

Netravali[35] has shown that, for the same number of levels, the MSSD quantizer has a better performance than quantizers designed on the basis of minimum mean-square quantizing error.

Sharma and Netravali[36] have studied a number of different quantizers and taken account of visual threshold criteria in their design. They measured the visual thresholds by dividing the picture into two halves with luminance L_0 and L_0+e . Then, by controlling the

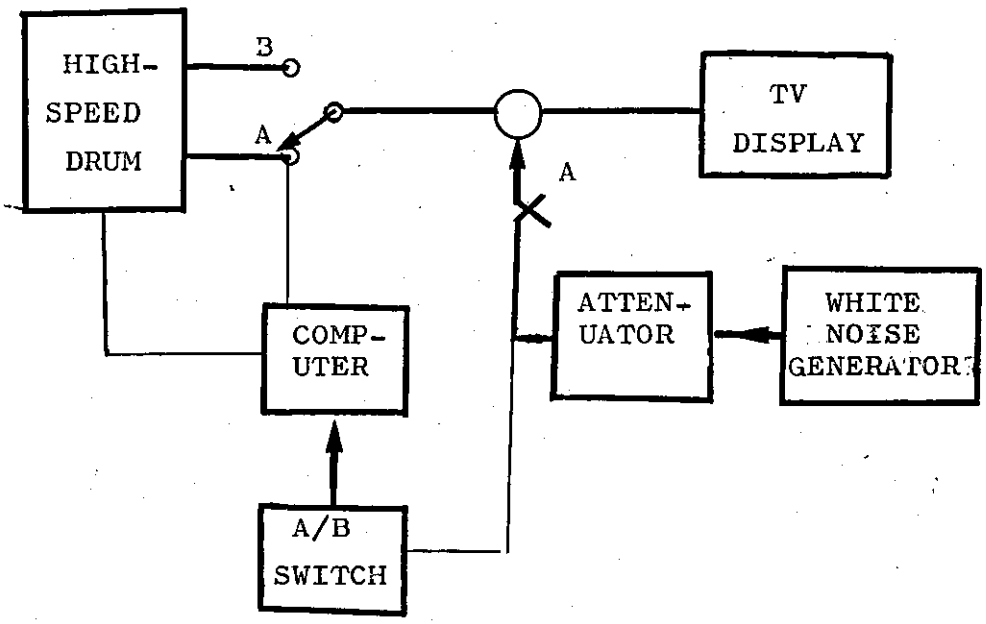

FIGURE 2.5 - Experimental set-up

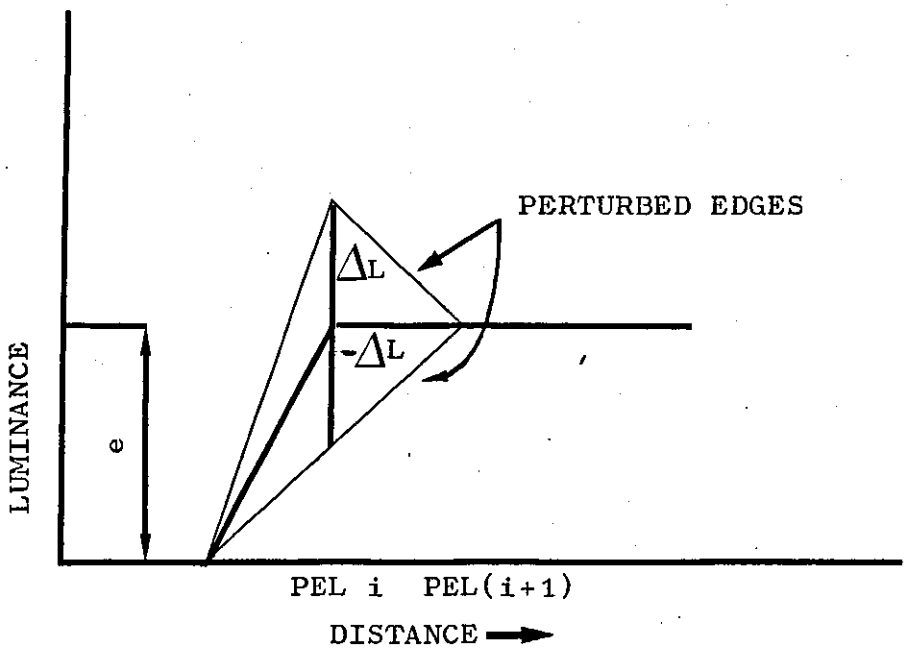

FIGURE 2.6 - Determinations of visual threshold

perturbation ΔL of the sample at the edge, the visual threshold T(è) can be determined Fig.(2.6).

Results of several such tests have shown that the threshold increases monotonically with respect to e[36]. In order to keep the quantization error below the visual threshold, a sufficient number of quantizing levels is required. For insufficient quantizing levels it becomes impossible to keep the quantization error below the visual threshold.

Sharma and Netravali[36] have given a geometric design procedure for a minimum number of levels according to

$$\left|Q(e) - e\right| \leqslant (1+\epsilon)\, T(e)$$

where Q(e) is the quantizer output function and ϵ is the constraint factor; for example, for $\epsilon = 0$, the quantization noise is constrained to be at or below the visual threshold. As ϵ is increased, the number of levels required decreases at the expense of some visual distortion. The geometric design of a quantizer according to the visibility function T(e) for a minimum number of quantizing levels in the range -A to A is shown in Fig.(2.7).

2.4. STATISTICAL CONSIDERATION OF VIDEO CODING.

Source encoding techniques for video signals are able to provide utilization of a given communication

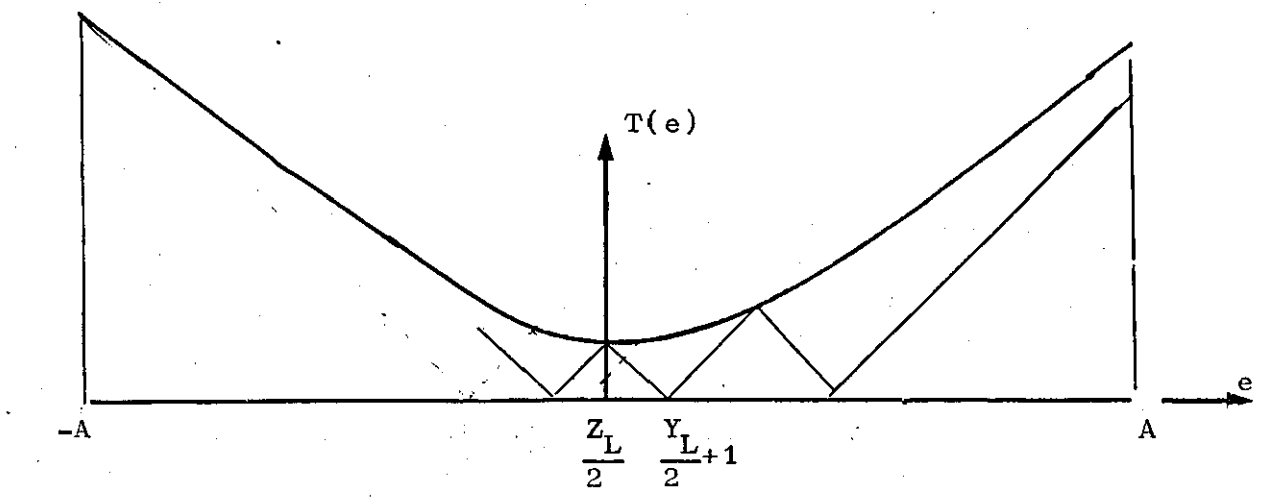

(a)

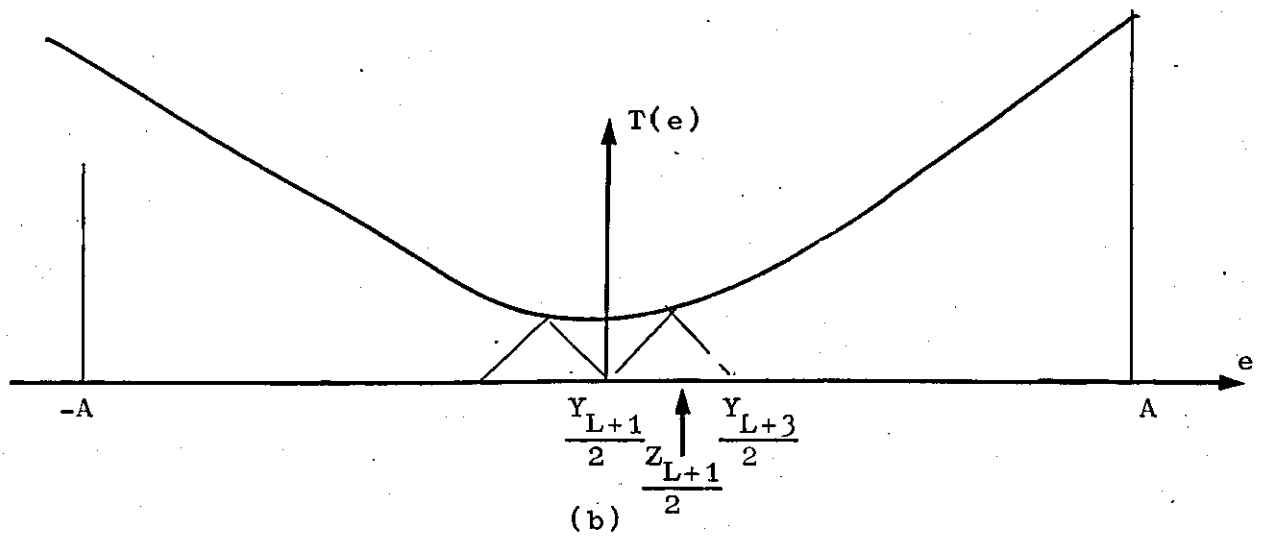

(b)

FIGURE 2.7 - Geometric quantizer design procedure for minimum number of levels

a: symmetric quantizer for even L

b: symmetric quantizer for odd L

system. For all these schemes the transmission rate can be determined considering characteristics of the human observer and the properties of the source which can be analysed by statistical methods.

In a digital coding system the continuous band limited video signal is sampled. After sampling the video signal can be described as a random process of discrete statistically dependent samples, whose amplitudes are in a continuous, or, after quantization, in a discrete form. Each sample corresponds to one picture element. The statistical dependencies of these samples extends both over a line and from line to line. Because of these statistical dependencies, it is necessary to use the general model of a source with memory for mathematical analysis. Assuming that each sample is statistically dependent only on a limited number of preceding samples, the Markov source model can be applied to this special physical source. Then the video signal is represented by a discrete Markov process (see Section 2.3.1.).

In the case of pictures, this means that the present picture element S_0 is assumed to be statistically dependent on n previously transmitted samples from the same or previous scan lines. According to [37] this dependency is expressed by conditional probabilities $P(S_0/S_1, S_2....S_n)$ and the entropy is approximated by the conditional entropy of the Markov source.

$$H(S_0/S_1 \ldots S_n) = - \sum_{S_0} \ldots \sum_{S_n} P(S_0, S_1 \ldots S_n)$$

$$\text{Log } P\ (S_0/S_1 \ldots . S_n) \qquad (2.33)$$

The average information content per word emitted from a source is often referred to as the entropy of the signal and can be defined as

$$H_0 = - \sum_i P_i \text{ Log } P_i \qquad (2.34)$$

From equations (2.33) and (2.34) the redundancy of a source with memory is

$$R = H_0 - H(S_0/S_1 \ldots . S_N) \qquad (2.35)$$

In order to take advantage of the redundancy of the signal to reduce the transmitted bit-rate, it is necessary to construct a variable length code to match the statistics of the signal. Entropy coding with minimum redundancy was developed independently by Shannon and Fano[38] and by Huffman[39]. These methods generate a variable length code which produces bits at a non-uniform rate[40-45].

The combination of DPCM and entropy coding has been studied by O'Neal[46]. He has shown in theory that DPCM with a uniform quantizer using entropy coding may yield an increase of 5.6dB in the SNR compared with

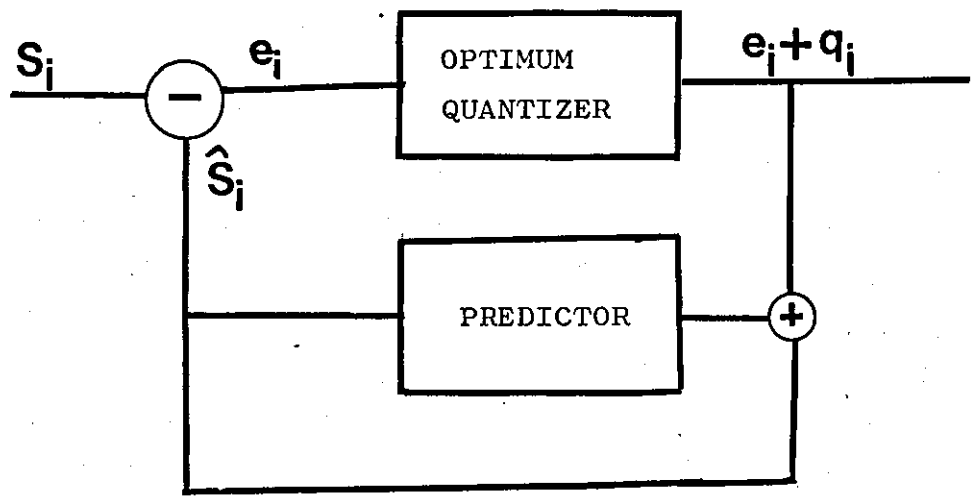

(a)

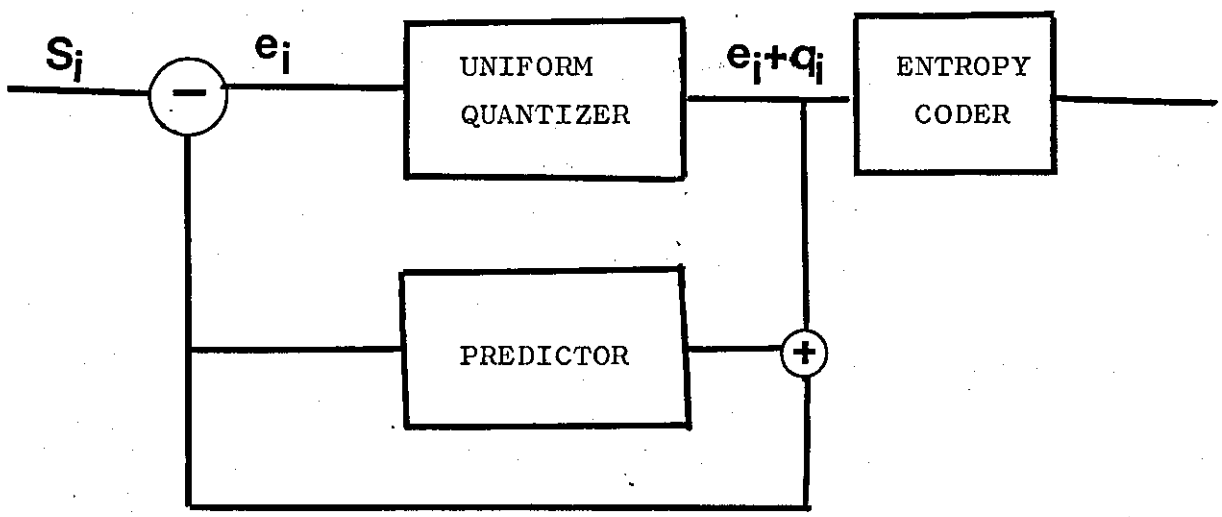

(b)

FIGURE 2.8 - Two dimensional DPCM to be compared

a: DPCM system without entropy coding

b: DPCM system with entropy coding

that of an equivalent DPCM system with an optimum non-linear quantizer (Fig.2.8). However, the 5.6dB improvement may be difficult to achieve with practical hardware.

2.5. DIGITAL COLOUR TELEVISION.

There are two types of colour television coding methods. One is known as component coding, in which a composite colour television signal is first separated into a luminance component and two chrominance components. The components are then encoded individually [47-51]. The second method is known as 'composite coding' in which a composite colour signal is encoded directly without component separation [52-58].

Component coding is an obvious choice because it is independent of the choice of colour standards and the problems of transcoding between, for example, the PAL and SECAM systems. However, component coding equipment tends to be complicated because it needs an input signal separation process, an output composite signal synthesising process and digital time division demultiplexing and multiplexing processes.

Of the two methods- composite coding and component coding- attention is now concentrated on the latter. A brief review of relevant composite coding work is given as an introduction at the beginning of each chapter. The paper by Limb, Rubinstein and Thompson [59] presents a comprehensive review of coding of colour

television signals, also giving the background of colour signal representation and colour perception.

Finally, in this chapter, for the benefit of the non-specialized reader, we give a brief description of analogue colour television systems.

2.6. COLOUR TELEVISION SYSTEMS.

The various colour television systems; NTSC, PAL and SECAM are now summarized. For more comprehensive concepts of colour television the interested reader can refer to the books by Carnt and Townsend[60] and Sims[61] which cover all major colour television systems.

Pearson[62] introduces the principles of monochrome and colour television signal properties and the psycho-visual properties of human vision. He also presents the process of video signal formation as a three-dimensional sampling operation with the help of Fourier expansion.

The fundamental concept of colour television is based on the chromitacity principle where most colours can be produced as a linear combination of three primary colours. In colour television, the commonly used primaries are red(R), blue(B) and green(G).

The primary colour signals are obtained by a three pick-up tube camera. In this camera the televised scene is separated into three primary pictures by dichroic mirrors Fig.(2.9). A dichroic mirror has the property of reflecting a selected colour and passing all other colours. Additional filters are placed in front of each tube to give the camera the desired spectral response

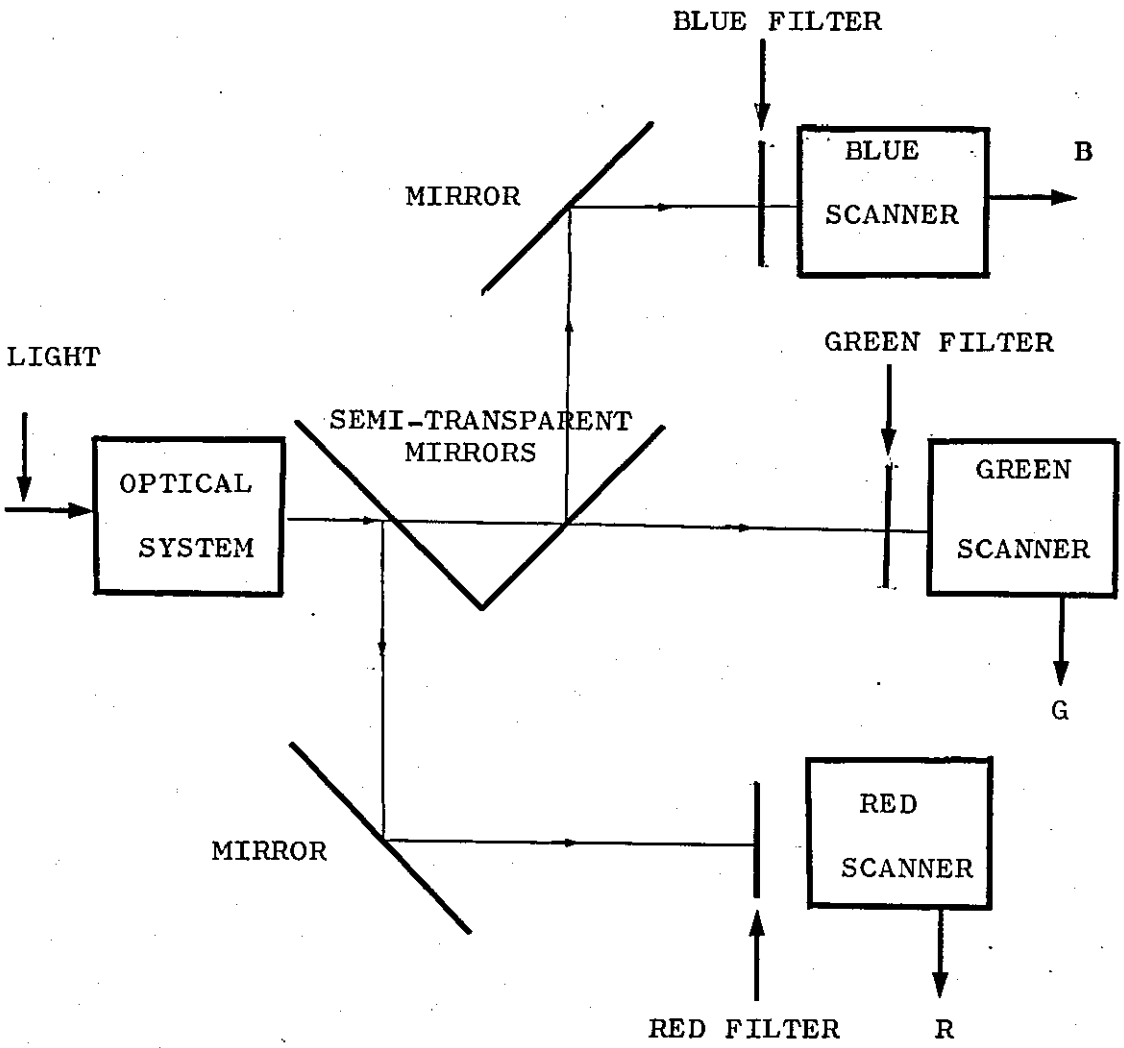

FIGURE 2.9 - Basic arrangement of the tricolour camera

because the response of the human eye is not uniform within the visible spectrum. A typical curve of the response of the eye in terms of brightness is shown in Fig.(2.10)

Considerations of compatibility require that a black and white (monochrome) signal be obtainable from the colour signal. Compatibility necessitates, in the first place, the following two conditions:

a) The colour transmission must remain within the frequency channel provided for black and white transmission.

b) The transmission of the luminance signal Y should allow satisfactory monochrome operation.

As is shown in Fig.(2.10),the visual sensation of brightness, witha peak near the yellow-green is not uniform throughout the visible spectrum. Thus, the signal having a response similar to the human brightness sensation is

$$Y = 0.30R + 0.594G + 0.11B \qquad (2.36)$$

The condition of compatibility, therefore, requires that the three primary signals are delivered in these proportions. It is consequently sufficient to add to the transmission two other independent linear combinations of the primary signals. These additional signals, which are known as chrominance or colour difference signals are;

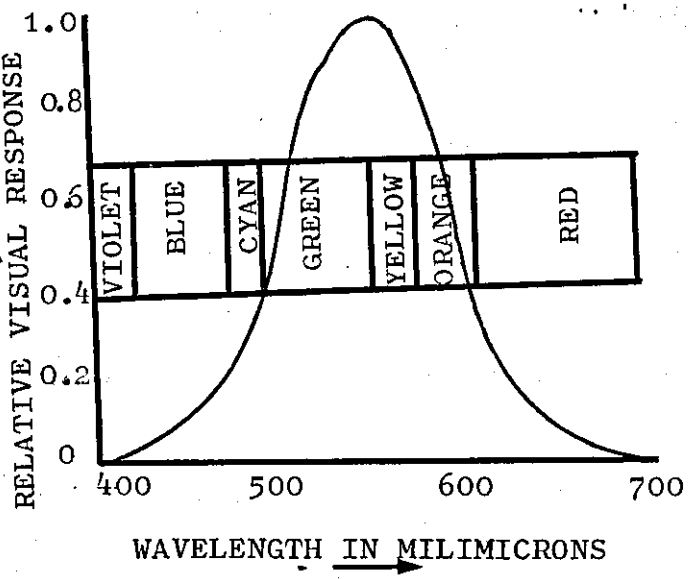

FIGURE 2.10 - The sensitivity of the human eye throughout the visible spectrum

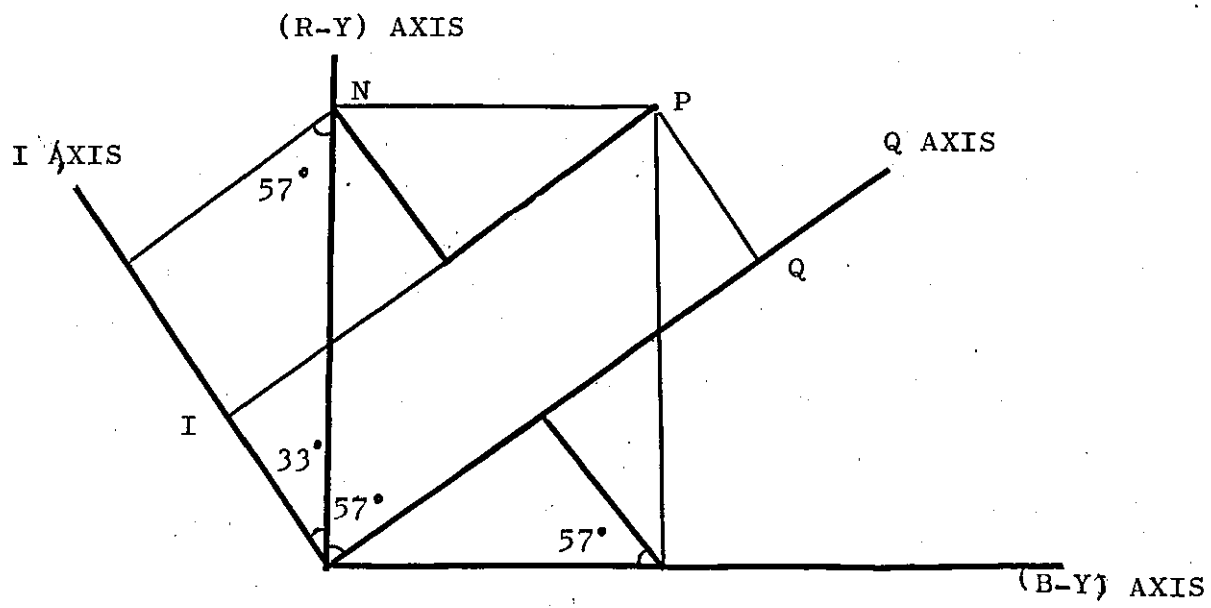

FIGURE 2.11 - Derivation of I and Q from (R-Y) and (B-Y)

$$R-Y = 0.7R - 0.59G - 0.11B$$
$$B-Y = -0.3R - 0.59G + 0.89B$$
$$G-Y = -0.3R + 0.41G - 0.11B \qquad (2.37)$$

R-Y and B-Y are chosen because their maximum values are greater than G-Y.

Thus a compatible colour television system may be set up by transmitting a monochrome signal (Y) plus two chrominance signals. The Y signal is transmitted so that existing monochrome receivers can reproduce the black and white picture. The chrominance signals modulate a sub-carrier near the high frequency end of the video channel. Methods of modulating the sub-carrier with chrominance information differ and they will therefore be described separately for the NTSC, PAL and SECAM systems.

2.6.1. THE NTSC SYSTEM.

To combine the two chrominance signals into a single signal, use is made of a technique known as two phase or quadrature modulation. Here the chrominance signals are applied to two balanced modulators, the carrier is suppressed and a simple modulated chrominance signal formed in this system can be defined as

$$S = V \text{ Cos } \omega_{sc}t + U \text{ Sin } \omega_{sc}t \qquad (2.38)$$

where V = 0.877 (R-Y) and U = 0.493 (B-Y) are the

weighted values of the colour difference signals.

In most forms of the NTSC signal, the two chrominance sub-carriers are advanced by 33° from their U and V axes Fig.(2.11)to give

$$S = I \cos (\omega_{sc}t + 33^{\circ}) + Q \sin (\omega_{sc}t + 33^{\circ}) \qquad (2.39)$$

where

$$I = V \cos 33^{\circ} - U \sin 33^{\circ}$$
$$= 0.74\ (R-Y) - 0.27\ (B-Y)$$

and

$$Q = V \sin 33^{\circ} + U \cos 33^{\circ}$$
$$= 0.48\ (R-Y) + 0.41\ (B-Y) \qquad (2.40)$$

The sub-carrier frequency is chosen to be an odd multiple of half line frequency to allow the chrominance and luminance components to interleave with minimal interaction.

2.6.2. THE PAL (Phase Alternation Line) SYSTEM.

With the PAL system the weighting factors are similar to those used for R-Y and B-Y in the NTSC system.

$$V = 0.877\ (R-Y)$$
$$U = 0.493\ (B-Y) \qquad (2.41)$$

The main difference between the PAL system and the NTSC system is that in quadrature modulation the phase of the sub-carrier for the V component is reversed at line frequency. Thus, the modulated chrominance signal is defined by the equations

$$u = U \sin(\omega_{sc} t),$$
$$v = \pm V \cos(\omega_{sc} t) \qquad (2.42)$$

The positive sign of V refers to the odd lines of the first and second fields and the even lines of the third and fourth fields.

The phase reversal of the V component protects the system against differential phase distortion in the transmission system at the expense of a slight reduction in saturation. In the decoder, the output from each demodulator is delayed by one line (64μs) and direct and delayed signals are added as shown in Fig. (2.12). There is, however, the inherent drawback in this process of a reduction in vertical chrominance resolution.

The frequency of the sub-carrier in the PAL system is

$$f_s = (284 - \tfrac{1}{4})\, f_L + 25 \text{ Hz} \qquad (2.43)$$

where f_L is the line frequency and is equal to

$$f_L = 15.625 \text{ KHz}$$

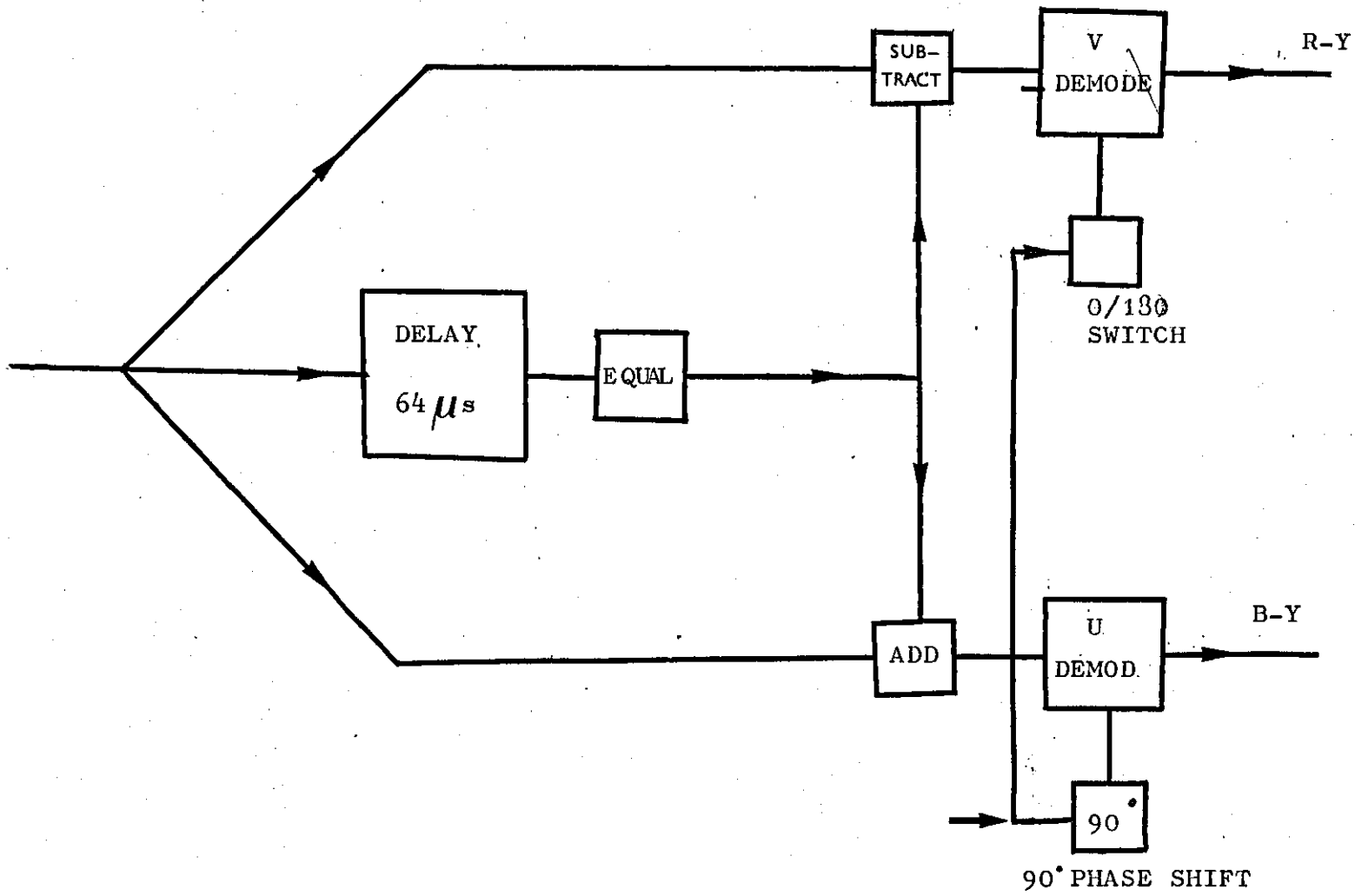

FIGURE 2.12 - Block diagram of PAL decoder using the delay line method

In the NTSC system the sub-carrier frequency is equal to an odd multiple of half the line frequency. In the PAL system, the sub-carrier frequency is almost equal to an odd multiple of quarter the line frequency and the v component is switched by 180^{o} on each consequtive line. This produces a one quarter line off set for the V components and a three quarter line off set for the U component Fig.(2.13). If the half line off set of the NTSC system had been used, the phase alternation of the v component would have produced components at harmonics of the line frequency which would increase the visibility of the sub-carrier signal in monochrome reception. For the same reason the 25Hz ($\frac{1}{2}$ cycle per field) is added to the quarter line offset frequency.

In order to establish the reference sub-carrier phase and to synchronize the switching of the V axis, the demodulator is supplied with a burst of ten cycles of sub-carrier following the line synchronizing pulse. The phase of the colour burst is 225^{o} with respect to 'U' on even lines of the first and second and odd lines of the third and fourth fields, and 135^{o} on odd lines of the first and second, and even lines of the third and fourth fields respectively.

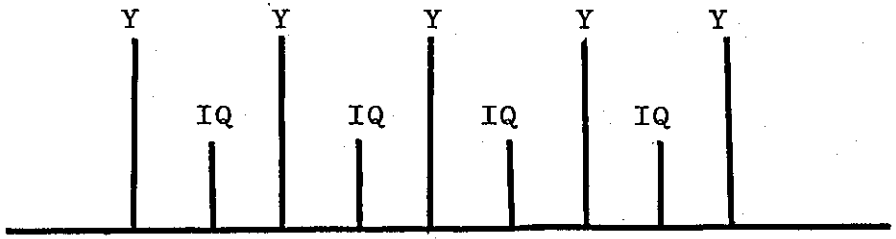

(a)

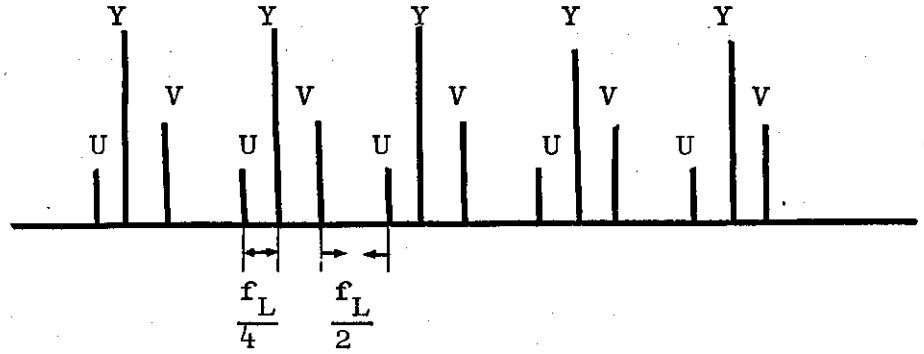

(b)

FIGURE 2.13 - Frequency spectra
a: NTSC with half line offset
b: PAL with quarter line offset

2.6.3. THE SECAM (Sequential Colour and Memory) SYSTEM.

The SECAM system has passed through several stages of development, one of the latest of which will be described in this sub-section.

In contrast to the situation in the NTSC and PAL systems, in the SECAM system the two chrominance signals are sent in line sequence; each one modulates the sub-carrier in turn for the duration of one scanning line Fig.(2.14). A reduction in the vertical chrominance resolution thus results.

The weighted colour difference signals are

$$D'_R = -1.9(R-Y)$$

and

$$D'_B = 1.5(B-Y) \qquad (2.44)$$

Because only one chrominance signal is transmitted at a time, cross-talk between the colour difference signals is avoided and it is not necessary to use the quadrature modulation technique of NTSC and PAL. Instead, frequency modulation is used. The weighted colour difference signals before modulation are pre-emphasised having a transfer function G(f) where

$$G(f) = \frac{1+j(f/f_1)}{1+j(f/g.f_1)} \qquad (2.45)$$

$g = 3.0$ and $f_1 = 85$ KHz

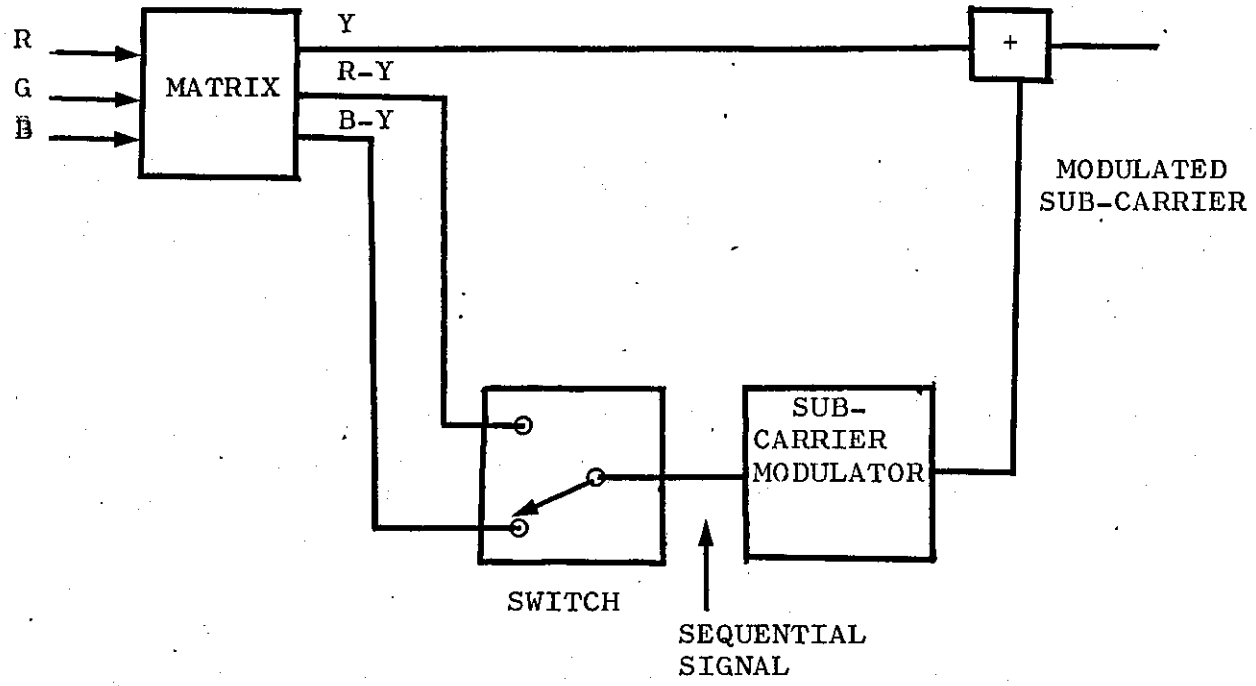

FIGURE 2.14 - Simplified diagram of the SECAM coder

The output signal is now applied to the frequency modulator. The frequency of the chrominance sub-carrier has the following nominal value on lines modulated by signal D'_R :

$$f_{SR} = 282\ f_L = 4.406\ 25\ \text{MHz}$$

and on lines modulated by signal D'_B

$$f_{SB} = 272\ f_L = 4.250\ 00\ \text{MHz}$$

where f_L is the line frequency.

The nominal frequency deviation obtained for unit amplitude modulation signal is

$$\Delta f_R = 280\ \text{KHz} \quad \text{for } D'_R \text{ lines} \tag{2.46}$$

and

$$\Delta f_B = 230\ \text{KHz} \quad \text{for } D'_B \text{ lines} \tag{2.47}$$

The maximum value of deviation is limited to the following values;

for D'_R: $+350 \pm 35$ KHz and -500 ± 50 KHz

for D'_B: $+500 \pm 50$ KHz and -350 ± 35 KHz

The modulated chrominance signal, before being added to the luminance signal, is passed through a filter which reduces the relative amplitude of the centre frequencies. This improves the chrominance signal to noise ratio and the compatibility of the system. At the receiver a filter with the inverse characteristic (bell-shaped) is used before the demodulator.

The colour sub-carrier is suppressed during the line and field blanking intervals. The sub-carrier is regenerated at its nominal undeviated frequency during the back porch of the line synchronizing pulses. To ensure that each colour signal sequence is fed to the correct demodulator, line identification signals, consisting of nine lines of frequency modulated sub-carrier, are transmitted during the field blanking period. These signals consist of bursts of sub-carrier frequency modulated by the following signals transmitted in line sequence.

a) D'_R, varying linearly from 0 to +1·25 from the beginning of the line for 15 μs, followed by a period at level +125.

b) D'_B, varying linearly from 0 to -1.5 from the beginning of the line for 20 μs, followed by a period at level -1.5.

CHAPTER III

ONE DIMENSIONAL DPCM

3.1. INTRODUCTION.

The television picture is composed of lines and fields, and the correlation between pels along a line and in both successive lines and fields has led to the development of predictors that are said to operate in one, two and three dimensions respectively.

In one dimensional picture coding the estimated value of S_i, $\hat{S}_i$, is predicted from previous pels along the line and should be a close replica of S_i. All predictors exploit the correlation in a signal (an uncorrelated signal is unpredictable) and the higher the correlation the more accurate will be the predictor. Further, areas of the picture in one or more fields often have correlation coefficients exceeding 0.98, enabling the predictor design to proceed on the basis that the area in which the sample to be predicted resides may be considered as a constant luminance,hue zone. Of course, this is not always true, and the predictor may perform less well unless some form of motion detector is used.

In the case of monochrome pictures, one, two or three dimensional prediction can be achieved without complication. For colour pictures, however,due to the presence of the sub-carrier, the prediction must be arranged according to sample phases that

are related to the sampling frequency, which affects not only the transmitted bit-rate but ease of hardware implementation.

3.2. THE SAMPLING FREQUENCY.

In most previous work[52,54,63,64] the sampling frequency of composite colour signals is simply related to the sub-carrier frequency. This minimizes intermodulation products between harmonics of the sampling and sub-carrier frequencies[65] and is also important in differential coding. For example, by selecting the sampling frequency (f_s) to be three times the sub-carrier frequency (f_{sc}), the third previous picture elememnt (pel) along the line is a good prediction of the pel under consideration, providing that hue (H), saturation (S) and luminance (Lu) only change slowly.

This value of f_s is considerably greater than the Nyquist rate $f_N = 2f_m$ where f_m is the highest frequency in composite signal s(t), and will increase the bandwidth of the digitally encoded signal relative to the minimum obtainable. This consequently led to the development of sub-Nyquist sampling[66] at $f_s = 2f_{sc}$; $f_{sc} < f_m$. This technique also enables satisfactory results to be obtained but is inherently more complex, requiring the 'combing out' of aliased components. In general, it is desirable that the sampling frequency is simply related to both line and

sub-carrier frequencies. In the case of the NTSC system, this can be achieved without complication (the sub-carrier frequency is a multiple of half-line frequency). In the PAL system the relationship between the sub-carrier and line frequencies is complex due to the sub-carrier having a quadrative line and half field frequency off set.

$$f_{sc} = (284 - \tfrac{1}{4})\, f_{line} + \tfrac{1}{2} f_{field} \qquad (3.1)$$

3.2.1. SAMPLING FREQUENCY: AN INTEGRAL MULTIPLE OF LINE FREQUENCY.

The relationship between the colour sub-carrier frequency f_{sc} and the line frequency f_L is given by equation (3.1). To remove the effect of the quarter line off set, we multiply both sides of this equation by 0.8.

$$0.8f_{sc} = 227f_L + 20 \qquad (3.2)$$

The sampling frequency f_s is selected to retain an approximately integral relationship with f_L. Thus,

$$f_s = 0.8f_{sc} \cdot n = 227f_L\, n + 20n \qquad (3.3)$$

where n is a positive integer.

Three values of n are of interest

$$n = 3, \quad f_s = 2.4f_{sc} = 681f_L + 60 \tag{3.4}$$

$$n = 4, \quad f_s = 3.2f_{sc} = 908f_L + 80 \tag{3.5}$$

$$n = 5, \quad f_s = 4.0f_{sc} = 1135f_L + 100 \tag{3.6}$$

For n = 3,4 and 5, the 'slip frequencies' 60, 80 and 100 Hz respectively, cause a slip of half a period of one cycle of the sub-carrier. If a signal is converted from a sampling rate based on line frequency ($f_s = 227f_Ln$), to a corresponding rate based on sub-carrier frequency ($f_s = 0.8f_{sc}n$), then, during the period of each field there is a horizontal displacement between the top and bottom of the picture of about 1/5000 of the picture width. Consequently, vertical lines are represented by an angle $< 0.2^{\circ}$ from their correct position. This small divergence is insignificant[67].

If we consider the case of $f_s = 2.4f_{sc}$, the sampling frequency is slightly below the Nyquist rate resulting in the alias components at the edge of the spectrum possibly causing visible interference. Further, since they are situated at an integral multiple of line frequency, the possibility of combing out these components is out of the question. For $f_s = 3.2f_{sc}$ (n=4), apart from the difficulty of prediction similar to that obtained when $f_s = 2.4f_{sc}$, the disadvantage is the high sampling

frequency. $f_s = 4f_{sc}$ (n=5) is probably the most desirable sampling frequency, being simply related to the line (ignoring the slip frequency of 100 Hz) and sub-carrier frequencies. The only drawback again is the high sampling frequency.

It is clear that the integral relationship between f_s and f_L aids the removal of the blanking intervals enabling picture bits to occupy these intervals, consequently reducing the transmitted bit-rate.

A further advantage occurs in that the sample points produce the orthogonal array shown in Fig.(3.1a) which repeats from frame to frame. If intermodulation products occur, however, the system will become vulnerable because most of the energy in the luminance signal is distributed around multiples of the line frequency. As f_s has an integral relationship with f_L, intermodulation products will fall on these spectral components at multiples of f_L causing visual interference.

3.2.2 SAMPLING FREQUENCY: AN INTEGRAL MULTIPLE OF HALF LINE FREQUENCY.

The advantage of using this relationship between f_s and f_L is that intermodulation and luminance components do not interfere.

Multiplying both sides of equation (3.1) by 0.4j and equating it to f_s yields

$$f_s = 0.4f_{sc}j = 113.5j\ f_L + 10j \qquad (3.7)$$

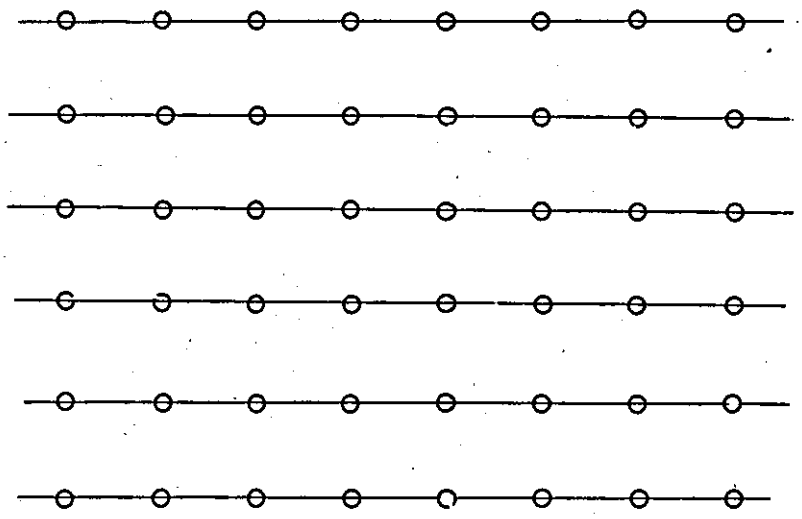

(a)

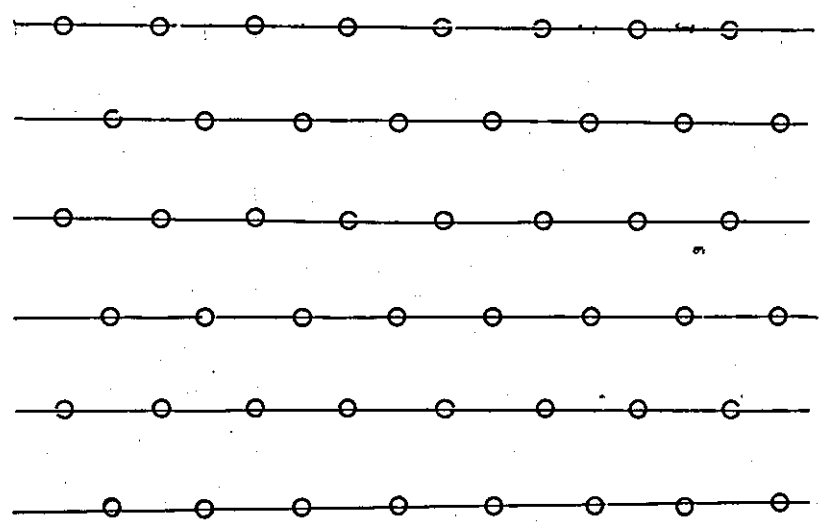

(b)

FIGURE 3.1 - Resulting pattern of samples

a: sampling frequency is a multiple of line frequency

b: sampling frequency is an odd multiple of half line frequency

If j is an odd integer (e.g. = 5 and 7)

$$f_s = 2f_{sc} = 567.5f_L + 50 \quad j=5 \tag{3.8}$$

and

$$f_s = 2.8f_{sc} = 794.5f_L + 70 \quad j=7 \tag{3.9}$$

The resulting pattern of sample points is shown in (3.1b)

3.3. PREDICTION FROM PREVIOUS PELS ALONG THE SCAN LINE.

The composite PAL signal can be represented as

$$S = Lu + C \sin (2\pi f_{sc} t + \varphi) \tag{3.10}$$

where Lu, C and φ represent the luminance, saturation and hue respectively and

$$C = \pm \sqrt{V^2 + U^2} \tag{3.11}$$

$$\varphi = \pm \tan^{-1}(V/U) \tag{3.12}$$

where the negative sign represents the PAL inversion of the V component which occurs on alternate lines. The signal is sampled at a rate f_s to yield a sequence of picture elements.

$$S_i = Lu + C \sin (2\pi \tilde{f}i + \varphi) \tag{3.13}$$

where

$$\tilde{f} = \frac{f_{sc}}{f_s} \tag{3.14}$$

The value of the i^{th} pel given by equation (3.13) is to be predicted from the three previous pels, S_{i-1}, S_{i-2} and S_{i-3} along the scan line. The coefficients $\{a_k\}$ of this one dimensional predictor will be derived as functions of $\tilde{f}$, equation (3.14) enabling the coefficients to be selected for varying sampling rates[68].

A linear predictor constructs its predicted sample value as the weighted summation of previous pels

$$\hat{S}_i = \sum_{n=1}^{3} a_n S_{i-n} \tag{3.15}$$

The coefficients $\{a_k\}$ are now found as follows: From eqn.(3.13) the first and third previous samples S_{i-1} and S_{i-3} are determined and added together

$$S_{i-1} + S_{i-3} = 2Lu + 2C \text{ Sin } (2\pi \tilde{f} (i-2) + \varphi) \cdot \text{Cos } (2\pi \tilde{f}) \tag{3.16}$$

By noting that the second previous sample is

$$S_{i-2} = Lu + C \text{ Sin } (2\pi \tilde{f}(i-2) + \varphi) \tag{3.17}$$

it is seen that the sine terms in eqns. (3.16) and (3.17)

can be eliminated to give an expression for the luminance component

$$Lu = \frac{S_{i-1} + S_{i-3} - 2.S_{i-2} \text{ Cos } 2\pi\tilde{f}}{2\ (1 - \text{Cos } 2\pi\tilde{f})} \qquad (3.18)$$

A second expression for Lu is now sought. Adding the present sample S_i to the second previous sample S_{i-2} gives

$$S_i + S_{i-2} = 2Lu + 2C \text{ Sin } (2\pi\tilde{f}(i-1) + \varphi) \cdot \text{Cos } (2\pi\tilde{f}) \qquad (3.19)$$

and combining this sum with

$$S_{i-1} = Lu + C \text{ Sin } (2\pi\tilde{f}(i-1) + \varphi) \qquad (3.20)$$

yields

$$Lu = \frac{S_i + S_{i-2} - 2S_{i-1} \text{ Cos } (2\pi\tilde{f})}{2(\ 1 - \text{Cos } 2\pi\tilde{f})} \qquad (3.21)$$

Equating eqns, (3.18) and (3.21)

$$S_i = S_{i-1}\ (1+2 \text{ Cos } 2\pi\tilde{f}) - S_{i-2}\ (1+2 \text{ Cos } 2\pi\tilde{f}) + S_{i-3} \qquad (3.22)$$

By assuming that Lu, C and φ are constant for S_i, S_{i-1}, S_{i-2} and S_{i-3} we have obtained two expressions for S_i,

equation (3.13) which depends on Lu, C and φ, and equation (3.22) which is a function of S_{i-1}, S_{i-2}, S_{i-3} and $\tilde{f}$.

If the assumption that over four samples, Lu, C and φ are constant (or generally change by a small amount) is reasonable, then S_i in eqn. (3.22) can be made equal to $\hat{S}_i$ in eqn. (3.15), when the three coefficients become

$$\left.\begin{aligned} a_1 &= 1 + 2\,\mathrm{Cos}\,2\pi\tilde{f} \\ a_2 &= -a_1 \\ a_3 &= 1 \end{aligned}\right\} \qquad (3.23)$$

By changing the sampling rate, thereby altering $\tilde{f}$, the changes that need to be made to $\{a_k\}$ are simple and given by eqn. (3.23). Table 3.1. shows a_1, a_2, a_3 for a number of values of $f_s/f_{sc} = \tilde{f}^{-1}$. f_s/f_{sc} = 2.4, 3.2 and 4.0 correspond to the case where f_s is, to a close approximation, an integral multiple of line frequency whilst f_s/f_{sc} = 2 and 2.8 apply when f_s is an integral multiple of half line frequency. f_s/f_{sc} = 2 is the so-called sub-Nyquist sampling case (f_s/f_{sc} = 2.4 is below the Nyquist rate). The relationship f_s/f_{sc} = 2.5 is of particular value in two dimensional signal prediction and is considered in detail in the following chapter.

From eqn. (3.23) we observe that,

TABLE 3.1

Predictor coefficients for various sampling frequencies

$\frac{f_s}{f_{sc}}$	a_1	a_2	a_3
4	1	-1	1
3.2	0.2346	-0.2346	1
3.0	0	0	1
2.8	-0.2470	+0.2470	1
2.5	-0.6180	+0.6180	1
2.4	-0.7321	+0.7321	1
2.0	-1	1	1

$$\sum_{n=1}^{3} a_n = 1 \qquad (3.24)$$

a necessary criterion for stability when the predictor is used in the feedback loop of a DPCM encoder and, more significantly, a desirable characteristic for luminance prediction.

A simple same-line predictor that involves a delay of 5T, where T is a sample period, is produced by adding a further delay of 2T to give the predicted output $\hat{S}_i$,

$$\hat{S}_{4,i} = S_{i-5} \qquad (3.25)$$

This prediction can be used because $f_s = 2.5f_{sc}$ produces 5 samples in every two cycles of the sub-carrier. In a picture where the signal changes rapidly this prediction has the disadvantage of a relatively large prediction distance (two sub-carrier periods).

3.4. ACCOMMODATING ABRUPT LUMINANCE CHANGES.

Adaptive prediction similar to that used by Devereux[63] for $f_s = 3f_{sc}$ is now considered.

By assuming Lu, C and φ are approximately constant over sampling instants, i-1, i-2 and i-3, eqns.(3.22) and (3.23) are established from which the predicted sample is

$$\hat{S}_i = LK\ (-a_2\ S_{i-1} + a_2\ S_{i-2} + S_{i-3}) \qquad (3.26)$$

where LK is the leak factor and is $\leqslant 1$.

This prediction is used unless there is an abrupt change in the composite signal when the prediction is based on a previous sample. The previous sample employed depends on the value of f_s/f_{sc}. For example,

$$\text{if} \quad f_s/f_{sc} = 3.0;\ \hat{S}_i = LK_1\ S_{i-1} \qquad (3.27)$$

$$\text{if} \quad f_s/f_{sc} = 2.5;\ \hat{S}_i = LK_2\ S_{i-2} \qquad (3.28)$$

$$\text{or} \quad f_s/f_{sc} = 2.5;\ \hat{S}_i = LK_3\ S_{i-1} \qquad (3.29)$$

The predictors based on S_{i-1} and S_{i-2} are used for three consecutive sampling instants before the prediction given by equation (3.26) is restored.

This adaptive prediction strategy depends on detection of abrupt changes in the composite signal and is conceived for use in DPCM encoding (see Chapter II, Section 2.). Fig.(3.2a) shows an arbitrary composite signal having sharp changes in hue and luminance. The corresponding prediction errors when the prediction is based entirely on equation (3.26) or on a combination of eqns. (3.26) and (3.28) are shown in Figs. (3.2b) and (3.2c) respectively for $f_s/f_{sc} = 2.5$ and $LK_2 = 1$.

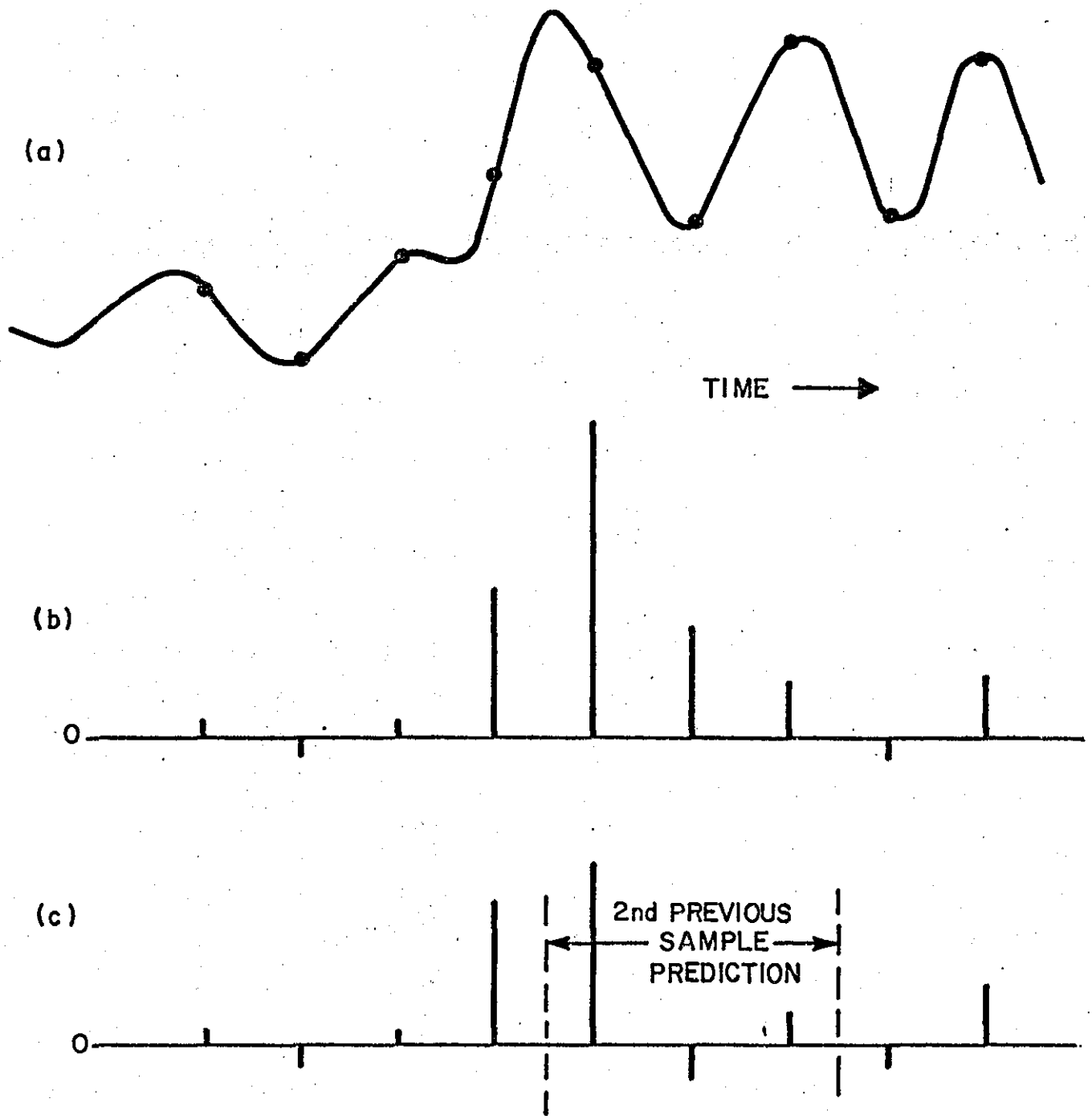

FIGURE 3.2 - One dimensional prediction

a: Arbitrary composite signal

b: Prediction error from prediction based on three previous samples.

c: Prediction error from prediction based on three previous samples or on the second previous sample

3.5. CODING PARAMETERS.

As a criterion of performance, signal to prediction error ratios (SNR_p)are used. The probability density function (pdf) of the error signal is also employed to compare various prediction techniques. In actual encoding, prediction of pels is based on the reconstructed picture elements for which a quantizer is needed. In the absence of a quantizer, the SNR_p and pdf are considered when the picture is based on the original pels.

All predictors have been simulated on the digital computer and the peak to peak signal to r.m.s. prediction error ratio, SNR_p and peak to peak signal to r.m.s. quantizing noise ratio SNR, were found for 16 lines of 100 percent saturated colour bar signals (see Appendix A).

$$SNR_p = 20 \text{ Log } \frac{V_{pp}}{\left[\frac{1}{N_1} \sum_{i=1}^{N_1} e_i^2\right]^{\frac{1}{2}}}$$

$$SNR = 20 \text{ Log } \frac{V_{pp}}{\left[\frac{1}{N_1} \sum_{i=1}^{N_1} q_i^2\right]^{\frac{1}{2}}} \qquad (3.30)$$

where N_1 is the number of samples involved in the measurement and q is the quantizing noise in the presence of the quantizer. The amplitude distribution of the prediction error is obtained by finding the number of sample values in each 512 quantum intervals* (-256-255).

* 1 quantum = spacing between adjacent 8 bit PCM levels.

These points are then normalized to produce the probability density function of the error signal. The probability density functions of three predictors are shown in Fig. (3.3).

The shapes of these curves are important in designing the optimum quantizers and in comparing the performance of different predictors. A poorer predictor will show a broader distribution of prediction errors.

3.6. QUANTIZER DESIGN PROCEDURE.

In Chapter II different quantizer design procedures were considered. Given the probability density function of the error signal P(e) and the number of quantizing levels N, the necessary conditions which define the optimum design of a quantizer are

$$Z_k = \frac{Y_{k-1} + Y_k}{2} \qquad 2 \leqslant k < N \tag{3.31}$$

$$\int_{Z_k}^{Z_{k+1}} (e - Y_k)\, P(e)\, de = 0 \tag{3.32}$$

Deviation of the above condition is given in Chapter II, Section 2.3.2.1. Further details have been discussed by Max [31], bearing in mind that e is a discrete variable and that $e-Y_k$ is the quantizing error for a typical input mapped on Y_k.

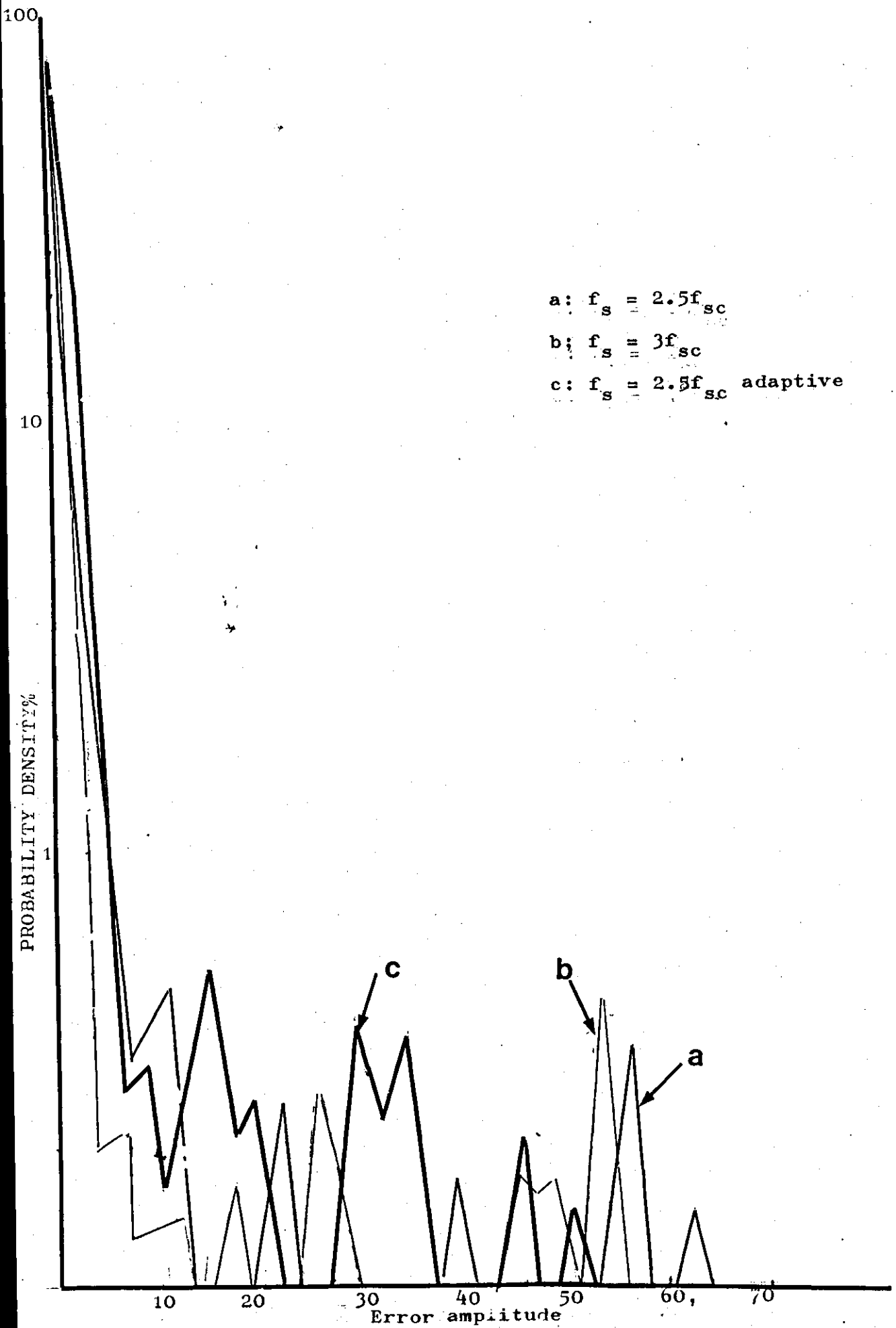

FIGURE 3.3 - Amplitude distribution of prediction error

For colour bar signals, probability density functions of error signals are different in shape for each predictor and it should be pointed out that the shape of the pdf will change from picture to picture. So, if the object is to compare different predictors for DPCM coding, it is best to carry this comparison out in the absence of the quantizer. Otherwise the quantizer should be adaptive according to the statistical variation of error signal. For speech signals, adaptation can be obtained without complication due to the relatively low speed of sampling and small number of quantization levels. The quantizer for broadcast quality television must be relatively primitive as it has to operate with a large number of quantizing levels and at a sampling rate 1000 times higher than used in telephony.

The following is a description of the algorithm used to carry out the design.

i) Suppose $P_1(e_i)$, $P_2(e_i)$.....$P_n(e_i)$ are the discrete probability density functions of the error signal for n different predictors. Instead of designing optimum quantizers for each of the n predictors, for simplicity, only, one quantizer is designed which is based on the average pdf's of the predictors.

$$P_{av}(e_i) = \frac{1}{N}\left[(P_1(e_i) + P_2(e_i) + \ldots P_N(e_i)\right] \qquad (3.33)$$

ii) Given the average probability density function

$P_{av}(e_i)$, the output levels Y_k are distributed according to the distribution of $P_{av}(e)$. Consequently, the input thresholds Z_k are defined by the condition (3.30). After finding all Z_k and Y_k the quantizer is included in the simulated DPCM loop. The new average pdf, $P'_{av}(e)$ is then obtained whose predictions are based on the reconstructed signals. The shape of the new pdf, $P'_{av}(e)$ is slightly different from that of $P_{av}(e)$. The quantizer design (based on $P'_{av}(e)$) is then modified by the experimental search procedure to obtain the pdf closest to $P_{av}(e)$.

The input range and quantized output levels for the 5 and 6 bit quantizers used in the experiments are shown in Table (3.2). In the case of the 64 level (6 bit) quantizer, the negative half of quantization law was given by changing the sign of the first 31 input ranges and quantized output levels, i.e. there were 33 positive and 31 negative quantization levels.

3.7. RESULTS.

The experiments were carried out using computer simulation. The input signal, a 100% saturated colour bar PAL signal, was applied to the A/D converter and the resulting 8 bit words were used prior to simulating DPCM with different predictors. This leads to the DPCM system shown in Fig.(2.1). The input sample x_i and the feedback sample $\hat{S}_i$ are 8 bit words resulting in a 9 bit

TABLE 3.2 - Quantizing laws

q-level number	32 LEVEL QUANTIZER		64 LEVEL QUANTIZER	
	INPUT	OUTPUT	INPUT	OUTPUT
33			161 ∿ 255	165
32	157 ∿ 256	172	153 ∿ 160	157
31	125 ∿ 156	140	145 ∿ 152	149
30	93 ∿ 124	108	137 ∿ 144	141
29	77 ∿ 92	84	129 ∿ 136	133
28	61 ∿ 76	68	121 ∿ 128	125
27	49 ∿ 60	54	113 ∿ 120	117
26	37 ∿ 48	42	105 ∿ 112	109
25	29 ∿ 36	32	97 ∿ 104	101
24	21 ∿ 28	24	89 ∿ 96	93
23	15 ∿ 20	17	81 ∿ 88	85
22	11 ∿ 14	12	73 ∿ 80	77
21	7 ∿ 10	8	65 ∿ 72	69
20	5 ∿ 6	5	57 ∿ 64	61
19	3 ∿ 4	3	51 ∿ 56	54
18	2	2	45 ∿ 50	48
17	1	1	39 ∿ 44	42
16	0	0	33 ∿ 38	36
15	-1	-1	29 ∿ 32	31
14	-2	-2	25 ∿ 28	27
13	-3 ∿ -4	-3	21 ∿ 24	23
12	-5 ∿ -6	-5	17 ∿ 20	19
11	-7 ∿ -10	-8	15 ∿ 16	16
12	-11 ∿ -14	-12	13 ∿ 14	14
9	-15 ∿ -20	-17	11 ∿ 12	12
8	-21 ∿ -28	-24	9 ∿ 10	10
7	-29 ∿ -36	-32	7 ∿ 8	8
6	-37 ∿ -48	-42	5 ∿ 6	6
5	-49 ∿ -60	-54	4	4
4	-61 ∿ -76	-68	3	3
3	-77 ∿ -92	-84	2	2
2	-93 ∿ -124	-108	1	1
1	-125 ∿ -156	-140	0	0

difference signal e_i. Non-linear quantization (see Section 3.6) is achieved by using a look-up table producing a 5 or 6 bit DPCM word L_i. The performance criterion was taken to be SNR.

Predicting the decoded sample S_i at both the transmitter and receiver (assuming no channel errors) from pels on the same line resulted in the SNR values shown in Table (3.3) being obtained for f_s/f_{sc} = 3.0 and 2.5. The left-hand column of the table gives the sample or samples used in the prediction. When three previous samples were used in the prediction the coefficients were calculated according to equation (3.23). When the first or second previous samples were used, L_k, L_{k1}, L_{k2} and L_{k3} in equations (3.26), (3.27) and (3.28) were all unity, and the DPCM encoder took the form shown in Fig.(3.4). When the quantizer level exceeded the threshold (equivalent to a quantization output level of 24) the switch was changed to produce the first or second previous sample, according to the value of f_s/f_{sc}, and the strategy described in Section (3.4). Row 6 in Table (3.3) corresponds to the prediction of eqn.(3.25) $\hat{S}_i = S_{i-2}$, while the last row uses either $\hat{S}_i = S_{i-5}$ or $\hat{S}_i = S_{i-2}$, the latter being used in the presence of a luminance jump. Thus, the prediction rules for rows 2, 4, 5, and 7 were adaptive according to the principle described in Section (3.4).

The peak to peak signal to r.m.s. prediction error ratio, SNR_p, was found for the predictor in the absence

SAMPLE PREDICTION BASED ON	SAMPLING FREQUENCY f_s	SNR_p, dB	NUMBER OF QUANTIZATION LEVELS	OVERALL SNR, dB
S_{i-3}	$3f_{sc}$	22.9	64	52.5
			32	46.7
S_{i-3} or S_{i-1}	$3f_{sc}$	24	64	52.8
			32	46.8
$S_{i-1}, S_{i-2}, S_{i-3}$	$2.5f_{sc}$	22.5	64	50.9
			32	44.4
$S_{i-1}, S_{i-2}, S_{i-3}$ or S_{i-1}	$2.5f_{sc}$	23.2	64	52.6
			32	46.3
$S_{i-1}, S_{i-2}, S_{i-3}$ or S_{i-2}	$2.5f_{sc}$	22.5	64	53.2
			32	47.7
S_{i-5}	$2.5f_{sc}$	20.6	64	49.6
			32	44.1
S_{i-5} or S_{i-2}	$2.5f_{sc}$	22.4	64	52.0
			32	46.1

TABLE 3.3 - SNR results of one dimensional DPCM

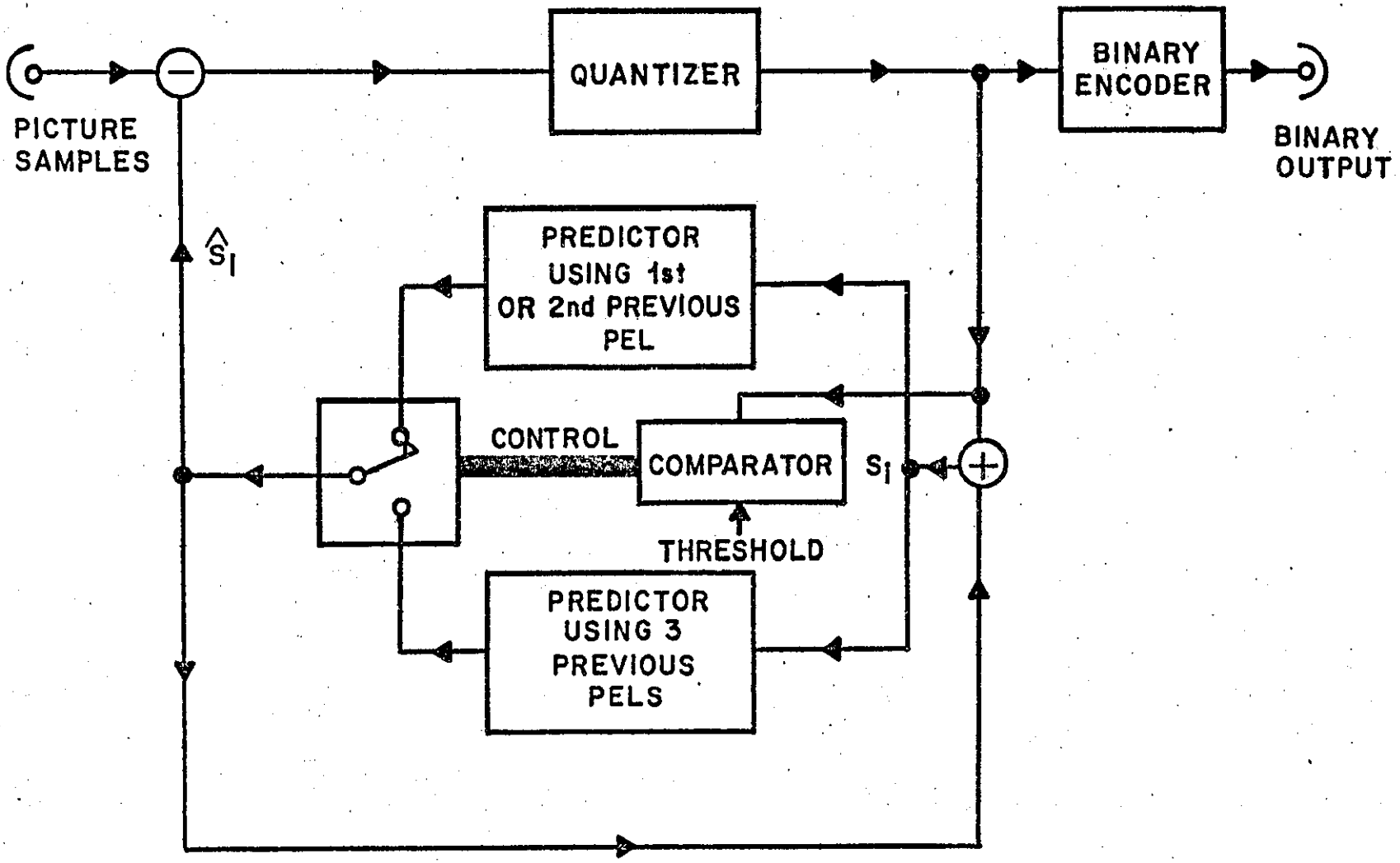

FIGURE 3.4 - One dimensional adaptive DPCM encoder

of the quantizer. The overall SNR was determined as the ratio of peak to peak input amplitude to r.m.s. quantization noise and is given for both the 32 and 64 level quantizers.

3.8. DISCUSSION.

In this chapter a simple predictor having three coefficients which can operate at any sampling rate has been described. As mentioned before, (see Section 3.2) the choice of sampling frequency depends on many factors. For comparative reasons, $f_s = 3f_{sc}$ and $f_s = 2.5f_{sc}$ (marginally above the Nyquist rate) were selected.

The results for predictors using the previous pel or pels along the same scan line Table (3.3), show that the SNR for $f_s/f_{sc} = 2.5$ is inferior to that for $f_s/f_{sc} = 3.0$. The fifth previous sample predictor, although simple, has an SNR which is 3dB worse than that of the predictor employing the previous pels. When the sampling frequency moves from $f_s = 3f_{sc}$ towards $f_s = 2.5f_{sc}$ the system becomes more vulnerable to rapid luminance transition. This is mainly because when the sampling frequency decreases from $3f_{sc}$ to $2.5f_{sc}$, the increased values of a_1 and a_2 will intensify the instability of the predictor during these transitions.

The stability of the predictor can be improved by using an adaptive strategy (see Section 3.4) which uses first or second previous sample prediction for three consecutive pels when there is a rapid transition.

The results for predictors using the adaptive version, Table (3.3), show that the SNR for $f_s = 2.5f_{sc}$ is a close approximation to that for $f_s/f_{sc} = 3.0$. The adaptation strategy is more effective in combating abrupt luminance changes than chrominance ones (particularly sharp hue variations).

3.9. Note on publication.

A paper entitled 'Non-integer sampling to subcarrier frequency ratios in DPCM of PAL signals', in co-authorship with Dr. R. Steele (Ph.D supervisor), has been published in Electronics Letters of IEE., Vol.15, No.16, August 1979. This paper is an abridged version of Chapter III.

CHAPTER IV

TWO DIMENSIONAL DPCM

4.1. INTRODUCTION.

In the last chapter one dimensional DPCM of colour television signals was discussed. Due to the high correlation that exists between samples on adjacent lines, better performance can often be obtained by employing two dimensional prediction.

In two dimensional prediction, the predicted value $\hat{S}_i$ of a pel $S_{i,j}$ can be obtained by a linear combination of the amplitude values of neighbouring pels occuring prior to $S_{i,j}$ in the same line and on preceding lines Fig.(4.1). For a monochrome signal the immediate horizontal and vertical neighbours of S_i can be used without complication. For colour television signals, because of the presence of the sub-carrier, prediction using immediately neighbouring pels cannot be achieved easily. Difficulties arise especially when PAL colour signals are used, due to the line alternation of the v component, bearing in mind that the strategy underlying any prediction algorithm is entirely dependent on selection of the sampling frequency and its relation to the sub-carrier frequency (see Chapter III, Section 3.2).

Two dimensional differential pulse code modulation (2D DPCM) has been extensively studied and is well documented[58,64,69,70,71,72]. Thompson[52] has proposed a predictor for PAL colour signals which uses the

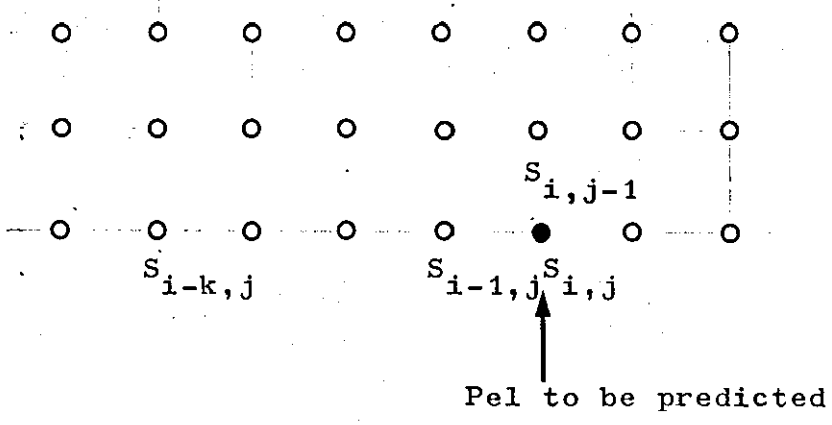

FIGURE 4.1 - Two dimensional prediction

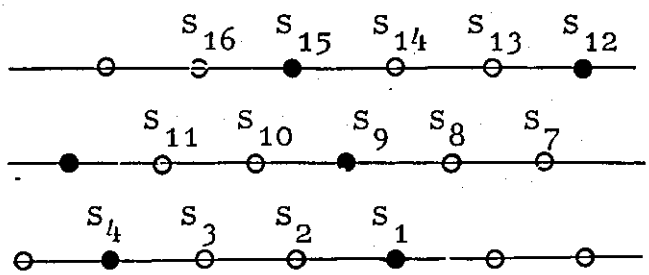

FIGURE 4.2 - Diagram of picture elements of PAL sampled at 13.3 MHz.

previous pel S_2 and congugate chrominance components of S_9 and S_{10} (S^*_{9c} and S^*_{10c})Fig.(4.2) to predict the pel S_1.

$$\hat{S}_1 = S_2 - S^*_{9c} + S^*_{10c} \qquad (4.1)$$

S^*_{9c} and S^*_{10c} are obtained by a simple modulation technique known as a PAL modifier in which modulation of the chrominance signal by a sinusaid of twice the sub-carrier frequency, generates additional components near $3f_{sc}$ which can be eliminated by a low pass filter.

In his paper Thompson has also examined the chrominance correction scheme in the case of NTSC signals which does not require a PAL modifier. An alternative approach is the all digital planar predictor which has been developed by Thompson[73]. For PAL colour signals, the planar is characterised by the three cyclic algorithms to overcome problems arising from the V-axis switch.

$$\hat{S}_1 = S_2 + S_8 - S_9$$

$$\hat{S}_2 = S_3 + S_{10} - S_{11}$$

$$\hat{S}_3 = S_4 + S_9 - S_{10} \qquad (4.2)$$

Devereux[74] has also examined a similar two dimensional prediction for PAL colour signals. In his

method a cyclic three-state prediction algorithm is used to cancel the effect of the phase reversal of the V component.

$$\hat{S}_1 = (S_4 + S_9)/2$$

$$\hat{S}_2 = (S_5 + S_8)/2$$

$$\hat{S}_3 = (S_6 + S_{10})/2 \qquad (4.3)$$

The prediction algorithms discussed above are established at a sampling rate of three times the sub-carrier frequency. In this chapter a two dimensional prediction technique is studied at various sampling rates. The two dimensional prediction which is described here comprises a combination of predictions along the scanning line (discussed in the previous chapter) and from previous lines.

4.2. TWO DIMENSIONAL PREDICTION.

The one dimensional prediction described in the previous chapter exploited the correlation of adjacent pels along a scan line. In this section the predictor utilizes the correlation of pels in between lines, and then considers the use of pels on the same line and on adjacent lines in the prediction process.

For PAL signals the sub-carrier, f_{sc}, is almost an odd harmonic of quarter line frequency,

$$f_{sc} = 1135\left[\frac{f_L}{4}\right] + 25 \qquad (4.4)$$

where f_L is the line frequency. As there are 625 lines per frame and 25 frames per second,

$$f_L = 25 \times 625 = 15625 \text{ Hz}$$

One scan line contains

$$(f_{sc}/f_L) = 283.7516 \qquad (4.5)$$

cycles of the sub-carrier. Therefore, the initial sub-carrier phase at the beginning of each successive line differs by

$$\varphi_{sc} = (1-0.7516)360 = 89.424 \text{ degrees} \qquad (4.6)$$

However, the V component of the chrominance signal changes by 180° on successive lines and also the phase of the sub-carrier on each alternate line changes by $2 \times 89.424 = 178.848^\circ$. The predictor must acknowledge these phase shifts by careful selection of the sampling frequency f_s. If f_s is not restricted to be an integral multiple of f_L, the number of samples in one line is N where,

$$\frac{f_s}{f_L} = N + F \qquad (4.7)$$

F is the fractional part of the ratio.

For 360 degrees (one cycle) of the sub-carrier, the sample period in degrees is

$$\theta = \frac{f_{sc}}{f_s} \times 360^{\circ} \tag{4.8}$$

The sample phase shift between lines is

$$\varphi_{sa} = (1-F)\left[\frac{f_{sc}}{f_s}\right]360^{\circ} \tag{4.9}$$

For

$$\varphi_{sa} = \varphi_{sc} \tag{4.10}$$

$$F = 1-0.2484\left[\frac{f_s}{f_{sc}}\right] \tag{4.11}$$

Substituting F into equation (4.7) gives

$$f_s = \frac{(1+N)}{284} \cdot f_{sc} \tag{4.12}$$

where N, an integer, is chosen to suit the required f_s.

4.2.1. PREDICTION USING PELS ON THE SECOND PREVIOUS LINE, $f_s = 2.5f_{sc}$.

The sampling frequency f_s is selected according to the following criteria:

1.) f_s exceeds the Nyquist rate, f_N, i.e. $f_s > f_N = 2.48f_{sc}$ for the PAL signal;

2.) f_s has a simple fractional relationship with f_{sc};

3.) f_s is selected using equation (4.12), which can be expressed as

$$f_s = \left[\frac{1+N}{71 * 4}\right] f_{sc} = \frac{K}{4} \; f_{sc} \qquad (4.13)$$

where K is a system parameter. For this value of f_s to be compatible with criterion (1.) $f_s \geq 2.48 f_{sc}$, $K \geq 10$. By selecting K=10, the lowest value of $f_s = 2.5 f_{sc}$ is obtained.

We now consider how the sample on the second previous line can be used to predict the current sample for $f_s = 2.5 f_{sc}$.

Applying equations (4.11) and (4.12), F = 0.379 and N = 709. However, some scan lines contain 709 pels while others have 710 pels. This variation of one pel is due to the fact that $F \neq 0$. A sector of the distribution of pels for $f_s/f_{sc} = 2.5 f_{sc}$ is shown in Fig.(4.3). For a plain area of the picture, pels S_1, S_2, S_3,... on line 1 have similar amplitude and phase to pels S_{1421}, S_{1422}, S_{1423},... on line 3. The PAL inversion of the v component occurs on intervening lines requiring more elaborate procedures to be adopted (as described in the next section) if samples on the even lines are to be used to predict pels on the odd lines. As can be seen

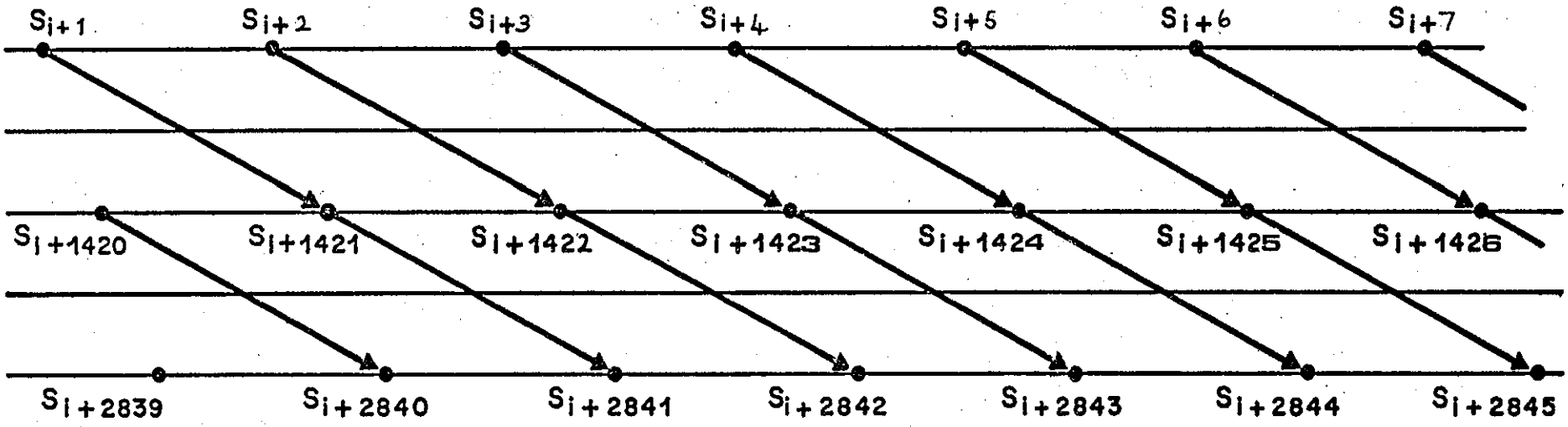

FIGURE 4.3 - Prediction using pels on the second previous line
$f_s = 2.5f_{sc}$

from the figure, to predict a picture element on the second previous line(be it odd or even) all that is required is a delay of $1420/f_s$. The predicted pel is therefore

$$\hat{S}_i = S_{i-1420} \tag{4.14}$$

The prediction distance associated with a delay of $1420/f_s$ is the same for each pel (except those at the ends of the lines) as shown by the arrows in Fig.(4.3).

A one dimensional predictor can now be incorporated to give a predicted value based on equations (3.22) and (3.23) in Chapter III,, and equation (4.14) above.

$$\hat{S}_i = AS_{i-1420} + B\,(a_1 S_{i-1} + a_2 S_{i-2} + a_3 S_{i-3}) \tag{4.15}$$

This prediction algorithm utilizes the correlation between pels delayed by 1,2,3 and 1420 sample periods, but within a prediction distance of 4 pel spacings. The system parameters A and B are usually close to 0.5, although the optimum values depend on the statistics of the signal.

A variant of this algorithm uses the adaptive strategy used in the previous chapter (section3.4)

$$S_i = AS_{i-1420} + B \begin{cases} a_1 S_{i-1} + a_2 S_{i-2} + a_3 S_{i-3} \\ \text{or} \\ LK_2 S_{i-2} \end{cases} \tag{4.16}$$

Further, the S_{i-1420} component could be omitted following an abrupt change in the picture in the vertical direction.

4.2.2. PREDICTION FROM PELS ON THE PREVIOUS LINE, $f_s = 2.5f_{sc}$.

Interline prediction similar to that used by Thompson[53] for $f_s/f_{sc} = 3$, can be achieved for $f_s = 2.5f_{sc}$. A periodic pattern of samples is produced of duration equal to two cycles of the sub-carrier, where the spacing between adjacent samples is, from equation (4.8), 144°. Seen on a transition state diagram, Fig.(4.4), the sample positions corresponding to states A,B,C,D and E are 144°, -72°, 72° and -144° and 0° relative to the U axis respectively.

Consider a vector centred on the origin of the U-V axis which rotates in an anti-clockwise direction during odd scan lines, and in a clockwise direction during even scan lines. Thus, in the case of the first scan line, which is odd, a succession of samples S_2, S_3, S_4, S_5, S_6, S_7,...S_{708}, S_{709} are generated according to the sequence of transition states B, C, D, E, A, B, C, D. For the second line, the sign of the V component is reversed and the transition diagram of Fig.(4.4b) applies. Samples S_{710}, S_{711}, S_{712}, S_{713}, S_{714}, S_{715}, S_{716},..S_{1417}, S_{1418} are produced for the transition states E,D,C,B,A,E,D..C,B. Consequently, S_4, S_3, S_2, S_6 and S_5 can be used to

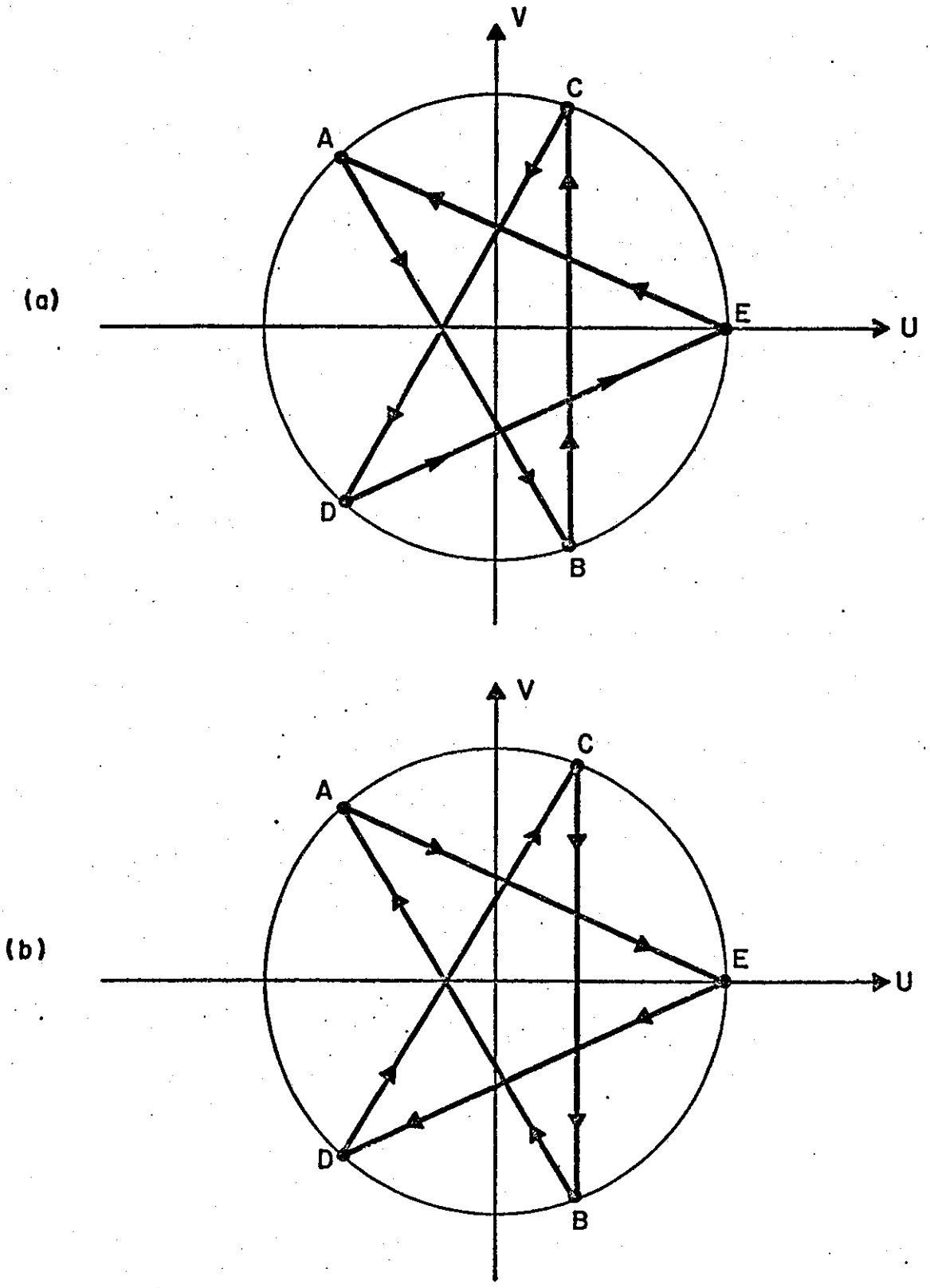

FIGURE 4.4 - Transition state diagram $f_s = 2.5f_{sc}$
a) odd lines
b) even lines

predict S_{711}, S_{712}, S_{713}, S_{714} and S_{715}, provided additional delays to 707T of 0, 2T, 4T, T and 3T, respectively, are available where T is the duration of one sample period $T = 1/f_s$. Figure (4.5) shows the initial parts of the first two scan lines for part of a picture having a constant Lu, C and φ. Both the u and v components slip by nearly 90° in subsequent scan lines and in addition the V component had its phase switched by 180° in alternate lines.

When more scan lines are considered, as shown in Fig.(4.6), the prediction pattern for the picture becomes apparent. Observe that the prediction pattern for samples associated with 'E' state transitions is a straight line in the figure, i.e., the 'prediction distance', except at line terminations, is constant and relatively small. The patterns for B and C zig-zag causing the prediction distance to vary between adjacent lines. The longest prediction distance occurs with the A and D states. These prediction patterns can be easily accommodated using the simple predictor shown by the solid lines in Fig.(4.7). Four delays of T seconds and one of 707T seconds, and a rotating switch combine to produce the predicted output $\hat{S}_{1,i}$

$$\hat{S}_{1,i} = S_{i-707-j} \qquad (4.17)$$

where j = 0,1,2,3,4 corresponding to transition states D, A, C, E, B respectively. As the switch rotates in

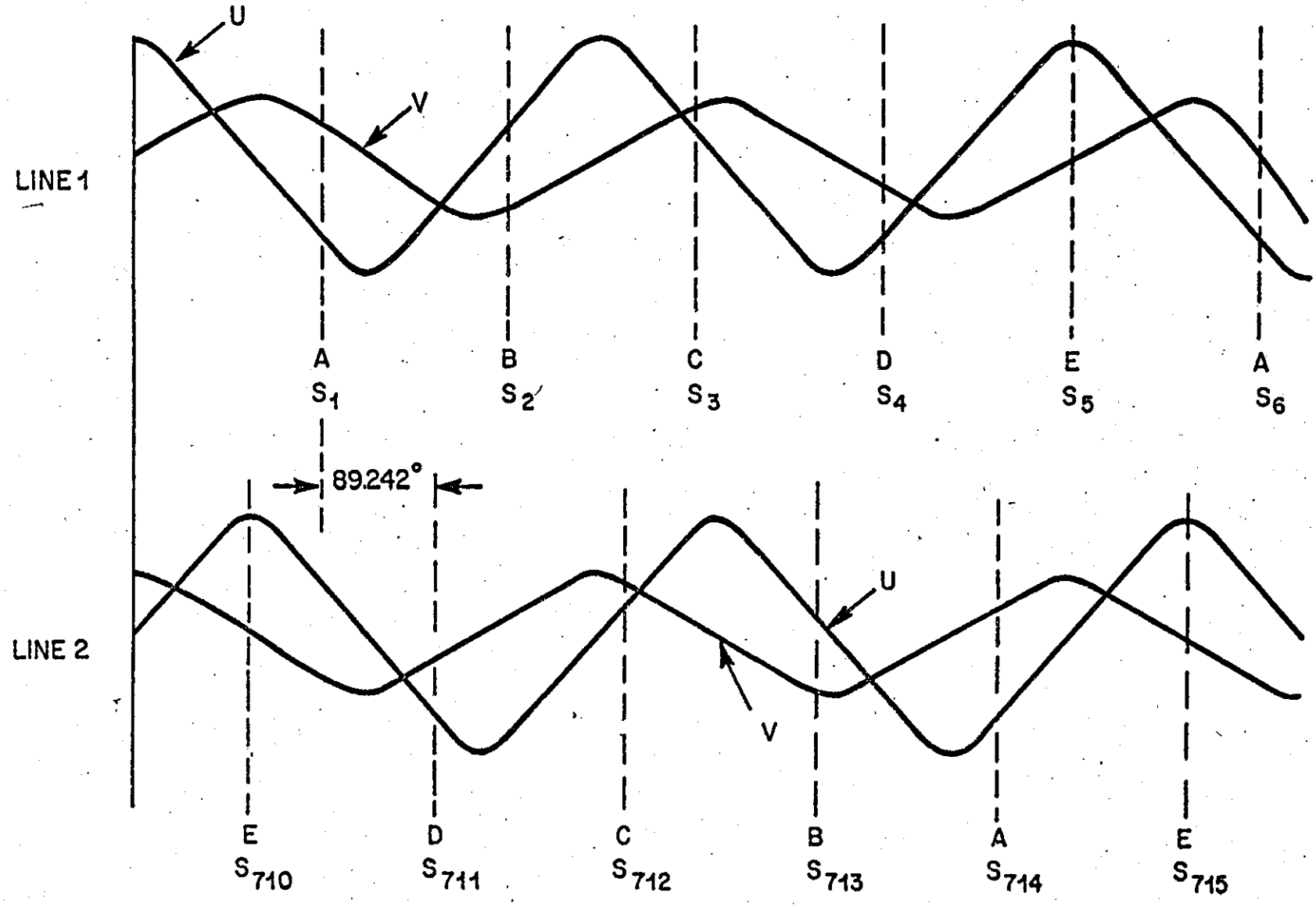

FIGURE 4.5 - Initial part of U and V component waveforms for the first two scan lines. Transition states and pel positions are marked.

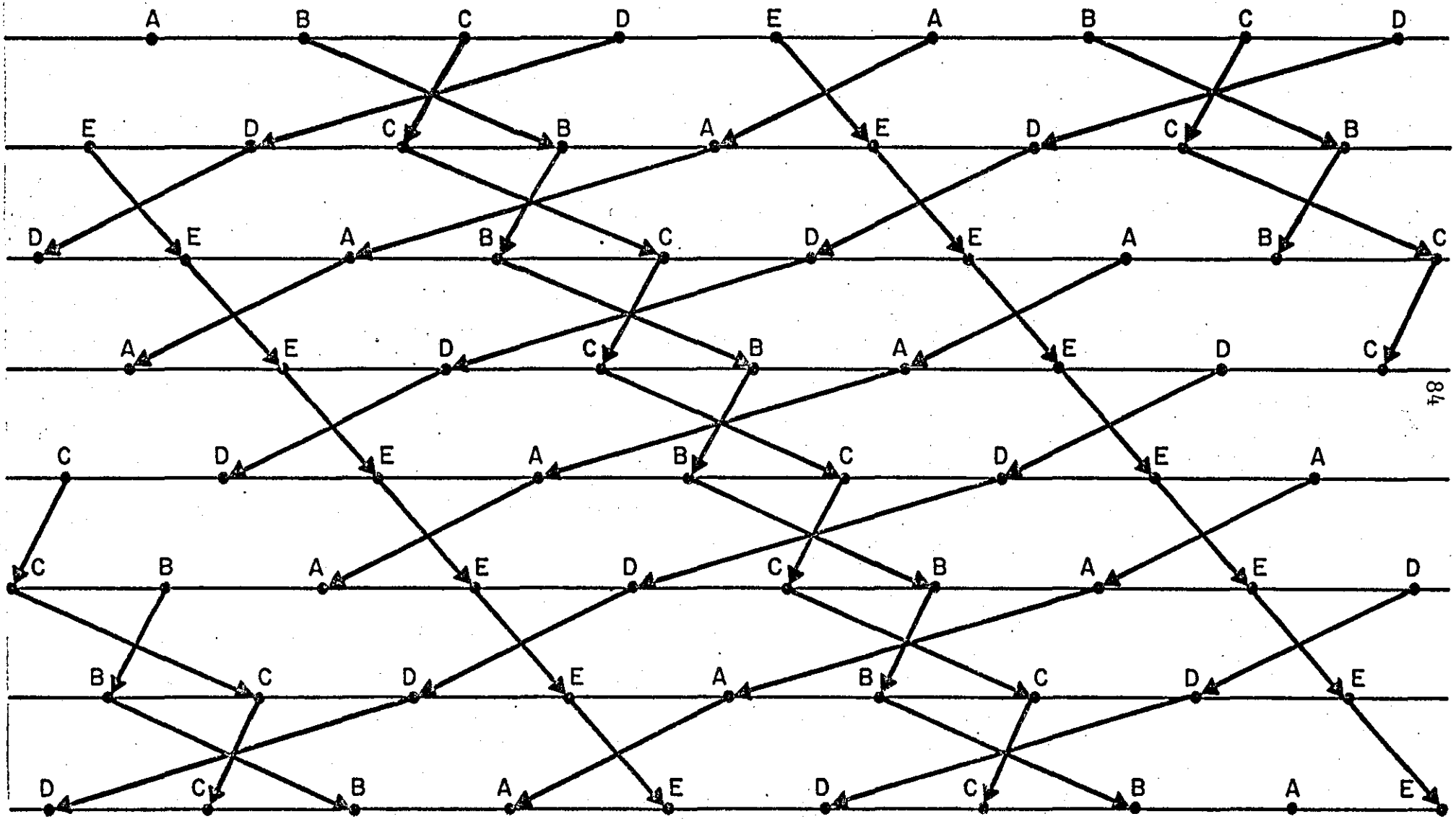

FIGURE. 4.6- Prediction Patterns for Predictions from pels on the previous line
$f_s = 2.5f_{sc}$

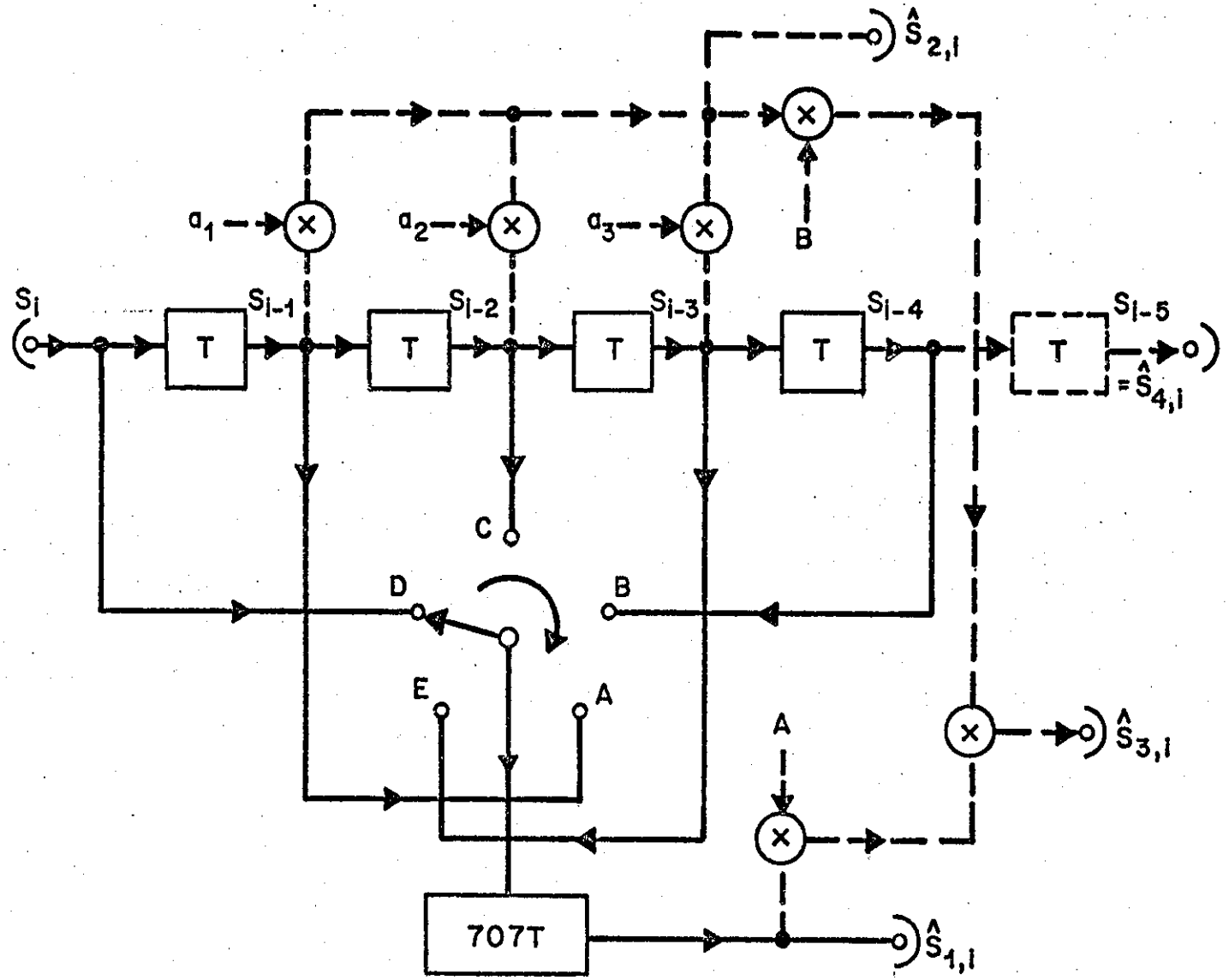

FIGURE. 4.7. Two dimensional Predictor

$f_s = 2.5 f_{sc}$

a clockwise direction the correct value of i is automatically selected irrespective of whether the input sample is on an odd or even line.

In order to generate $\hat{S}_{2,i}$ the pels S_{i-1}, S_{i-2} and S_{i-3} are available in the predictor, and hence by multiplying them by the appropriate a_1, a_2, a_3, the predicted output $\hat{S}_{2,i}$ can be formed. The coefficients a_1, a_2, a_3, are selected according to the theory given in Section (3.3). We now have available two predictor outputs based on one sample on the previous line ($\hat{S}_{1,i}$) and on three samples in the current line ($\hat{S}_{2,i}$). A better prediction can therefore be achieved by combining these two predicted samples:

$$\hat{S}_{3,i} = AS_{i-707-j} + B \sum_{n=1}^{3} a_n S_{i-n} \qquad (4.18)$$

where A and B are system parameters usually close to 0.5.

Alternatively, we can use the adaptive prediction of Section (3.4) to produce an equation similar to (4.16), where the second previous line component (S_{i-1420}) is replaced by a switched previous line component ($S_{i-707-j}$).

4.3. RESULTS.

The experiments were carried out using computer simulation. The input signal, a 100% saturated colour

bar PAL signal, was applied to the DPCM system using different types of two dimensional predictors. The 5 and 6 bit quantizers of Table (3.2)are used in the experiments. These quantizers were designed according to the average probability density function of most of the one and two dimensional predictors (see Chapteer III, Section3.6). The peak to peak signal to r.m.s. noise ratio SNR, and signal to prediction noise ratio SNR_p, are taken to be the measure of performance.

The prediction is based on samples along the same and on either the previous line or the second previous line. Table(4.1)shows the SNR results for the same quantizers and input signal used in connection with one dimensional DPCM (Chapter III), except that f_s/f_{sc} is always 2.5. The weighting of the samples along the same scan line as the sample being predicted is identical to that used in Table(3.3) Chapter III. The prediction for the sample used on either the previous or second previous line is $S_{i-707-j}$ and S_{i-1420}, respectively. By forming the predicted sample as the average of the previous and same line predictions the SNR values were obtained.

4.4. DISCUSSION.

A two dimensional predictor that avoids comb filtering by operating marginally above the Nyquist rate, is relatively simple to implement, achieves short pre-

TABLE 4.1 - SNR results of two dimensional DPCM

SAMPLE PREDICTION BASED ON		SNR_p, dB	NUMBER OF QUANTIZATION LEVELS	OVERALL SNR, dB
SAME LINE	PREVIOUS LINE			
$S_{i-1}, S_{i-2}, S_{i-3}$	S_{i-1420}	24.5	64	53.6
			32	46.6
$S_{i-1}, S_{i-2}, S_{i-3}$	$S_{i-707-j}$	25.8	64	54.0
			32	47.5
$S_{i-1}, S_{i-2}, S_{i-3}$ or S_{i-2}	S_{i-1420}	25.1	64	53.9
			32	48.0
$S_{i-1}, S_{i-2}, S_{i-3}$ or S_{i-2}	$S_{i-707-j}$	26	64	54.8
			32	48.9
S_{i-5}	S_{i-1420}	23.2	64	51.9
			32	46.3
S_{i-5}	$S_{i-707-j}$	24.6	64	53.0
			32	46.7

diction distances and SNR values that satisfy CCITT requirements, is proposed here. After deriving eqn. (4.12) and confining the sampling frequency f_s just to exceed the Nyquist rate, f_s was chosen to be $2.5f_{sc}$. By so doing, it was found that a simple predictor involving a fixed delay of $1420/f_s$ enabled predictions to be made from samples on the second previous line,(see Fig.4.3). Using the slightly more complex predictor Fig.(4.7), and phase-locked sampling, predictions were made from samples on the previous line, where the electronic switch rotating continuously in a clockwise direction automatically selected the correct delay.

The predictions based on previous lines exploit the vertical correlation in the picture. Combining the one dimensional predictors described in the previous chapter, and their adaptive variants, the correlation in the horizontal direction can also be utilized to achieve a two dimensional predictor based on 4 pels.

When the two dimensional predictor was combined with the one dimensional adaptive predictor at $f_s/f_{sc}=2.5$ the SNR increased by a further 2.5dB. From Table (4.1) it can be seen that by using the prediction based on a pel in the previous line compared to the second previous line the gain in SNR is just over a dB. It is therefore concluded that for $f_s/f_{sc} = 2.5$ the prediction,

$$\hat{S}_i = 0.5\, S_{i-707-j} + 0.5 \begin{cases} -0.618\, S_{i-1} + 0.618\, S_{i-2} \\ + S_{i-3} \\ \text{or} \\ S_{i-2} \end{cases} \qquad (4.19)$$

gave the best SNR of the systems tried. Of the two dimensional predictors discussed the easiest to implement is

$$\hat{S}_i = S_{i-5} + S_{i-1420} \qquad (4.20)$$

(see Table 4.1, row 6). The penalty in SNR is 3dB compared to the DPCM encoder using the predictor based on equation (4.19). The bit rate of 5 and 6 bit DPCM for $f_s/f_{sc} = 2.5$ is 55 and 66 Mb/s, to which supervisory, synchronization and error correcting bits may be added.

We emphasise that the theory in Section 4.2.1. is not dependent on the $f_s/f_{sc} = 2.5$ condition. Using eqn. (4.13) other f_s/f_{sc} ratios can be selected and predictors designed. Our choice of $f_s/f_{sc} = 2.5$ resulted in predictors that are relatively simple while operating above the Nyquist rate. They may have more application in studio work than in the transmission environment where the more complex DPCM codecs associated with $f_s/f_{sc} = 2.0$ may be prefered.

4.5. Note on publication.

A paper entitled 'Predictors for intra-frame encoding of PAL picture signals', in co-authorship with Dr. R. Steele, has been published in IEE Proc., Vol. 127, Pt.F, No. 3, June 1980. The paper is a version of the two dimensional DPCM described in this chapter.

CHAPTER V

BLOCK ADAPTIVE DPCM OF COLOUR TELEVISION SIGNALS.

5.1. INTRODUCTION.

The reduction of the sampling rate f_s, is one of the key factors for bandwidth compression of digitally encoded colour television signals. For example, sub-Nyquist sampling at $f_s = 2f_{sc}$ (where f_{sc} is the sub-carrier frequency) with 6 bits per sample yields 53 Mb/s [66], which is still relatively high compared with the 5.5 MHz bandwidth of analogue PAL signals. The demand for further bandwidth compression is still the main criteria in the encoding of broadcast quality colour television signals.

In the last few years the emphasis in picture coding has concentrated on the software and hardware implementation of more complex techniques. This is partially due to advances in the technology of digital processors and digital storage devices which have resulted in dramatic reductions in the size and cost of digital processing logic functions. Development of fast and massive digital memory and of digital logic has also given a good opportunity to consider more complex and sophisticated techniques. These are mostly adaptive techniques [75] such as adaptive transform coding [76-79], adaptive delta modulation [80-83] and adaptive DPCM [84-86]. These are able to follow

statistical variations in the input signal and therefore increase the encoding efficiency of these systems. For example, a DPCM system with an adaptive quantizer and adaptive predictor provides an improved performance since the adaptive quantizer step-size reduces both granular and slope-overload noise. The adaptive predictor provides a signal of smaller variance at the quantizer input than a fixed predictor.

In this chapter schemes which make use of short-term statistical properties of pictures, resulting in more efficient coding, are considered. In Section (5.2) a simple adaptive linear predictor with one coefficient is presented. The value of the weighting coefficient is updated for each block of incoming samples stored in the input buffer. Therefore, the weighting coefficient changes with a period of NT_s seconds, where T_s is the sampling period and N is the number of samples in each block.

In Section (5.3) the design procedure for a block adaptive quantizer comprising a combination of K non-uniform quantizers is studied. The proposed adaptive strategy is extended to the following systems;

i) block adaptive variable length quantizer:

ii) block adaptive fixed length quantizer:

Section (5.4) deals with the simulation results considering different sampling frequencies and various quantization schemes. Comparisons of these various

techniques, in terms of resulting bit-rate and signal to quantization noise ratios, are also presented.

5.2. ADAPTIVE PREDICTORS.

DPCM systems using a fixed optimized predictor generate a well behaved stationary differential signal if the original data is stationary. For optimal encoding of a non-stationary signal, the weighting coefficients of the predictor require changing according to the variation of the signal, thus generating stationary differential signals.

One approach is updating of the predictor coefficients a_j, using a sequentially adapting estimation technique such as the gradient search method[87]. Gibson and others[88] examined the application of Kalman filter algorithm and stochastic approximations[89,90] in updating the predictor coefficients for speech coding. However, the adaptation algorithm is complex and cannot be considered for real-time pictorial coding. In these methods the predictor coefficients are not transmitted but are extracted from the reconstructed signal at both the transmitter and receiver. This is known as backward estimation. It is clear that a prior knowledge of the statistics of the input samples (forward estimation) will produce more accurate prediction than backward estimation.

Atal and Schroeder[91] studied the performance of

such an adaptive system for speech signals. Their system can achieve very large SNR gains over PCM. However, its great complexity limits its application for real-time communications. Xydeas[92] presents a comprehensive review of various adaptive schemes used in speech coding. Due to the high sampling rate of television signals however, similar complex adaptive techniques may involve difficulties in hardware implementation.

The adaptation strategy which is described is based on the orthogonality principle of linear mean-square estimation [93]. The predictor coefficient is determined by optimizing the mean-square of the difference between the input signal values and predicted values of each block of incoming samples stored in a buffer[94].

If $S_{j+1}, S_{j+2}, \ldots S_{j+N}$ are the video sample values in the P^{th} block where $j = (P - 1)N$, the linear estimate of the sample S_m based on previous samples is denoted by the following equation;

$$\hat{S}_m = a_P \hat{\hat{S}}_m \qquad (5.1)$$

where $\hat{\hat{S}}_m$ is the unweighted estimated value and a_P is the weighting coefficient in the P^{th} block Fig. (5.1).

The error e_m between the sample S_m of the input signal and its predicted value $\hat{S}_m$ is given by

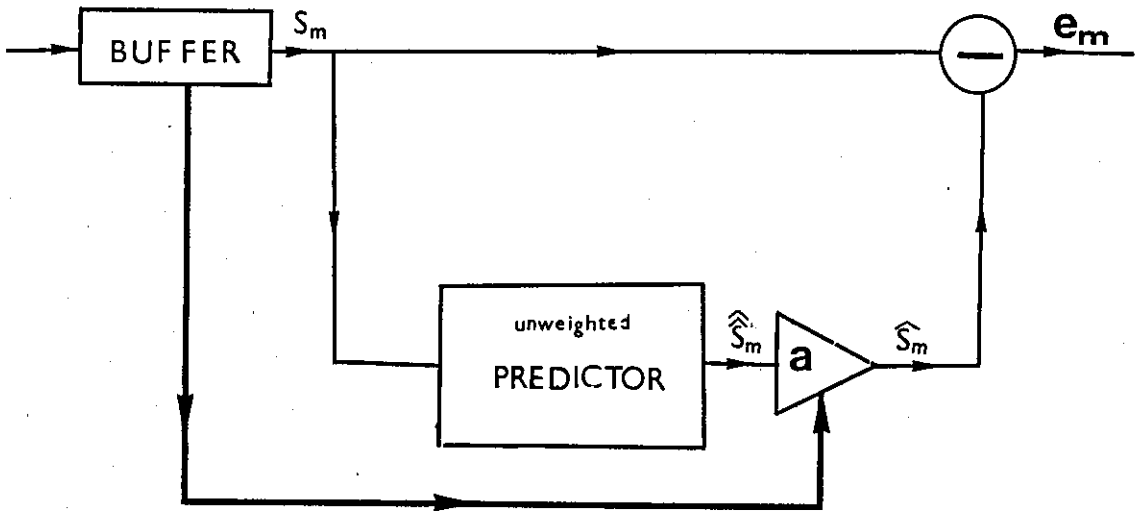

FIGURE 5.1 - Block adaptive predictor

$$e_m = S_m - \hat{S}_m \tag{5.2}$$

The mean-square error in the P^{th} block is

$$\sigma_e^2 = \frac{1}{N} \sum_{m=j+1}^{m=j+N} (S_m - \hat{S}_m)^2 \tag{5.3}$$

Given that the predictor coefficient is unchanged for each block of incoming samples, equation (5.3) can be written as

$$\sigma_e^2 = \frac{1}{N} \sum_{m=j+1}^{m=j+N} (S_m - a_P \hat{\hat{S}}_m)^2 \tag{5.4}$$

The optimum value of a_P can be found by equating the derivative of σ_e^2 with respect to a_P to zero.

$$\frac{\partial \sigma_e^2}{\partial a_P} = \frac{1}{N} \sum_{m=j+1}^{m=j+N} - 2\hat{\hat{S}}_m (S_m - a_P \hat{\hat{S}}_m) = 0 \tag{5.5}$$

Therefore,

$$a_P = \frac{\sum_{m=j+1}^{m=j+N} S_m \hat{\hat{S}}_m}{\sum_{m=j+1}^{m=j+N} (\hat{\hat{S}}_m)^2} \tag{5.6}$$

The minimum mean-square error can be obtained by substituting a_P in equation (5.4)

$$(\sigma_e^2)_{min} = \frac{1}{N} \sum_{m=j+1}^{m=j+N} S_m^2 - a_P^2 \frac{1}{N} \sum_{m=j+1}^{m=j+N} \hat{\hat{S}}_m^2 \tag{5.7}$$

To extend the algorithm in relation to the sampling frequency f_s and the sub-carrier frequency f_{sc}, two distinct cases are examined for $f_s = nf_{sc}$.

i.) when n is an integral value. In this case the best linear estimate of sample S_m should be based on the previous sample one sub-carrier period away, e.g.,

$$\hat{\hat{S}}_m = S_{m-n} \tag{5.8}$$

Substituting the above relation in equations (5.6) and (5.7) results in

$$a_P = \frac{\sum_{m=j+1}^{m=j+N} S_m S_{m-n}}{\sum_{m=j+1}^{m=j+N} (S_{m-n})^2} \tag{5.9}$$

and

$$(\sigma_e^2)_{min} = \frac{1}{N} \sum_{m=j+1}^{m=j+N} S_m^2 - a_P^2 \frac{1}{N} \sum_{m=j+1}^{m=j+N} (S_{m-n})^2 \tag{5.10}$$

$f_s = 2f_{sc}$, (n=2) (sub-Nyquist) and $f_s = 3f_{sc}$, (n=3) are two of the most important sampling rates which have been used in composite coding of PAL colour television signals [66,53].

ii.) when n is not an integral value [95]. It has been shown in Chapter III (eqn.3.26) that

$$\hat{\hat{S}}_m = - bS_{m-1} + bS_{m-2} + S_{m-3} \tag{5.11}$$

where

$$b = -(1+2 \text{ Cos } 2\pi \frac{f_{sc}}{f_s})$$

from equations (5.1) and (5.11)

$$\hat{S}_m = a_P (-bS_{m-1} + bS_{m-2} + S_{m-3}) \tag{5.12}$$

With respect to equation (5.12), equations (5.6) and (5.7) can be written as

$$a_P = \frac{\sum_{m=j+1}^{m=j+N} (S_m)(-bS_{m-1} + bS_{m-2} + S_{m-3})}{\sum_{m=j+1}^{m=j+N} (-bS_{m-1} + bS_{m-2} + S_{m-3})^2} \tag{5.13}$$

and

$$(\sigma_e^2)_{min} = \frac{1}{N} \sum_{m=j+1}^{m=j+N} S_m^2 - a_P \frac{1}{N} \sum_{m=j+1}^{m=j+N} (-bS_{m-1} + bS_{m-2} + S_{m-3})^2 \tag{5.14}$$

5.3. THE ADAPTIVE QUANTIZER.

The distribution (pdf) of the differences between the actual values of pels and the corresponding estimates is close to Laplacian, which the width of the distribution changes from block to block depending on the statistical variation of each block. Therefore, it is sensible to use various quantizing laws according to

that variation. Noll[96] examined a uniform quantizer with a step-size adaptation for speech signals. The adaptation is performed by a variable gain G_N prior to the quantizer and inverse gain G_N^{-1} prior to the predictor. G_N is proportional to the inverse of the variance of the difference signal Fig.(5.2). With this adaptive strategy Noll has increased the dynamic range of the quantizer, which is a very important factor in speech coding.

The technique which is described here is based on the selection of K possible non-uniform quantizers. The insertion of each quantizer in the DPCM loop depends on the variance of each block of incoming samples. Therefore the selection of each quantizer is controlled automatically by a set of K-1 threshold values $t_1, t_2, \ldots t_{k-1}$. The selected quantizer remains in the loop until the next decision is made (after NT_s seconds).

In applying the above technique, the following types of quantizers are considered.

i.) The block variable length quantizer (System A). As has been mentioned before, the probability density function of the differential values of pictorial material is close to Laplacian. The smaller the absolute value of a difference, the higher is its probability. To minimize the average number of bits per sample shorter code words must be assigned to the blocks containing highly probable differences and longer words to the blocks

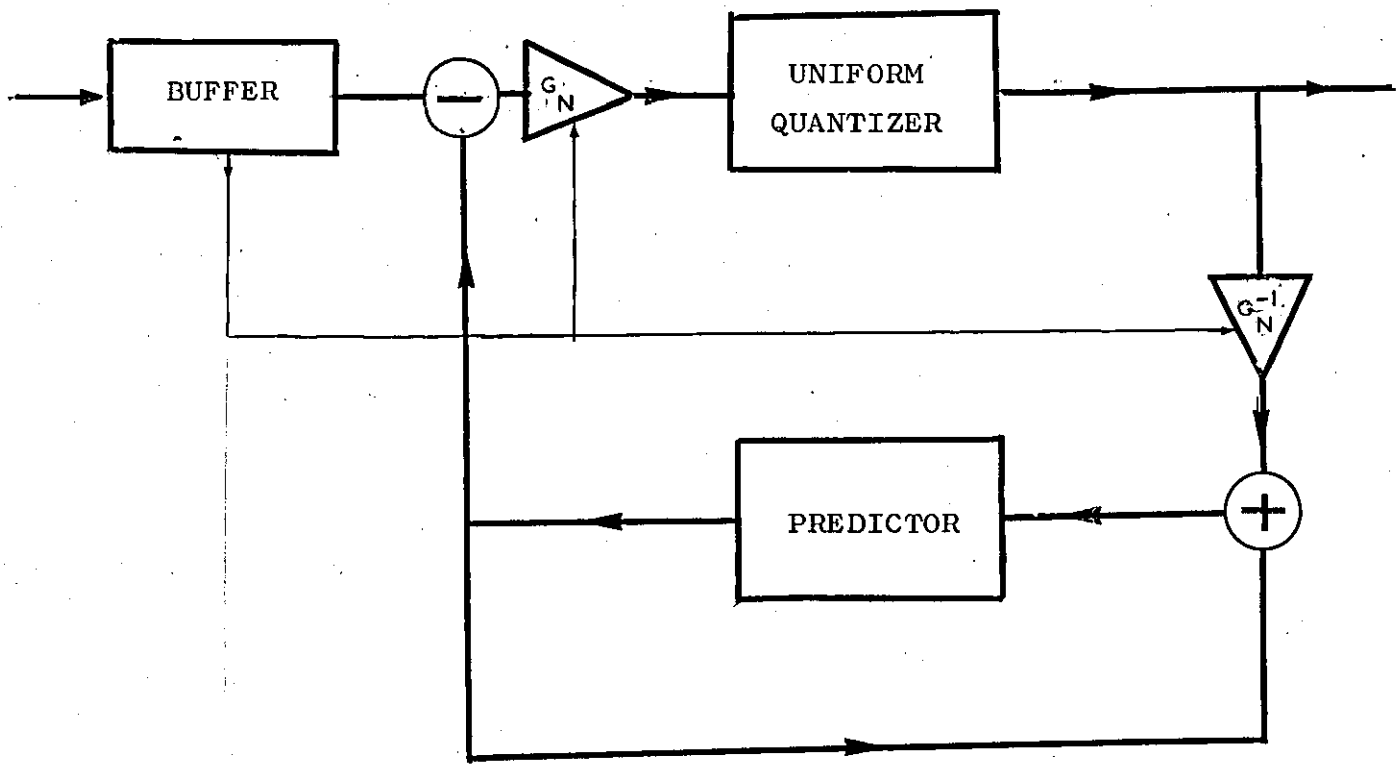

FIGURE 5.2 - Variable gain adaptive DPCM

with less probable differences.

Therefore, K non-uniform quantizers Q_1, Q_2,..Q_K are used, each having a different number of quantization levels, L_1, L_2,..L_K. The threshold values are established according to equations (5.10) and (5.14), depending on the sampling frequency. This is achieved by dividing the variances (σ_e^2) of all blocks into K categories with respect to L_1, L_2,..L_K.

Each non-uniform quantizer is designed according to the average probability density function (pdf) of the blocks which lie within its threshold values. In this way blocks with smaller values of σ_e^2 employ quantizers with smaller numbers of quantization levels.(less active picture regions).

This method produces bits at a varying rate from block to block; e.g. if P_1, P_2,..P_K represent the selection probabilities for quantizers Q_1, Q_2,..Q_K respectively, the average number of bits per sample of the system is

$$C_1 = P_1 \text{Log}_2 L_1 + P_2 \text{Log}_2 L_2 \ldots + P_K \text{Log}_2 L_K \qquad (5.15)$$

Information about the predictor coefficient and quantizer selection must be transmitted to the receiver in addition to the picture information. The average number of bits per sample required to transmit the overhead information (C_2) can be shown to be

$$C_2 = (\text{Log}_2 L_P + \text{Log}_2 K)/N \text{ bits/sample} \qquad (5.16)$$

where L_p is the number of quantization levels required to quantize the predictor coefficient. The overall bit-rate (B) is then

$$B = nf_{sc} (C_1 + C_2) \qquad (5.17)$$

ii.) The fixed length quantizer (System B).

This system is identical to System A except that here the number of quantization levels for all K possible quantizers are equal. Therefore, for smaller variances the encoder selects the quantizer with relatively more 'fine' quantization steps and vice-versa. This method increases the dynamic range of the system by reducing granular noise and slope overload distortion.

5.3.1. THE TRANSMISSION BUFFER.

In a variable length quantizer the bit-rate varies from block to block depending on the activity of the pictorial segments and the threshold values specified in the encoder. Therefore, a buffer is required to generate a constant transmission bit-rate. Because the signal must be reconstructed in proper time sequence after transmission, another buffer store must be provided at the receiver[97]. For television it may be possible to employ comparatively small stores as any loss due to overflow could be compensated by interpolation between neighbouring lines in the picture. However, reduction of the probability of overflow would require larger stores.

In the case of block variable length codec, it might be possible to use comparatively small stores by controlling the overflow. For example; suppose there is already an overflow in the P^{th} block and for the next incoming block an initial decision is made by a comparator to select the quantizer with the maximum code length (e.g. Q_1) Fig.(5.3). It would then be possible to change the comparator decision to select the quantizer with smaller code length (say Q_2) to prevent a further overflow in the incoming block.

No attempt has been made here experimentally to establish a reasonable size of the buffer. Several studies of this aspect in buffers have already been reported in the literature[98-101]

5.4. RESULTS AND DISCUSSION.

Several experimental tests were carried out using computer simulation and a 100% saturated PAL colour bar signal as input data.

The input samples were delayed by NT_s seconds (during which each block of N samples is stored in a buffer) and the predictor coefficient (a) and the variance of the difference signal (σ_e^2) calculated according to equations (5.9) and (5.10) for $f_s = nf_{sc}$ (n=2 and 3), and equations (5.13) and (5.14) for $f_s = 2.5f_{sc}$. The predictor coefficient is quantized by a 22 level non-uniform quantizer.

In the first part of the experiments the amplitude distribution of prediction error together with the peak

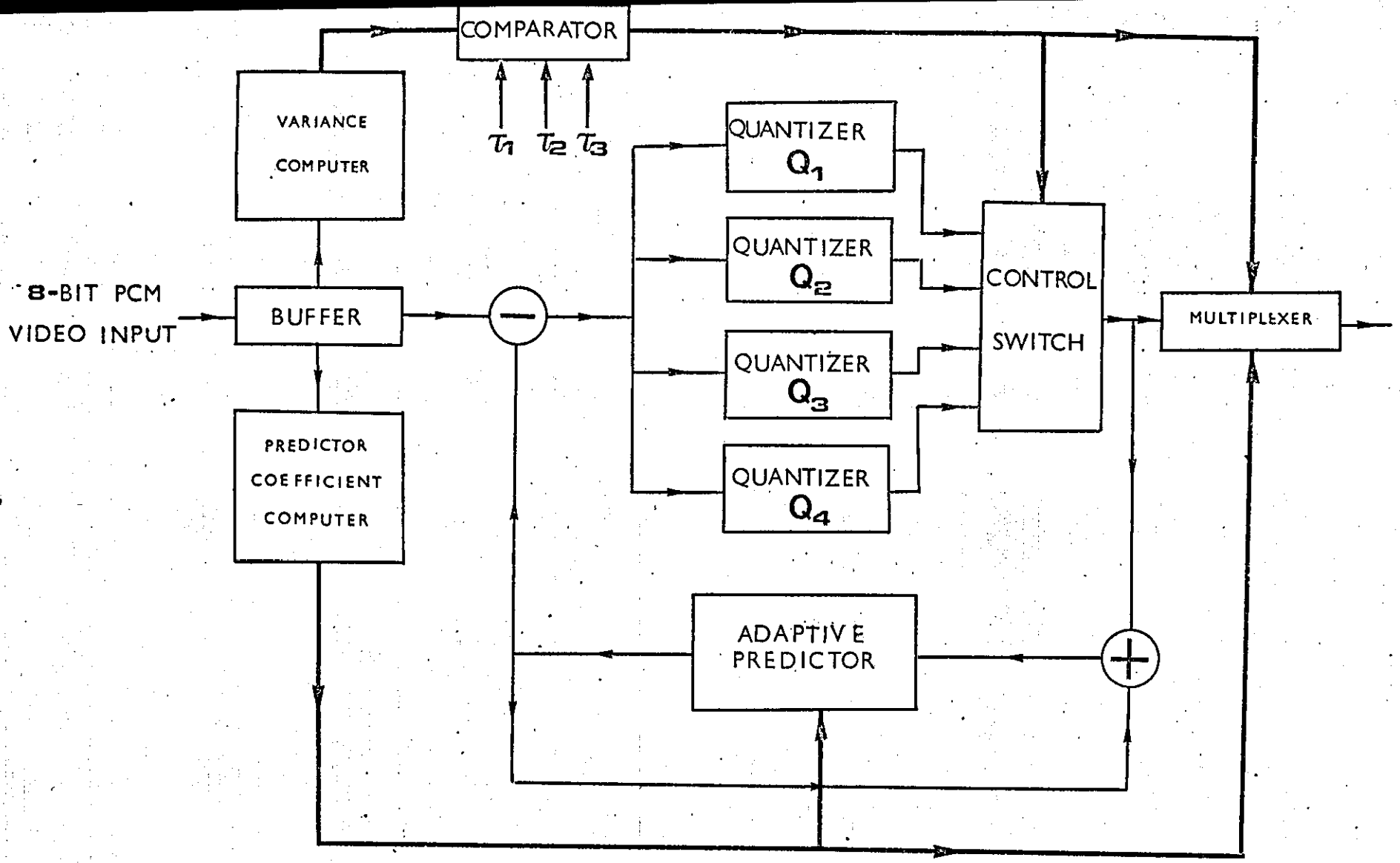

FIGURE 5.3 - Block adaptive DPCM

to peak signal to r.m.s. prediction noise ratio were measured. Figure (5.4) shows the amplitude distribution of prediction error of non-adaptive ($f_s = 3f_{sc}$) and adaptive ($f_s = 2.5f_{sc}$ and $3f_{sc}$) predictors in the absence of a quantizer. It can be deduced from this that adaptation results in the reduction of large prediction errors, which would otherwise cause severe system overload in the presence of a quantizer. Furthermore, this block adaptive prediction strategy shows the similarity and improvement in signal to prediction noise ratio for adaptive $f_s = 2.5f_{sc}$ and $f_s = 3f_{sc}$ irrespective of the selection of sampling frequency.

In the second part of the experiments a 100% saturated colour bar signal sampled at $f_s = 2f_{sc}$ and $f_s = 2.5f_{sc}$, was applied to the DPCM system of Fig.(5.3). The measure of performance was taken to be the peak to peak signal to r.m.s. quantization noise ratio SNR, and the resulting bit-rate. The results are classified into two groups and are shown in Tables (5.1) and (5.2) corresponding to the type of quantizer used.

Table (5.1) represents the results for the variable length quantizer. Four non-uniform quantizers Q_1, Q_2, Q_3,.. ..Q_4 with 4, 8, 16 and 32 levels respectively, have been used. The input range and quantized output levels of quantizers Q_1, Q_2, Q_3, Q_4 are shown in Table (5.3). In the case of the 32 level quantizer, the negative half of the quantization law was obtained by changing the sign of the first 2-16 input ranges and quantized output levels, i.e. there are 17 positive and 15 negative quantization

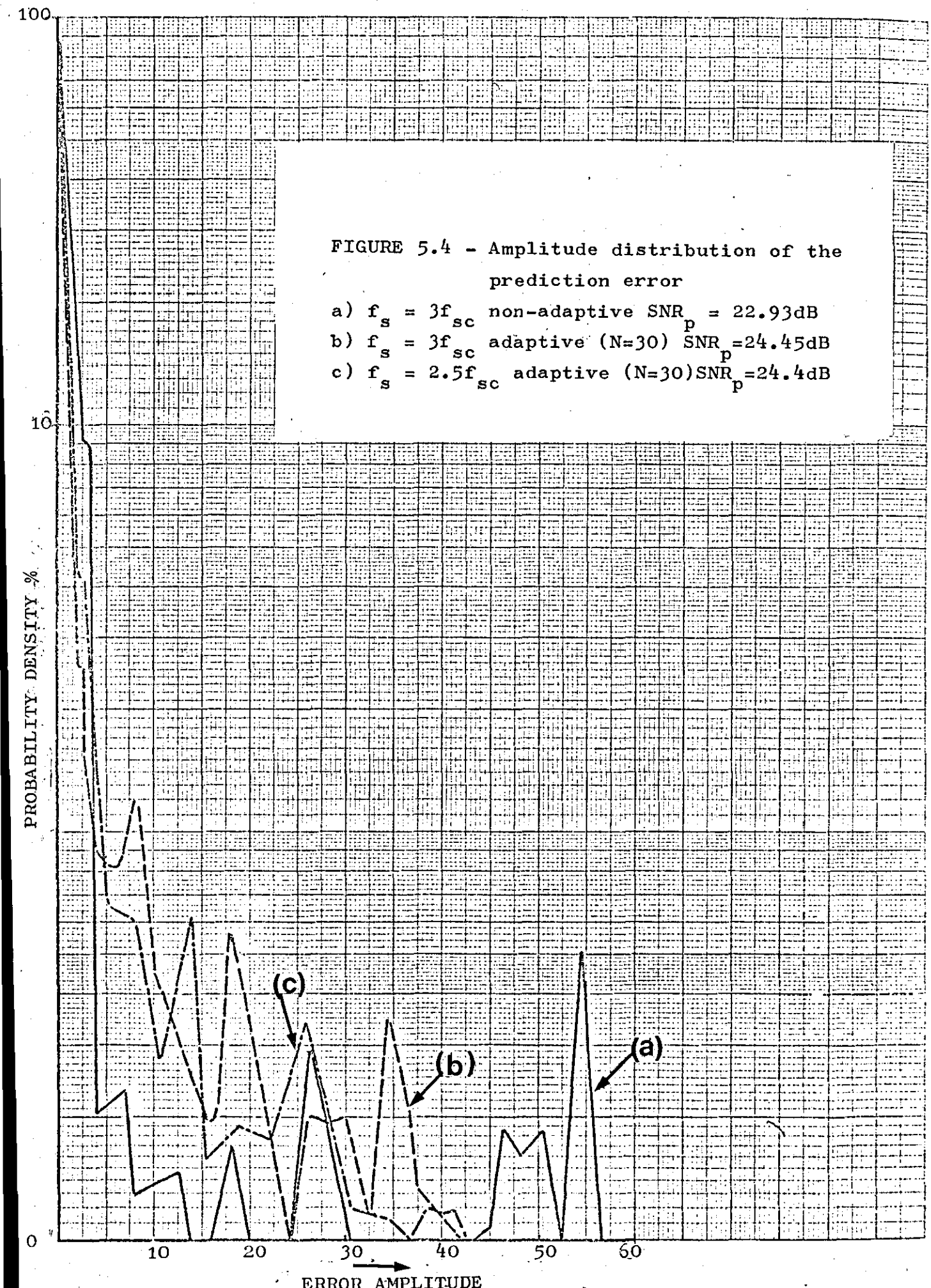

FIGURE 5.4 - Amplitude distribution of the prediction error

a) $f_s = 3f_{sc}$ non-adaptive $SNR_p = 22.93dB$

b) $f_s = 3f_{sc}$ adaptive (N=30) $SNR_p = 24.45dB$

c) $f_s = 2.5f_{sc}$ adaptive (N=30) $SNR_p = 24.4dB$

TABLE 5.1- RESULTS OF THE VARIABLE LENGTH BLOCK ADAPTIVE AND NON-ADAPTIVE DPCM

DPCM SYSTEM	SAMPLING FREQUENCY	BLOCK LENGTH	NUMBER OF QUANTIZATION LEVELS				OVERALL BIT-RATE $C=C_1+C_2$ Mb/s	SNR dB
			Q_1	Q_2	Q_3	Q_4		
BLOCK ADAPTIVE DPCM	$f_s=2f_{sc}$	15	4	8	16	32	28.34	50.02
BLOCK ADAPTIVE DPCM	$f_s=2.5f_{sc}$	15	4	8	16	32	35.9	48.8
BLOCK ADAPTIVE DPCM	$f_s=2f_{sc}$	100	4	8	16	32	41.0	47.5
BLOCK ADAPTIVE DPCM	$f_s=2.5f_{sc}$	100	4	8	16	32	52.8	46.7
NON ADAPTIVE DPCM	$f_s=2f_{sc}$	-	54				51.0	49.8
NON ADAPTIVE DPCM	$f_s=2.5f_{sc}$	-	54				63.78	48.2

TABLE 5.2- RESULTS OF THE 24 LEVEL FIXED-LENGTH BLOCK ADAPTIVE DPCM.

DPCM SYSTEM	SAMPLING FREQUENCY	BLOCK LENGTH	OVERALL BIT-RATE $C=C_1+C_2$ Mb/s	SNR dB
BLOCK ADAPTIVE DPCM	$f_s=2f_{sc}$	15	44.47	49.9
BLOCK ADAPTIVE DPCM	$f_s=2.5f_{sc}$	15	55.59	49.1
BLOCK ADAPTIVE DPCM	$f_s=2f_{sc}$	100	41.23	48.1
BLOCK ADAPTIVE DPCM	$f_s=2.5f_{sc}$	100	51.53	47.2

TABLE 5.3 - Quantizing laws for variable length quantizer

	QUANTIZER Q_1		QUANTIZER Q_2		QUANTIZER Q_3		QUANTIZER Q_4	
	INPUT	OUTPUT	INPUT	OUTPUT	INPUT	OUTPUT	INPUT	OUTPUT
17							123 to 255	130
16					35 to 255	42	107 to 122	115
15					25 to 34	30	91 to 106	98
14					17 to 24	19	75 to 90	83
13					12 to 16	14	63 to 74	66
12					8 to 11	9	53 to 62	59
11					5 to 8	6	43 to 52	46
10					2 to 4	3	35 to 42	39
9					1	1	27 to 34	30
8			4 to 255	5	0	0	21 to 26	23
7			2 to 3	2	-1	-1	15 to 20	18
6			1	1	-4 to -2	-3	10 to 14	11
5			0	0	-7 to -5	-6	7 to 9	8
4	2 to 256	2	-1	-1	-11 to -8	-9	4 to 6	5
3	1	1	-3 to -2	-2	-16 to -12	-14	2 to 3	2
2	0	0	-6 to -4	-5	-24 to -17	-20	1	1
1	-256 to -1	-1	-256 to -7	-9	-256 to -25	-30	0	0

TABLE 5.4 - Quantizing laws for fixed-length quantizer

	QUANTIZER Q_1		QUANTIZER Q_2		QUANTIZER Q_3		QUANTIZER Q_4	
	INPUT	OUTPUT	INPUT	OUTPUT	INPUT	OUTPUT	INPUT	OUTPUT
13	33 to 255	35	50 to 255	55	73 to 255	80	130 to 255	140
12	27 to 32	30	38 to 49	43	57 to 72	64	106 to 129	120
11	21 to 26	23	30 to 37	33	45 to 56	50	82 to 105	92
10	16 to 20	18	24 to 29	27	37 to 44	40	66 to 81	73
9	13 to 15	14	18 to 23	20	29 to 36	32	50 to 65	58
8	10 to 12	11	14 to 17	16	23 to 28	25	34 to 49	41
7	8 to 9	8	10 to 13	11	17 to 22	19	22 to 33	27
6	6 to 7	6	7 to 9	8	11 to 16	13	14 to 21	17
5	4 to 5	4	5 to 6	5	7 to 10	8	8 to 13	10
4	3	3	3 to 4	3	4 to 6	5	4 to 7	5
3	2	2	2	2	2 to 3	2	2 to 3	2
2	1	1	1	1	1	1	1	1
1	0	0	0	0	0	0	0	0

levels.

Table (5.2) shows the results for fixed length quantizer with four possible non-uniform quantizers each having 24 quantization levels. The positive half of the input range and quantized output levels are shown in Table (5.4).

The quantizers of Tables (5.3) and (5.4) are designed according to the discussion in Section (5.3), for the sampling frequency of $f_s = 2f_{sc}$ and a block length of 15 samples (N=15). For the purpose of comparison, the results in the case of N=100 are shown in Tables (5.1) and (5.2) using the quantizers of Tables (5.3) and (5.4) respectively. The results of non-adaptive DPCM using a 54 level non-uniform quantizer are also included in Table (5.1).

Optimization of the system requires careful consideration of all the factors involved in the adaptation strategy. The most important of these are threshold values, block lengths and the number of quantizers. The interaction of these factors make the overall optimization of the system a considerable task.

The threshold values play an important role in the systems performance in terms of SNR and resulting bit-rate, especially in the case of variable length quantizer. For example; if the comparator in Fig.(5.3) selects the 4 or the 16 level quantizer instead of the 8 level quantizer (as a result of a bad decision), this would cause severe system overload or unnecessarily increase the bit-rate for the incoming block of data.

As mentioned earlier, threshold values were determined by dividing whole blocks of data into four categories with regards to the number of quantization levels used, and according to their distribution (pdf) in which they are distinguished by their variances. Since each quantizer is selected according to the variance (σ_e^2), and, to a somewhat lesser degree, to the shape of the distribution of each block of samples, the accuracy of the decision reduces as the number of quantizers increases

Another important parameter which affects the system performance is the block length (N), as the number of quantizers depends on this also. For large block lengths the probability of each block covering a relatively quiet area of the picture reduces considerably. As an example; in the case of N=100 the selection probability of the 4 level quantizer reaches zero and it is therefore seldom selected.

For variable length coding it has been established that the block length of 15 samples is the optimum length for colour bar signals, given that four non-uniform quantizers with 4, 8, 16 and 32 levels with threshold values of 5, 28, and 270 are used. For example; as the block length decreases from N=100 to its optimum length (N=15), the overall bit-rate (including overhead information) drops from 41.0 to 28.3 Mb/s (Table 5.1). A further reduction in the block length causes an overall increase in the bit-rate due to the overhead information

(equation 5.16). In the case of the fixed length quantizer, it is found that for a sampling frequency of $f_s = 2f_{sc}$, block length of N=15 and threshold values of 24, 65 and 960, quantizers with 24 levels are required to obtain a similar SNR. There is thus an increase of 16 Mb/s in the bit-rate compared with that of the variable length quantizer. At the same time, however, it does not require a buffer prior to the transmission channel. Furthermore, non-adaptive DPCM with a comparable SNR requires a 52 level quantizer which yields a bit-rate at 51.0 Mb/s for $f_s = 2f_{sc}$ and 63.78 Mb/s for $f_s = 2.5f_{sc}$.

Thus, the application of this block adaptive strategy highlights the fact that substantial bit-rate reduction can be obtained compared with the corresponding non-adaptive schemes (see Tables (5.1) and (5.2)). As a result the variable length quantizer at both $f_s=2f_{sc}$ and $f_s = 2.5f_{sc}$ can produce a 44 percent reduction in the bit-rate without any loss in SNR.

Finally, it is important to point out that with the variable length quantizer a minimum bit-rate of 28.34 Mb/s is achieved at $f_s = 2f_{sc}$ (sub-Nyquist rate) with some added complexity in combing out the aliased components (see Appendix B), yielding a 50dB SNR. This clearly shows the possibility of transmitting a broadcast quality colour television signal at the proposed European 34.368 Mb/s hierarchical level.

5.5. Note on publications.

A first paper entitled 'Block Adaptive Prediction of Colour Television Signals' has been published in Electronics Letters of IEE, Vol.16, No.6, March 1980. This paper is an abridged version of the block adaptive predictor described in Section (5.2).

A second full length paper entitled 'Bandwidth Compression of Digital Colour Television Signals Using Block Adaptive DPCM' has been accepted for publication and is to be published in the October issue of IEE Proc. Pt.F. This paper is a brief version of Chapter VI.

CHAPTER VI

BLOCK ADAPTIVE DPCM OF SECAM SIGNALS

6.1. INTRODUCTION.

Differential pulse code modulation is one of the most efficient ways of coding composite PAL or NTSC signals. Block adaptive DPCM has been discussed in detail in the previous chapter for composite PAL colour signals, and it should be emphasised that a similar algorithm is equally applicable to the NTSC system. One of the problems which exists in efficient predictive coding of composite SECAM signals (the principle of which system has been discussed in Chapter II), is the frequency variation of the sub-carrier.

In the SECAM system the two chrominance signals ($D_R = -1.9(R-Y)$ and $D_B = 1.5(B-Y)$) are frequency modulated and sent in line sequence. The modulated chrominance signals are then passed through an r.f. pre-emphasis filter and added to the luminance component.
The frequency of the chrominance sub-carrier has the following nominal value;

on lines modulated by signal D_R

$$f_{SR} = 282 f_L = 4.40625 \text{ MHz} \qquad (6.1)$$

on lines modulated by signal D_B

$$f_{SB} = 272 f_L = 4.250 \text{ MHz} \qquad (6.2)$$

where f_L is the line frequency.

The maximum frequency deviation, including the effects of video pre-emphasis, is equal to the following values;

for D_R +350 and -500 KHz

for D_B +500 and -350 KHz

In SECAM the frequency of the sub-carrier changes according to hue and saturation. There is therefore no advantage in relating the sampling frequency to the sub-carrier frequency. Devereux has stated that, for minimum impairment, the sampling frequency f_s for SECAM should be an integral multiple of line frequency f_L [102].

6.2. LINEAR PREDICTION OF SECAM.

Due to the amplitude and frequency variations of the sub-carrier, an accurate prediction of composite SECAM signals cannot be easily achieved.

For example, the simplest method is to sample the SECAM signal at $f_s = 3f_{oc}$ (f_{oc} being the centre frequency of the sub-carrier) using third previous sample prediction. This technique may give satisfactory results but the prediction is not very accurate when the sub-carrier frequency deviates. Therefore, to increase the accuracy of

the prediction, a more sophisticated method should be employed.

Design of an efficient prediction scheme requires a prior knowledge of the statistical variations of the signal. One example of the application of such statistics is the block adaptive prediction technique which has been studied in the previous chapter in the case of PAL colour television signals[94,103]. This technique, however, can be applied to the SECAM system providing a specific prediction algorithm is employed.

In this chapter various adaptive and non-adaptive prediction schemes are considered.

6.3. DESCRIPTION OF THE PREDICTION SCHEMES.

Consider the composite SECAM signal to be sampled at a rate f_s into a sequence S_m, S_{m-1}, S_{m-2}.... As previously discussed,(see Chapter III), for a uniformly coloured area, the sample S_m can be estimated from the three previous samples according to the following relationship;

$$\hat{\hat{S}}_m = (-bS_{m-1} + bS_{m-2} + S_{m-3}) \qquad (6.3)$$

where $\hat{\hat{S}}_m$ is defined as the unweighted estimated value and

$$b = -(1+2 \text{ Cos } 2\pi \frac{f_o}{f_s}) \qquad (6.4)$$

f_o is the sub-carrier frequency for the specific coloured area.

As can be deduced from the above equations, the value of b changes according to the variation of sub-carrier frequency. The linear prediction of sample S_m can be shown to be;

$$\hat{S}_m = a(-bS_{m-1} + bS_{m-2} + S_{m-3}) \qquad (6.5)$$

where 'a' is the overall weighting coefficient (see Fig. 6.1).

With regard to the above prediction, the following adaptive and non-adaptive prediction algorithms are described.

6.3.1. BLOCK ADAPTIVE PREDICTION BASED ON OPTIMIZATION OF 'b'.

In this scheme the data is first divided into blocks, each containing N samples. For a fixed value of a=1, the coefficients -b and b change with a period of NT_S second (T_S is the sampling period) corresponding to the statistical behavior of each block of incoming samples stored in the input buffer. Suppose S_{j+1}, S_{j+2}....S_{j+N} are the video sample values of the P^{th} block stored where j=(P-1)N; the error between the sample S_m of the input signal and its predicted value $\hat{S}_m$ can be written as

$$e_m = S_m - \hat{S}_m \qquad (6.6)$$

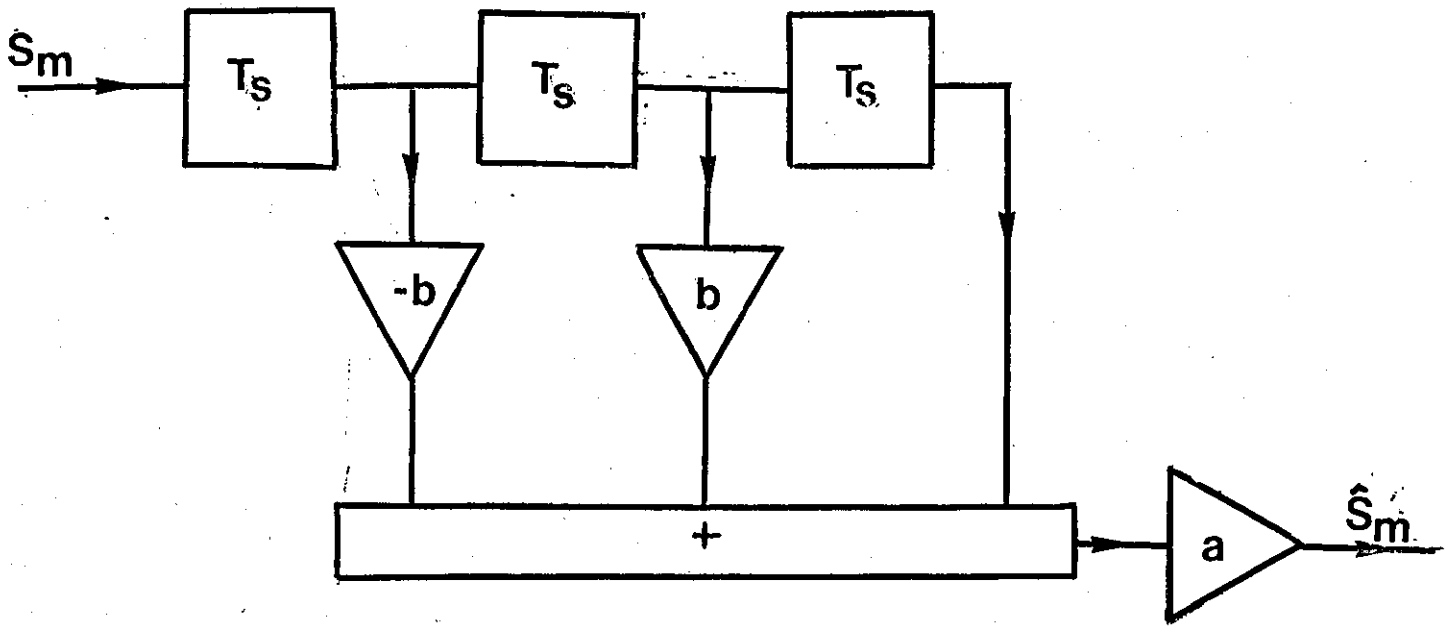

FIG. 6.1 - Predictor

or

$$e_m = S_m - S_{m-3} - b(-S_{m-1} + S_{m-2}) \qquad (6.7)$$

The mean-square prediction error in the P^{th} block is

$$\sigma_e^2 = \frac{1}{N} \sum_{m=j+1}^{m=j+N} \left[(S_m - S_{m-3} - b(S_{m-2} - S_{m-1})\right]^2 \qquad (6.8)$$

The optimum value of 'b' can be obtained by equating the derivative of the above equation to zero.,

$$\frac{\partial \sigma e^2}{\partial b} = 1/N \sum_{m=j+1}^{m=j+N} -2(S_{m-2} - S_{m-1})\left[S_m - S_{m-3} - b\right.$$

$$\left.(S_{m-2} - S_{m-1})\right] = 0 \qquad (6.9)$$

Therefore, the optimum value of 'b' is

$$b_{opt} = \frac{\sum_{m=j+1}^{m=j+N} (S_{m-2} - S_{m-1})(S_m - S_{m-3})}{\sum_{m=j+1}^{m=j+N} (S_{m-2} - S_{m-1})^2} \qquad (6.10)$$

6.3.2. BLOCK ADAPTIVE PREDICTION BASED ON OPTIMIZATION OF 'a'.

Given that the coefficients '-b' and 'b' are unchanged, the optimum value of 'a' has been previously obtained in the case of PAL colour signals (see Chapter V, eqn.5.13) and can be written as

$$a_{opt} = \frac{\sum_{m=j+1}^{m=j+N} S_m(-bS_{m-1} + bS_{m-2} + S_{m-3})}{\sum_{m=j+1}^{m=j+N} (-bS_{m-1} + bS_{m-2} + S_{m-3})^2} \qquad (6.11)$$

where

$$b = -(1+2 \text{ Cos } 2\pi f_{sc}/f_s)$$

where f_{sc} is the sub-carrier frequency of the PAL colour signal.

This technique has been studied here under the following conditions:

i.) fixing the value of 'b' according to the centre frequency f_{oc} of the SECAM sub-carrier

$$b = -(1+2 \text{ Cos } 2\pi f_{oc}/f_s) \qquad (6.12)$$

ii.) fixing the value of 'b' in line sequence (switched predictor) on lines modulated by D_R

$$b_R = -(1+2 \text{ Cos } 2\pi f_{SR}/f_s) \qquad (6.13)$$

on lines modulated by D_B

$$b_R = -(1+2 \text{ Cos } 2\pi f_{SB}/f_s) \qquad (6.14)$$

where f_{SR} and f_{SB} are the mean sub-carrier frequencies on lines D_R and D_B respectively.

The switched predictor, which is controlled sequentially by line frequency, is shown in Fig.(6.2).

6.3.3. NON-ADAPTIVE PREDICTION.

For the purpose of comparison fixed predictors are also considered here. In this system the overall weighting coefficient 'a' is fixed at its optimum value and 'b' is obtained according to equation (6.12) for the standard predictor, and equations (6.13) and (6.14) for the switched predictor.

6.4. SIMULATION AND EXPERIMENTAL RESULTS.

In DPCM encoding systems, an estimate of each input sample is subtracted from the actual input sample. The difference is then quantized, binary encoded and transmitted.

The DPCM system using block adaptive and fixed predictors described in the previous section has been simulated on a digital computer. The input signal was a 100 percent saturated SECAM colour bar signal Fig.(6.3). With respect to the earlier discussion, the sampling frequency has been fixed at integral multiples of line frequency $f_s = 816 f_L = 12.75$ MHz.

The input range and quantized output levels for a 32 level non-uniform quantizer used in the simulation are shown in Table(6.1). In the case of block adaptive prediction, each block of 17 samples (N=17) is buffered and the short-term optimum coefficient for the segment calculated.

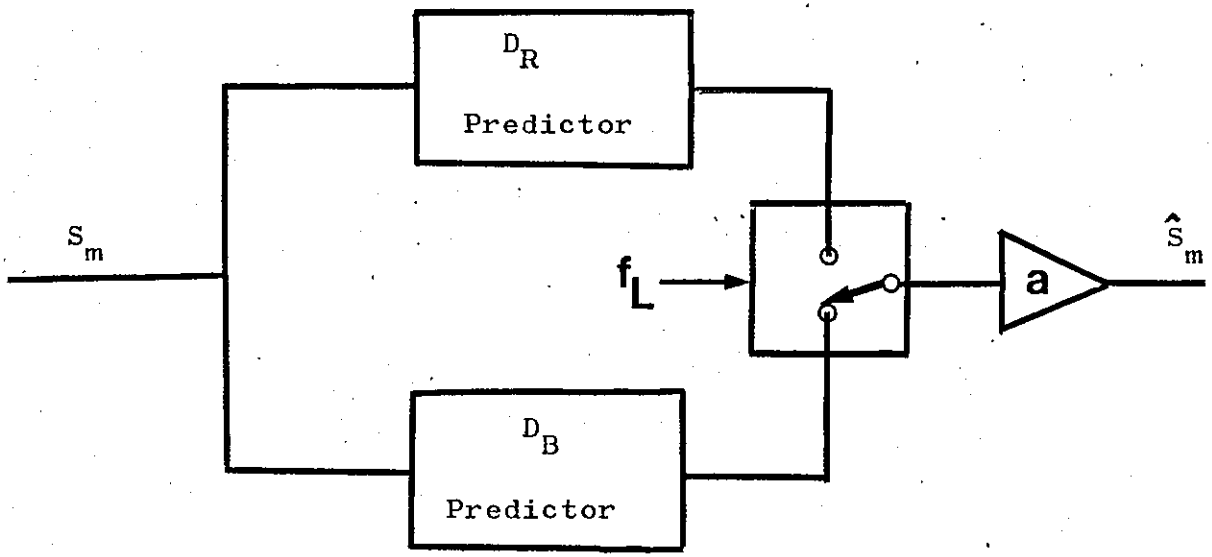

FIG.6.2 Switched Predictor.

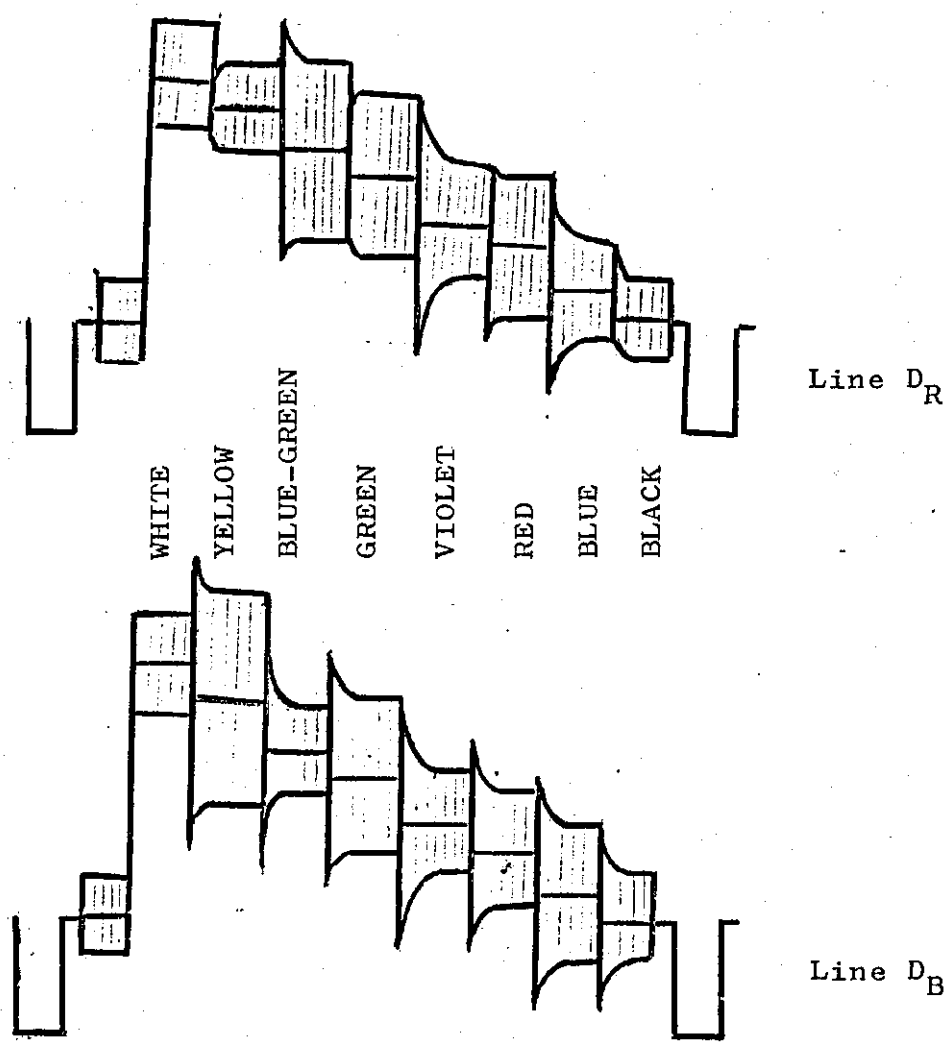

FIG.6.3 Composite Signal for 75 % ampl., 100% saturated colour bar pattern.

The results for various DPCM systems using adaptive and non-adaptive DPCM are shown in Table (6.2). In the results the signal to quantizing noise ratio SNR and signal to prediction noise ratio SNR_p (in the absence of the quantizer) have been used as the criteria for performance and comparison.

6.5. DISCUSSION AND CONCLUSIONS.

Comparisons of various adaptive and non-adaptive DPCM systems for digital encoding of the SECAM colour bar signal indicate that the block adaptive prediction technique based on optimization of 'b' eqn.(6.10), can produce the highest SNR. This verifies the effectiveness of this adaptation strategy where the predictor can adapt itself to the sub-carrier frequency variation.

The other adaptive technique which has been used in the previous chapter for PAL[103] is based on optimization of 'a' and has been considered here for the purpose of comparison. As can be deduced from Table(6.1), the performance of this system in terms of SNR and SNR_p is inferior to the former technique. To extend this technique a switched predictor has been used to reduce the effect of frequency variations on the predictor with the fixed value of 'b'. However, the improvement in SNR is negligible.

In this chapter adaptive prediction, where the adaptation was based on optimizing the predictor parameter 'a' or 'b' have been studied. A further possible technique is to

TABLE 6.1 - Quantizing Characteristic.

No.	INPUT	OUTPUT
17	133 to 255	140
16	117 to 132	124
15	101 to 116	108
14	89 to 100	93
13	73 to 88	77
12	61 to 72	66
11	49 to 60	54
10	37 to 48	43
9	27 to 36	32
8	19 to 26	22
7	13 to 18	15
6	8 to 12	10
5	5 to 7	6
4	3 to 4	3
3	2	2
2	1	1
1	0	0

The negative half of the quantization law is given by changing the sign of the input range and quantized output levels nos. 2-16.

TABLE 6.2 - SNR results of 5 bits adaptive and non-adaptive DPCM systems.

DPCM System	Prediction Parametres		SNR_p dB	SNR dB
	b	a		
Block Adaptive Predictor	variable	1	29.82	52.33
Block Adaptive Predictor	variable	0.97	29.85	52.44
Block Adaptive Predictor	0.06	variable	28.03	50.63
Block Adaptive Switched Predictor	c_R=0.13 c_B=0.0	variable	28.16	51.02
Non-Adaptive Switched Predictor	c_R=0.13 c_B=0.0	fixed	27.75	48.28
Non-Adaptive Predictor	0.06	fixed	27.61	47.86

optimize both parameters 'a' and 'b' for each block of incoming samples one at a time. For example, for a=1, the optimum 'b' can be calculated according to eqn.(6.10), and consequently for this value of 'b' the optimum 'a' is obtained according to eqn.(6.11). Although with this method the overall optimization can be obtained, it will double the computation time within one block period and will probably inflict too great a hardware penalty.

CHAPTER VII

RECAPITULATION

7.1. INTRODUCTION.

As is shown throughout this thesis, the objective of the research reported here is the application of differential pulse code modulation and related techniques to the encoding of broadcast quality colour television signals in order to reduce the high bit-rate necessary for the transmission of high quality digital television signals. Two approaches are considered;

i.) reduction of sampling frequency and

ii.) the development of novel adaptive techniques to improve encoding performance.

Initially a simple approach was taken and the possibility of reducing the sampling frequency by developing a prediction algorithm with little added complexity considered. As a result, a simple predictor having three coefficients was developed for DPCM encoding of composite PAL or NTSC colour television which can operate at any desired sampling frequency. Predictions based on previous pels along the line were derived for the case $f_s/f_{sc} = 2.5$. To improve the results, a simple adaptive strategy was then employed to handle rapid luminance changes. As a result, this simple adaptive strategy showed a significant improvement in encoding performance.

Next, two dimensional predictions were considered, and a sampling frequency of 2.5 times the sub-carrier

frequency was established for this purpose. Two dimensional predictors which utilize the correlation of pels between lines as well were designed and used in DPCM encoding of PAL colour bar signals. Two dimensional DPCM showed a significant improvement in encoding performance compared with one dimensional DPCM. Up to this point attention was directed to the design of predictors which were generally non-adaptive, or if adaptive, the adaptation algorithm was simple to implement. However, the bit-rate for 5 and 6 bit DPCM for $f_s/f_{sc} = 2.5$ is 55 and 66 Mb/s which is still relatively high compared with 5.5MHz. For broadcasting the obvious goal is to reduce the bit-rate of the video signal to somewhat less than 34.368 Mb/s[104,105] without significant loss of picture quality, such that a complete television signal can be accommodated within the 34.368 Mb/s multiplex level. For this reason, it was soon realized that a further substantial bit-rate reduction could not be realized by using simple classical schemes. Therefore, more complex techniques such as adaptive schemes which the statistical variations can be taken into account were next considered. As adaptive schemes can increase the complexity of a DPCM encoder considerably, simplified encoding algorithms were sought.

In the first stage a novel block adaptive prediction scheme for colour television signals was developed. In this scheme the input data is partitioned into blocks of

N samples and a criterion based on optimization of mean-square prediction error within each block of incoming data chosen. Next the quantization process was considered. To take advantage of some of the mathematics developed for adaptive predictors, two block adaptive quantization strategies were established. One operated on a fixed length basis to improve the SNR performance of the system, while the other made use of variable length code to encode the quiet region of the picture with smaller code length and vice-versa. As a result, the aim of reducing the bit-rate of PAL colour bar signals below the hierarchical level of 34 Mb/s was achieved. Since the adaptation algorithm which was employed in the case of PAL signals can also be applied to NTSC signals, the idea of employing a similar strategy for digital coding of composite SECAM signals was then considered.

To deal with frequency variation of the SECAM sub-carrier, a new algorithm was developed which resulted in a significant improvement in system performance compared with other relevant techniques.

In the following section of this chapter the main results of the investigations are reviewed.

7.2. NON-INTEGER SAMPLING TO SUB-CARRIER FREQUENCY RATIOS

In Chapter III a predictor based on three previous pels along a scan line was examined for DPCM encoding

of composite PAL signals. The predictor coefficients were described in terms of the ratio of sampling frequency f_s to colour sub-carrier frequency f_{sc}. To evaluate the effectiveness of the method, a ratio of $f_s/f_{sc} = 2.5$ was considered (giving 5 samples in 2 cycles of the sub-carrier). The predictor in the encoder and decoder made their predictions on the three previous samples along the scan line by means of computer simulation for colour bar signals. The performance was inferior to third previous sample prediction ($f_s/f_{sc}=3$), degradation arising when the colour change in the colour bar signal causes jumps in the luminance level. In this situation the predictor having $f_s/f_{sc} = 2.5$ with coefficients a_1, a_2 ($a_1 = -0.618$) causes very poor predictions ($a_1 = 0$ for $f_s/f_{sc} = 3$) The predictions were improved by using a simple adaptive algorithm which uses previous (or second previous) sample prediction for three consequtive pels when there is a rapid change in the luminance level. The results for the predictors using the previous pel or pels along the same scan line showed that the SNR for $f_s/f_{sc} = 2.5$ is a close approximation to that for $f_s/f_{sc} = 3.0$ and that the adaptive version produced a small improvement in SNR compared to the non-adaptive case. The adaptive strategy is more effective in combating abrupt changes in luminance rather than in chrominance (particularly sharp hue variations).

Fifth previous sample prediction ($f_s/f_{sc} = 2.5$ giving 5 samples in two cycles of the sub-carrier) was also

examined and showed an SNR which is 3dB inferior to that of the predictor employing three previous pels.

7.3. PREDICTORS FOR INTRAFRAME ENCODING OF PAL PICTURE SIGNALS.

Following the one dimensional prediction of Chapter III, the concept of two dimensional prediction was introduced in Chapter IV. $f_s/f_{sc} = 2.5$ was originally established for the purpose of two dimensional prediction, the reason for this being to compensate for sample phase shift in relation to sub-carrier phase shift in successive lines. The resulting distribution of pels showed that for a plain coloured area of the picture, the prediction distance associated with a delay of $1420/f_s$ (pels on the second previous line) is the same for each pel. Furthermore, to exploit the vertical correlation more efficiently, the possibility of previous line prediction was studied. For PAL signals and $f_s = 2.5f_{sc}$, a cyclic five state prediction algorithm was developed to deal with the V-axis switch.

With the aid of computer simulation, two dimensional DPCM using a non-uniform quantizer was examined. The prediction was based on samples on the same and on either the previous or the second previous line. By forming the prediction as the average of the previous and same line predictions SNR values were obtained. As a result, two dimensional DPCM using the predictions based on a pel in the

previous line gained just over 1dB SNR advantage compared to that for the second previous line. Computer simulation results also indicate that a further 2.5dB increase in SNR can be obtained when the two dimensional predictor is combined with the one dimensional adaptive predictor.

It is therefore concluded that for $f_s = 2.5f_{sc}$, this combined strategy gives the best SNR of the system. Also, the easiest two dimensional DPCM which uses the fifth previous pel along the line was examined. However, this system showed worse results when compared to the other two dimensional systems examined in this thesis.

It is emphasised that the motivation behind this work is to develop a two dimensional prediction technique which can operate at a sampling rate above the Nyquist rate but well below $f_s = 3f_{sc}$. The result is a 13.3 MHz reduction in the bit-rate compared with that for $f_s = 3f_{sc}$ for 6 bit DPCM. However, at the same time there is the disadvantage of a greater prediction distance in some cases.

7.4. BANDWIDTH COMPRESSION OF DIGITAL COLOUR TELEVISION SIGNALS.

After considering all possibilities in earlier investigations for reduction of the bit-rate, it was concluded that a substantial bit-rate reduction is not possible by reducing the sampling frequency or developing more complex

non-adaptive techniques. As a result, the concept of a new adaptive DPCM encoder was introduced in Chapter IV. In this adaptive scheme, the pictorial data is first divided into small blocks and then the input samples are delayed by one block period, during which time the system can calculate new parameters according to the statistical variation of each block of incoming samples stored in the input buffer. The new parameters are then transmitted to the receiver (in addition to the main information) prior to the corresponding block of data.

A generalised adaptation algorithm for either PAL or NTSC signals which can operate at any desirable sampling frequency was developed. In the first part of the experiments an adaptive prediction technique was examined in which the predictor coefficient was calculated for each block of incoming samples for sampling frequencies of $f_s = 3f_{sc}$ and $f_s = 2.5f_{sc}$.

Computer simulation confirmed the notion that smaller block sizes were superior in performance to larger blocks, at the expense of greater bit-rate. Further, comparison of adaptive and non-adaptive predictors in terms of amplitude distribution of prediction error and signal to prediction noise ratio indicated that adaptive predictors reduce large prediction errors and thus increase the signal to prediction noise ratio by about 1.5dB.

The next stage of the investigation concentrated on developing an adaptive quantization technique in harmony with the adaptive prediction strategy. The result was

a block adaptive quantizer comprising a combination of 4 non-uniform quantizers. The selection of each quantizer was dependent on the activity of each block of pictorial data and was judged by a set of threshold values according to the variance of the samples in the block stored in the buffer. Two different approaches were used: one was variable length quantizer in which each quantizer has a different number of quantization levels; the other was fixed length quantizer with the same number of quantization levels for each quantizer.

The adaptive DPCM system which comprises a combination of block adaptive predictor and block adaptive quantizer, has been computer simulated. Comparisons with non-adaptive DPCM have been made in terms of bit-rate. In the case of fixed length adaptive quantizer, a reduction of about 6.5 Mb/s can be obtained which, compared with a reduction of 23 Mb/s in the case of the variable length quantizer, is less significant. It is therefore concluded that adaptive DPCM with variable length quantizer can achieve a significant reduction in bit-rate without loss of picture quality in terms of SNR. As a result, a bit-rate of only 28.3 Mb/s was achieved with a 50dB SNR at a sampling frequency of twice the sub-carrier frequency (with some added complexity in combing out the aliased components). A buffer is also required for a constant transmission bit-rate. The significance of this adaptive DPCM system is that it is capable of transmitting high quality colour television signals at somewhat below the

34.368 Mb/s multiplex level.

With the NTSC system, colour difference signals modulate a sub-carrier in amplitude and phase in a way similar to PAL. Thus, the one dimensional adaptive prediction algorithm which was developed in Chapter IV, can equally be applied to the NTSC system in its present form. However, in the next stage of the investigation, a similar adaptive algorithm was applied to the SECAM system. Although the results were satisfactory, it was felt that there should be a better prediction algorithm which can cope with frequency variations for the SECAM sub-carrier. Consequently a novel prediction algorithm in which the predictor can adapt itself efficiently to those variations was developed. Experimental results show that an improvement in SNR of about 4.5dB is obtained compared with the standard non-adaptive system.

Finally, we feel any further investigation in relation to the schemes presented in this thesis should be based on hardware realization of these schemes. Also, the use of two dimensional block adaptive prediction may offer further reduction in bit-rate and should be carefully investigated.

APPENDIX 1

PAL SYSTEM I SPECIFICATION AND COLOUR BAR GENERATION

The principles of PAL colour signals are given in Chapter II, Section 2.6.2. In this Appendix some specifications required for broadcast quality television and colour bar generation are given as follows;

number of lines per frame: 625,

line frequency: 15.625 KHz,

field frequency: f_f = 50 Hz,

video bandwidth: 5.5 MHz (0dB),

chrominance bandwidth:

at 1.3MHz < 3dB attenuation relative to low frequencies,

at 4.0MHz < 20dB attenuation relative to low frequencies.

The upper chrominance sideband will be restricted by the video bandwidth of 5.5MHz. The amplitude-frequency characteristic of the chrominance signal is approximately Gaussian.

The saturation of a colour bar signal can be defined from the expression

$$\text{Saturation\%} = \left[1 - \left(\frac{E_{min}}{E_{max}}\right)^{\gamma}\right] 100$$

where E_{max} and E_{min} are the maximum and minimum of R, G, and B respectively during coloured bars and γ is the gamma exponent. A 100% saturated colour bar signal is a comp-

osition of 100% amplitude and 100% saturation with white and black.Fig.(A1.1). The Table shown below, gives peak to peak amplitude of chrominance components and peak luminance components with specified chrominance angles with respect to the U axis. Line n refers to the odd lines and line n+1 to the even lines of the first and second fields.

COLOUR	LUMINANCE	PEAK-TO-PEAK CHROMINANCE			CHROMINANCE ANGLE( )IN DEGREES	
	Y	U AXIS U	V AXIS V	TOTAL C	LINE n	LINE n+1
White	0.700	0	0	0	-	-
Yellow	0.620	0.612	0.140	0.627	167	193
Cyan	0.491	0.206	0.861	0.885	283.5	76.5
Green	0.411	0.405	0.721	0.827	240.5	119.5
Magenta	0.289	0.405	0.721	0.827	60.5	299.5
Red	0.209	0.206	0.861	0.885	103.5	256.5
Blue	0.080	0.612	0.140	0.627	347	13.0
Burst	0	0.212	0.212	0.300	135	225

The generation of a colour bar signal can be arranged according to particular amplitudes and phases related to each bar (see above Table). The instantaneous voltage of the composite colour signal can be defined as

$$S(I) = Y + U \sin\left(2\pi \frac{f_{sc}}{f_s} I\right) \pm V \cos\left(2\pi \frac{f_{sc}}{f_s} I\right) \quad (A1.1)$$

or

for $\varphi = \tan^{-1}(V/U)$

and $C = \sqrt{U^2 + V^2}$

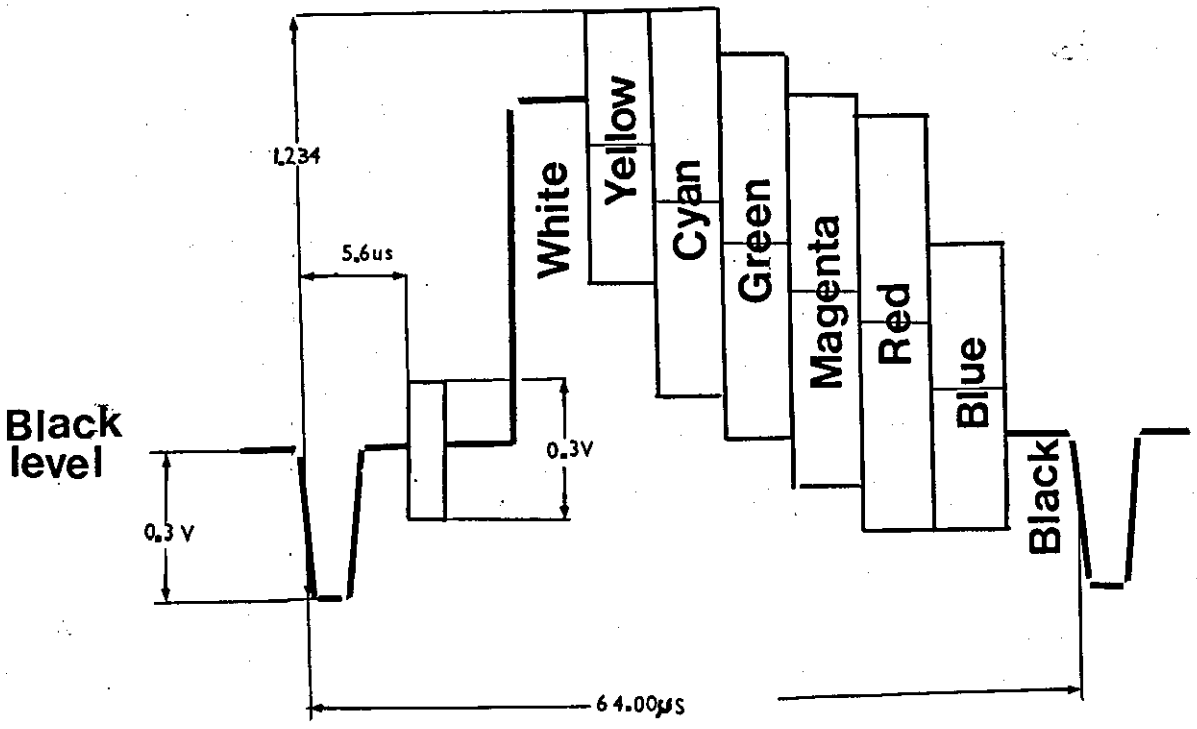

FIGURE A1.1 - The line waveform of a 100% saturated colour bar signal.

Equation (A1.1) can be represented as

$$S(I) = Y \pm C \sin\left(2\pi \frac{f_{sc}}{f_s} I \pm \varphi\right) \qquad (A1.2)$$

Thus, the sample values of a colour bar signal can be obtained according to the levels of synch pulses, bursts and bars which are given in Fig.(A1.1).

Special treatment is required for transitions from one bar to the next. It is therefore important that the transition time should be compatible with the system bandwidth for both luminance and chrominance in order to meet the specifications of PAL system I transmissions.

For an appropriate edge shape for luminance transitions, the spectrum of the edge should be adjusted in order to produce zero frequency components at the sub-carrier frequency, thus reducing cross-colour effect. The transition that has been chosen[110] for the luminance edge is obtained by integration of the 2T pulse (raised cosine), thus,

$$F(t) = 0.5\left[t + T + \frac{T}{\pi} \sin\frac{\pi t}{T}\right] \qquad (A1.3)$$

for $T = \frac{1}{f_{sc}}$, the first spectrum zero occurs at sub-carrier frequency[110].

For chrominance transition, the form of spectrum is chosen to be Gaussian[106]. Its frequency response can be shown as

$$H(f) = \exp\left[-2\pi^2 f^2 \sigma^2\right] \qquad (A1.4)$$

where the value of σ^2 (standard deviation) can be determined approximately according to the roll off in frequency response (3dB for 1.3MHz and 20dB for 4.0MHz). The impulse response of the equation (A1.4) in the time domain is;

$$F(t) = \frac{1}{\sqrt{2\pi\sigma^2}} \int_{-\infty}^{t} \exp\left[-\frac{t^2}{2\sigma^2} \right] dt \qquad (A1.5)$$

For $\frac{t}{\sigma} = \tau$, the above equation can be shown as

$$F(t) = \frac{1}{\sqrt{2\pi}} \int_{-\infty}^{\tau\sigma} \exp\left[-\tau^2/2 \right] d\tau \qquad (A1.6)$$

A plot of this is shown in Fig.(A1.2) and this determines the envelope of the chrominance transitions.

Having discussed the luminance and chrominance transitions, a computer programme was written to generate three sets of bars at sampling frequencies $f_s = 2f_{sc}$, $f_s = 2.5f_{sc}$ and $f_s = 3f_{sc}$. Figure (A1.3) illustrates the construction of two typical transitions; Yellow-Cyan and Green-Magenta for $f_s = 2.5f_{sc}$. The completed 16 line colour bar samples were then converted into 8-bit code words and were subsequently used as the data input throughout this thesis.

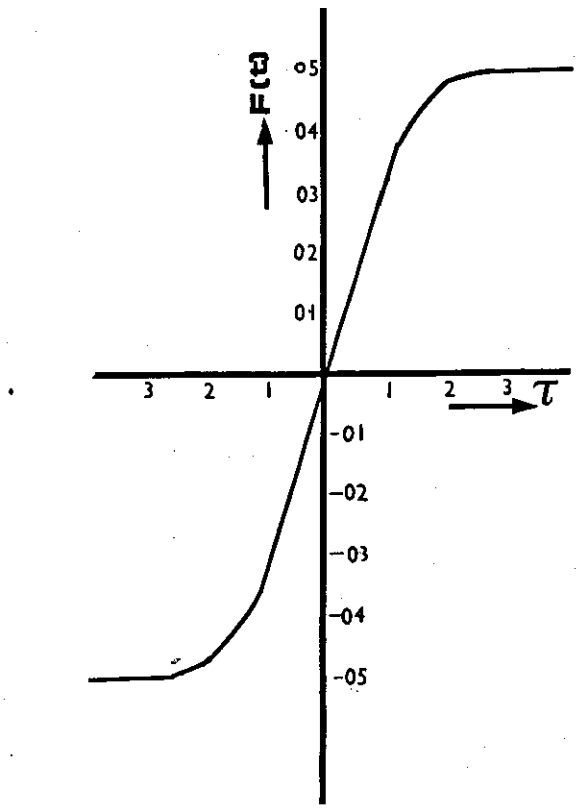

FIGURE A1.2 - Chrominance transition envelope obtained from equation (A1.6)

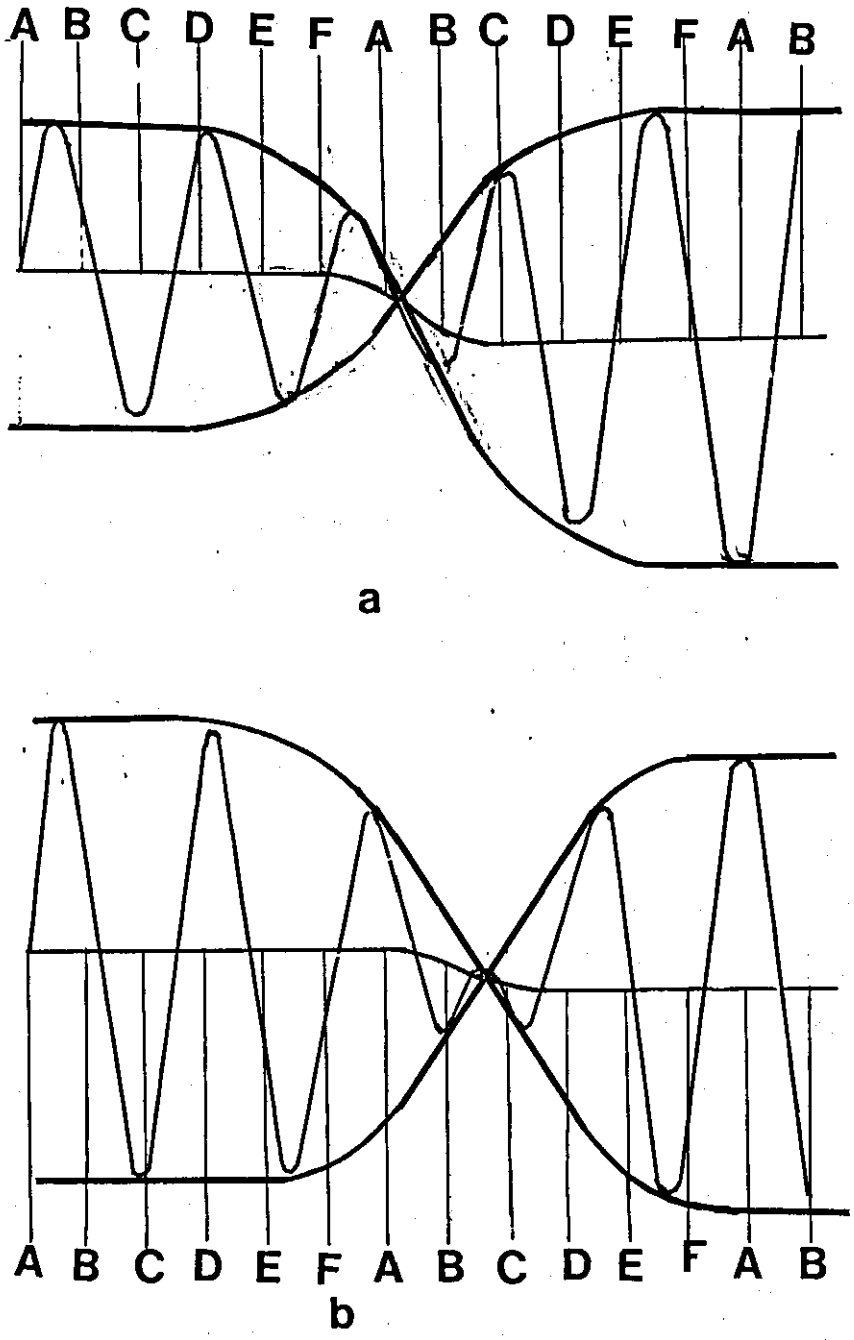

FIGURE A1.3 - Transitions reconstructed from computed values $f_s = 2.5f_{sc}$

a: Yellow-Cyan transition

b: Green-Magenta transition

APPENDIX 2

SUB-NYQUIST FILTERS

Sampling above the Nyquist rate is necessary due to the fact that aliasing components will be present in the baseband and this will result in distortion of the modulating signal. This, however, presupposes that the modulating signal occupies the whole of the baseband spectrum. In a video signal, this is not so and it is possible to sample at a sub-Nyquist rate and to extract the original video without appreciable distortion. This is mainly because most of the energy contained in the spectrum of monochrome signals is concentrated at multiples of line frequency. Thus, for sampling frequency (f_s) at an odd multiple of half the line frequency and below the Nyquist rate, the alias components will be reflected from f_s at intervals of f_L and interleave between the video spectral lines. The required monochrome spectrum can be separated from the aliasing components by the actions of a comb filter. It has been shown[66] that due to certain properties of the PAL television signal, it is possible with only slight impairment of the final picture quality, to sample at a rate exactly twice the sub-carrier frequency with a particular phase relationship. In order to separate the

wanted components from aliased components it is necessary to employ a comb filter at the receiving end. This filter should have a comb response for frequencies above $2f_{sc} - f_m$, where f_m is the maximum baseband frequency. Pre-comb filtering, prior to sampling, is also required to improve the performance. Figure (A2.1) shows a form of analogue comb filter using a one line delay[66]. The necessary comb filtering to remove aliasing components can be performed digitally rather than by using analogue filters[108,107]. In this way the analogue input signal is first sampled at $4f_{sc}$ followed by an A/D conversion with an 8 bit accuracy. The sampling frequency is phase-locked in such a way that samples are taken at phase angles of 45°, 135°, 225° and 315° with respect to the U component. A pre-digital comb filter (Fig. A2.2) is then used to remove high frequency components at odd multiples of half line frequency (which would otherwise produce alias components at multiples of line frequency) and is simultaneously converted to $f_s = 2f_{sc}$ (Fig.A2.2). A digital post comb filter is also required at the receiving end (before D/A conversion) to convert the sample rate from $2f_{sc}$ back to $4f_{sc}$ and at the same time remove the high frequency alias components at odd multiples of half line frequency. Figures (A2.2a) and (A2.2b) show block diagrams of digital pre and post comb filters suggested by Taylor[106]. In Fig.(A2.2a) data at $4f_{sc}$[17,74] enters the filter and is processed

entirely at $2f_{sc}$(8.87 MHz). The switch shown on the left schematically represents that samples of input data are switched alternately to the line paths. In practice, this is achieved by bi-phase $2f_{sc}$ clock-pulses. In Fig.(A2.2b) the full comb filter for up-conversion of data from $2f_{sc}$ to $4f_{sc}$ is shown. The data is processed at $2f_{sc}$ rate as far as S_1 and S_2, whereas the final adder operates at $4f_{sc}$. The diagram shows the output from the filter comprising low frequency information from line N+1 only, and the high frequency components from lines N and N+1.

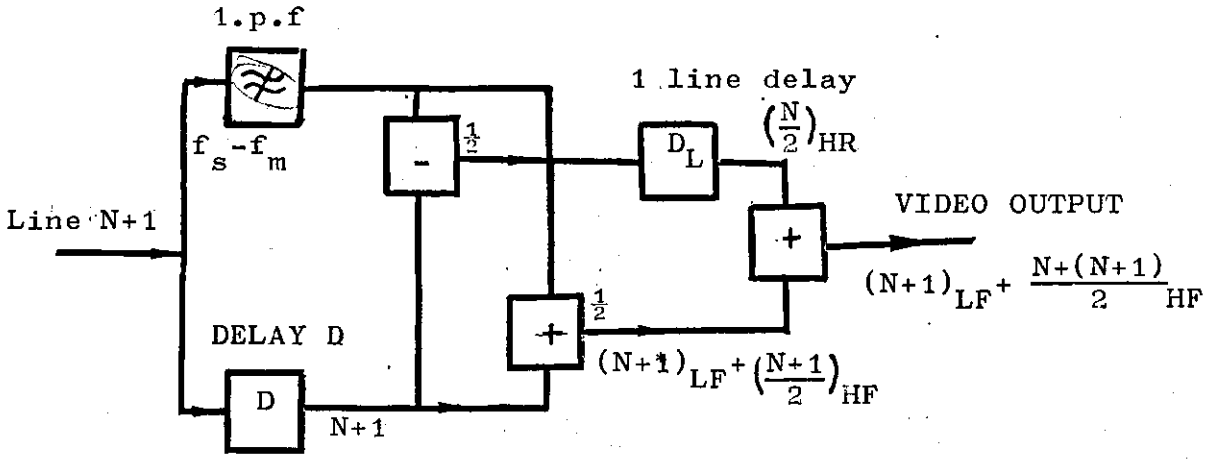

FIGURE A2.1 - Analogue comb filter

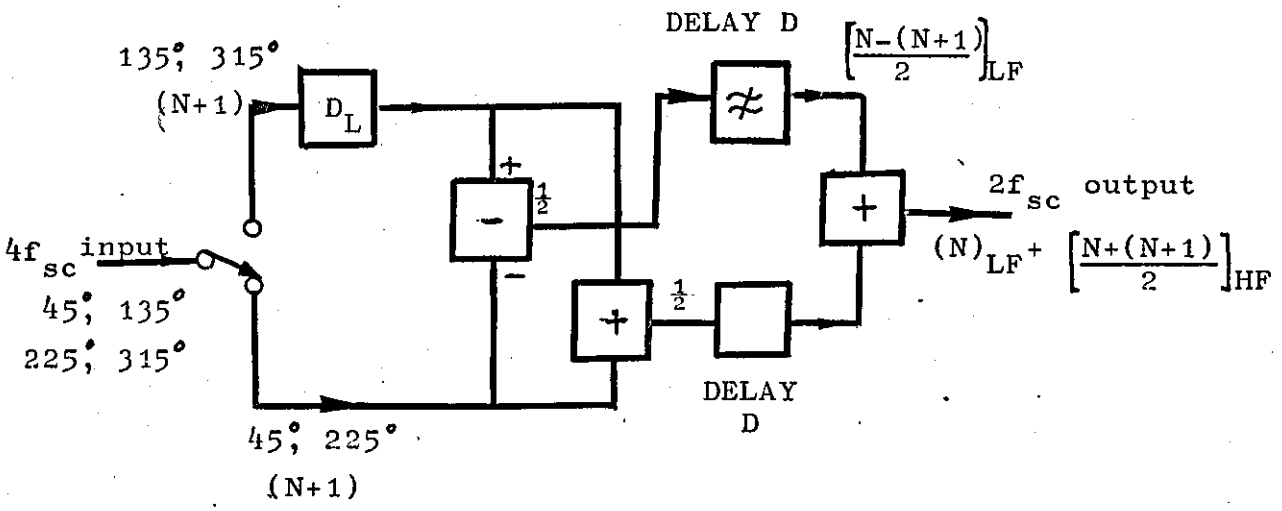

(a)

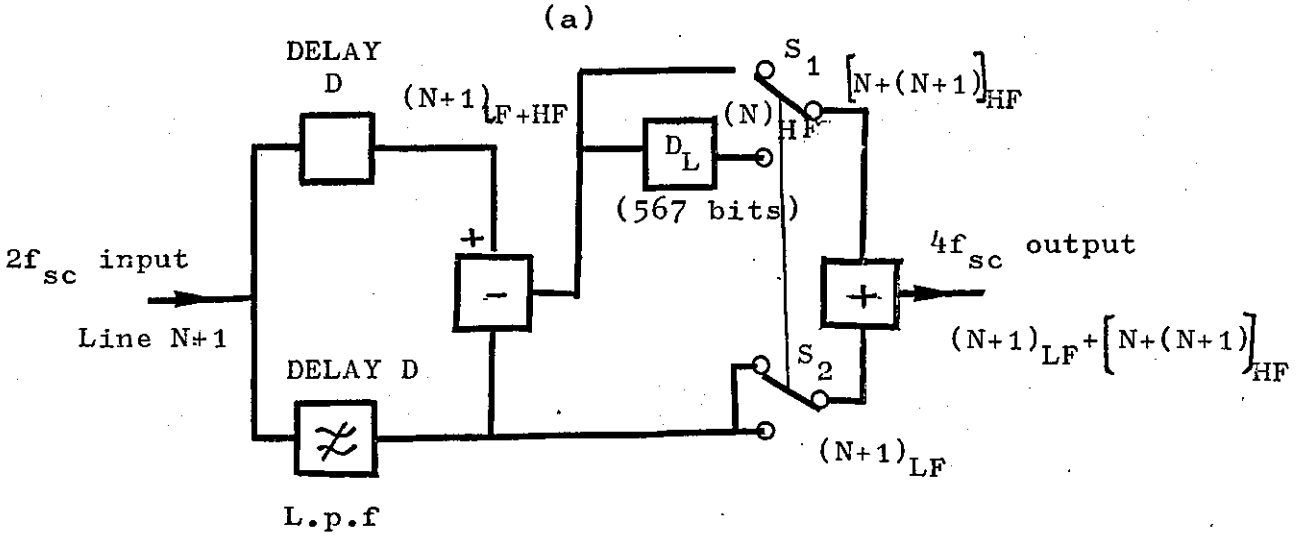

(b)

FIGURE A2.2 - Digital comb filter extracted from ref.110

a: pre comb filter for down conversion

b: post comb filter for up conversion

REFERENCES

1. ANDREWS, C.A., DAVIS, J.M., SCHWARTZ, G.R.:'Adaptive Data Compression'. Proc. IEEE, Vol.55, No.3, (1967), pp.267-277.

2. USCEE: University of Southern Califonia Electrical Engineering, Report, 1968.

3. PRATT, W.K., ANDREWS, H.C., KANE, J.:'Hadamard Transform Image Coding'. Proc. IEEE, Vol.57, No.1, (1969), pp.55-68.

4. WALKER, R.:'Hadamard Transformation - A Real-Time Transformer for Broadcast Standard PCM Television; Theory and Application of Walsh and Other Non-Statistical Functions'. Hatfield Polytechnic, June, 1973.

5. WINTZ, P.A.:'Transform Coding'. Proc. IEEE, Vol.60, No.7, July 1972, pp.809-820.

6. HABIBI, A.:'Hybrid Coding of Pictorial Data'. IEEE TRANS. on COMM., Vol.COM-22, No.5, May 1974, pp.614-624.

7. DELORAINE, E.M. and REEVES, A.H.:'The 25th Anniversary of Pulse Code Modulation'. IRE Proceedings, Vol.48, pp.1546-1561 (Sept.1960).

8. GOODALL, W.M.:'Television by Pulse Code Modulation'. B.S.T.J., Vol.1, pp.33-49, Jan. 1951.

9. CARBREY, R.L.:'Video Transmission Over Telephone Cable Pairs by Pulse Code Modulation'. IRE Proceedings, Vol.48, pp.1546-1561, Sept.1960.

10. HUANG, T.S.:'PCM Picture Transmission'. Spectrum, Vol.2, No.12, pp.37-60, Dec.1965.

11. PRATT, W.K.:'Bibliography on Digital Image Processing and Related Topics'. University of Southern California, USCEE Report 453, Sept.1973.

12. CATTERMOLE, K.W.:'Principles of Pulse Code Modulation'. (book); London Illiffe, 1973 (second impression.)

13. HOESHELF, D.F.:'Analogue to Digital/Digital to Analogue Conversion Techniques'. (book); John Willey and Sons,Inc., New York, 1968.

14. SCHMIDT, H.:'Electric Analogue/Digital Conversions'. (book); Van Nostrand Reinhold Co., 1970.

15. DEVEREUX, V.G.:'Pulse Code Modulation of Video Signals: 8 Bit Coder and Decoder'. BBC Report EL-42, 1970/25.

16. HORNA, O.A.:'A 150 Mbps A/D and D/A Conversion System'. COMSAT Technical Review, Vol.2, No.1, Spring 1972, pp.39-72.

17. FLETCHER, R.E.:'A Video Analogue to Digital Convertor'. International Broadcasting Convention (IBC) '74, IEE Conf. Publication No.119, pp.47-57.

18. CUTLER, C.C.:'Differential Quantization of Communication Signals'. Patent No.2, 605, 361, July 29, 1952 (Applied for June 29, 1950).

19. OLIVER, B.N.:'Efficient Encoding'. B.S.T.J. 31, July 1952, pp.724.

20. HARRISON, C.W.:'Experiments with Linear Prediction in Television'. B.S.T.J. 31, July 1952, pp.764-783.

21. ELIAS, P.:'Predictive Coding'. IRE Trans. Inform. Theory IT-1, March 1955, pp.16-33.

22. GRAHAM, R.E.:'Predictive Quantization of T.V. Signals'. Wescon Convention Record, Part 4, August 1958, pp.147-156.

23. O'NEAL, J.B., Jr.,:'Predictive Quantization Systems (Differential Pulse Code Modulation) for the Transmission of Television Signals'. B.S.T.J. 45, No.5 (May-June 1966), pp.689-721.

24. CONNOR, D.J., PEASE, R.F.W., and SCHOLES, W.G.: 'Television Coding Using Two-Dimensional Spatial Prediction'. B.S.T.J.50, March 1971, pp.1049-1061.

25. KUMMEROW, T.:'Statistics for Efficient Linear and Non-Linear Picture Encoding'. PROC. 1972 Int 1. Telemetering Conf. 8, pp.149-161.

26. THOMA, W.:'Video Transmission Network with Intraframe DPCM and Optional Interframe Coding'. PROC 1972 Int 1. Conf. on Communications 39, pp.1-5.

27. HABIBI, H. and ROBINSON, G.S.:'A Survey of Digital Picture Coding'. Computer(IEEE Computer Soc. Magazine), Vol.7, No.5, May 1974, pp.22-34.

28. PAPOULIS, A.:'Probability, Random Variables, and Stochastic Processes'. McGraw-Hill Book Company, International Student Edition, pg.39.

29. O'NEAL, Jr.,J.B. and STROH, R.W.:'Differential PCM for Speech and Data Signals'. IEEE TRANS on COMM, March 1974.

30. PANTER, R.F. and DITE, W.:'Quantization Distortion in Pulse-Count Modulation with Non-uniform Spacing of Levels'. Proc. IRE, Vol.39, Jan. 1951, pp.44-48.

31. MAX, J.:'Quantizing for Minimum Distortion'. IRE Trans Inform. Theory, Vol.IT-6, March 1960,pp.7-12.

32. NITADORI, K.:'Statistical Analysis of DPCM'. Electron. Commun., Vol.48, Feb.1965.

33. CANDY, J.C. and BOSWORTH, R.H.:'Methods for Designing Differential Quantizers Based on Subjective Evaluations of Edge Business'. B.S.T.J., Vol.51, Sept.1972, pp.1495-1516.

34. THOMA, W.:'Optimizing the DPCM for Video Signals Using a Model of the Human Visual System'. Picture Coding Symposium, West Germany, 1974.

35. NETRAVALI, A.N.:'On Quantizers for DPCM Coding of Picture Signals'. IEEE TRANS on Inform. Theory, Vol.IT-23, No.3, May 1977.

36. SHARMA, D.K. and NETRAVALI, A.N.:'Design of Quantizers for DPCM Coding of Picture Signals'. TRANS on COMM., Vol. COM-25, No.11, Nov.1977.

37. GALLAGER, R.G.:'Information Theory and Reliable Communications'. (Book). New York, John Willey (1968).

38. SHANNON, C.E.:'A Mathematical Theory of Communication'. B.S.T.J. 27, 1948, pp.379-423 (Part I), pp. 623-656 (Part II).

39. HUFFMAN, D.A.:'A Method for the Construction of Minimum Redundancy Codes'. Proc.IRE, 1952 pp.1098-1101.

40. LIMB, J.O.:'Entropy of Quantized Television Signals'. Proc. IEE, 1968, 115, 1, pp.16-20.

41. REID, D.F.:'Some Bit-Rate Reduction Methods Which Preserve Information in Broadcasting Quality Digital Video Signals'. BBC Report EL-97.

42. RICE, R.F.:'An Advanced Imaging Communication System for Planetary Exploration'. Proc. of SPIE, Vol.66, August 1975, pp.70-89.

43. RICE, R.F. and PLAUNT, J.R.:'Adaptive Variable-Length Coding for Efficient Compression of Space Craft Television Data'. IEEE TRANS on COMM. TECH., Vol.COM-19, No.6, pp.889-897.

44. MAY, C.L. and SPENCER, D.J.:'ERTS Image Data Compression Technical Evaluation'. Final Report for NASA Contract NASS-21746, April 1974.

45. GOYAL, S.K. and O'NEAL, J.B.:'Entropy Coded DPCM Systems for Television'. Proc. of the National Telecommunications Conf., San Diego, California, Dec. 2-4, 1974, pp.72-76.

46. O'NEAL, J.B.:'Entropy Coding in Speech and T.V. DPCM Systems'. IEEE TRANS on INFORM. THEORY, Vol.17, Nov.1971, pp.758-761.

47. GOLDING, L.S.:'DITEC-A Television Communication System for Satellite Links'. 2nd Int'l Conf. on Digital Satelite Communications, 1972.

48. SAWADA, K. and KOTERA, H.:'32 Mb/s Separate Coding of Broadcasting Colour Television Signals'. Paper Tech. Group, on Communication Systems, IECE, Jap.,CS76-145, 1976.

49. STENGER, L.:'Quantization of T.V. Chrominance Signals Considering the Visibility of Small Colour Differences'. IEEE TRANS on COMM., Vol. Com-25, No. 11, Nov. 1977, pp.1393-1406.

50. PIRSCH, P. and STENGER, L.:'Statistical Analysis and Coding of Colour Video Signals'. Acta Electronica, 19, 4, 1976, pp.277-287.

51. RUBINSTEIN, C.B. and LIMB, J.O.:'Statistical Dependence Between Component of Differentially Quantized Colour Signals'. IEEE TRANS on COMM. Vol. COM-20, Oct.1972, pp.890-899.

52. THOMPSON, J.E.:'Differential Encoding of Composite Television Signals Using Chrominance Corrected Prediction'. IEEE TRANS on COMM., COM-22,8,1974.

53. THOMPSON, J.E.:'Data Compression of Composite Colour Television Signals Using Planner Prediction'. 3rd In't Conf. on Digital Satelite Comms., 1975

54. IIJIMA, Y. and ISHGURO, T.:'Differential Pulse Code Modulation of NTSC Colour Television Signals'. Paper Tech. Group, on Commun. Systems, IECE Jap., CS73-74, 1973.

55. IIJIMA, Y. and SUZUKI, N.:'Experiments on Higher Order DPCM of NTSC Television Signals'. NEC Central Research Laboratories Report, 1974.

56. SAWADA, K. and KOTERA, H.:'Study on Direct Predictive Coding of Colour T.V. Signals'. Paper Tech. Group, on Commun. System, IECE Jap., CS76-45, 1976.

57. SAWADA, K. and KOTERA, H.:'32 Mb/s Transmission of NTSC Colour T.V. Signals by Composite DPCM Coding'. IEEE TRANS on COMM. Vol. COM-26, No.10, Oct.1978.

58. ISHIGURO, T., IINUMA, K., KOGA, T., AZAMI, S., and MUNE, T.:'Composite Interframe Coding of NTSC Colour Television Signals'. National Telecommunication Conf., Dallas, Texas, Dec. 1976.

59. LIMB, J.O.;'RUBINSTEIN, C.B., and THOMPSON, J.E.:'Digital Coding of Colour Video Signals- A Review'. IEEE TRANS., 1977, COM-25,pp.1349-1385.

60. CARNT, P.S. and TOWNSEND, G.B.:'Colour Television'. (book);
Vol.1:'The NTSC System Principles and Practice'. 1969.
Vol.2:'PAL, SECAM and Other Systems'.1969
London (Illiffe) Newnes-Butterworth,1969.

61. SIMS, H.V.:'Principles of PAL Colour Television and Related Systems'. (book); London (Illiffe) Newnes-Butterworth, 1969.

62. PEARSON, D.E.:'Transmission and Display of Pictorial Information'. (book); Pentech Press 1975.

63. DEVEREUX, V.G.:'Differential Coding of PAL Signals Based on Differences Between Samples One Sub-Carrier Period Apart'. BBC Report 1973/7.

64. HATORI, Y. and YAMAMATO, H.:'Direct Predictive Coding by Comb Filter Integration'. Tech. Group, on Image Engineering, IECE Jap., IE-75-109, 1975.

65. THOMPSON, J.E.:'Requirements for Digital Transmission of Broadcast Standard Colour Television Signals'. British Post Office Memorandum R16.2/140.

66. DEVEREUX, V.G.:'Sub-Nyquist Sampling of PAL Colour Signal'. BBC Report, RD 1975/14, Jan.1975.

67. BALDWIN, J.L.E.:'Sampling Frequencies for Digital Coding of Television Signals'. IBA Tech. Review, Vol.9, Sept. 1976, pp.32-36.

68. GHARAVI, H. and STEELE, R.:'Non-Integer Sampling to Sub-Carrier Frequency Ratios in DPCM of PAL Signals'. Electron. Lett., 1979, 15, 16, pp.483-484.

69. THOMPSON, J.E.:'Differential Coding for Digital Transmission of PAL Colour Television Signals'. IEE Conv., Int. Broadcasting Concession, Sept. 1972, pp.26-32.

70. CONNOR, D.J., BRAINARD, R.C. and LIMB, J.O.:'Intra-frame Coding for Picture Transmission'. IEEE PROC., Vol.60, July 1972, pp.779-791.

71. LIMB, J.O. and MOUNTS, F.W.:'Digital Differential Quantizer for Television'. B.S.T.J., Vol.48, Sept.1969, pp.2583-2599.

72. LIMB, J.O., RUBINSTEIN, C.R. and WALSH, K.A.:'Digital Coding of Colour Picturephone Signals by Element-Differential Quantization'. IEEE TRANS. COMM., Vol. COM-19, Dec.1971,pp.992-1005.

73. THOMPSON, J.E.:'Data Compression of Colour Television Signals Using Planar Predictions'. The third international conference on Digital Satelite Communication, Kyoto, Japan, Nov.1975.

74. DEVEREUX, V.G.:'Differential Coding of PAL Colour Signals Using Same-Line and Two-Dimensional Prediction'. BBC RD 1975/20.

75. HABIBI, A.:'Survey of Adaptive Image Coding Techniques'. TRANS. on COMMUN. Vol. COM-25, No.11, Nov.'77.

76. DILLARD, G.M.:'Application of Ranking Techniques to Data Compression for Image Transmission'. NTC 75 Conference Record, Vol.1, pp.22-18 to 22-22.

77. ANDERSON, G.B. and HUANG, T.S.:'Piecewise Fourier Transformation for Picture Bandwidth Compression'. IEEE TRANS. on COMMUN. TECH., Vol. COM-19, April 1971, pp.133-140.

78. KNAUER, S.C.:'Real-Time Video Compression Algorithm for Hadamard Transform Processing'. Proc. of SPIE, Vol.66, August '75, pp.58-69.

79. COX, R.V. and TESCHER, A.G.:'Generalized Adaptive Transform Coding'. 1976 Picture Coding Symposium, Asilomar, CA, Jan. 28-30.

80. ABATE, J.E.:'Linear and Adaptive Delta Modulation'. Proc. of IEEE (special issue on Redundancy Reduction), Vol.55, No.3,March 1967, pp.298-308.

81. JAYANT, N.S.:'Adaptive Delta Modulation with a One-Bit Memory'. B.S.T.J., Vol.49, No.3, March 1970, pp.321-342.

82. WINKLER, M.R.:'High Information Delta Modulation'. IEEE International Conv. Rec., pt.8, 1963, pp.260-265.

83. HAWKES, T.A. and SIMONPIERI, P.A.:'Signal Coding Using Asynchronous Delta Modulation'. IEEE TRANS on COMMUNS., Vol. COM-22, No.3, March 1974, pp.346-348.

84. VIRUPAKSHA, K., O'NEAL, J.B., Jr.,:'Entropy Coded Adaptive Differential Pulse Code Modulation (DPCM) for Speech'. IEEE TRANS. on COMM., Vol. COM-22, No.6, June 1975, pp.777-778.

85. READY, P.J. and SPENCER, D.J.:'Block Adaptive DPCM Transmission of Images'. NTC '75 Conference Record, Vol.2, pp.22-10 to 22-17.

86. MAXEMCHUK, N.F. and STULLER, J.A.:'An Adaptive Intra-frame DPCM Codec Based Upon Non-Stationary Image Model'. B.S.T.J., July-August 1979, Vol.58, No.6.

87. CUMMISKEY, P.:'Adaptive DPCM for Speech Processing'. Ph.D. Dissertation, Newark College of Engineering, Newark, N.J.,1973.

88. GIBSON, J.D., JONES, S.K., and MELSA, J.L.:'Sequentially Adaptive Prediction and Coding of Speech Signals'. IEEE TRANS. on COMMUN., Vol. COM-22, Nov. 1974, p.1789.

89. SAGE, A.P., MELSA, J.L.:'Estimation Theory with Application to Communication and Controls'. (book); McGraw-Hill, 1971.

90. JAZWINSKI, A.H.:'Stochastic Processes and Filtering Theory'. N.Y. Academic, 1970.

91. ATAL, B., SCHROEDER, M.R.:'Adaptive Predictive Coding of Speech Signals'. B.S.T.J., Vol.49, No.8, Oct.'78, pp.1973-1986.

92. XYDEAS, C.S.:'Differential Encoding Techniques to Speech Signals'. Ph.D. Thesis, 1978, Loughborough University.

93. PAPOULIS, A.:'Probability, Random Variables, and Stochastic Processes'. (book); McGraw-Hill, International Student Edition.

94. GHARAVI, H.:'Block Adaptive Prediction of Colour Television Signals'. Elect. Lett., Vol.16, No.6, March 1980, pp.226-228.

95. GHARAVI, H. and STEELE, R.:'Predictors for Intraframe Encoding of PAL Picture Signals'. IEE Proc. Pt.F, June 1979.

96. NOLL, P.:'A Comparative Study of Various Quantization Schemes for Speech Encoding'. B.S.T.J., Vol.54, No.9, pp.1597, Nov.1975.

97. BUDRIKIS, Z.L.:'Theoretical Finite Sample Statistics of Run-Length Coded T.V. Picture Signals'. P.M.G. Res. Lab., Melbourne, Australia, Commonwealth Austral. Rep. 5352, 1961.

98. POPP, D.J.:'Buffer Considerations for Data Compression of Non-Stationary Video Data'. IEEE TRANS on COMMUN., COM-18, No.2, April 1970.

99. BUDRIKIS, Z.L., HULLET, J.L., PHIET, D.Q.:'Transient Mode Buffer Stores for Non-Uniform Code T.V.'. IEEE TRANS on COMM. TECH., COM-19, 6, 1971, pp.913-922.

100. MEDLIN, J.E.:'Buffer Length Requirements for a Telemetry Data Compression'. Nat. Telemetering Conf., Washington,D.C., May 1962.

101. SCHWARTZ, G.R.:'Buffer Design for Data Compression Systems'. IEEE TRANS on COMMUN. TECH., Vol. COM-16, August 1968, pp.606-615.

102. DEVEREUX, V.G.:'Comparison of Picture Impairments Caused by Digital Coding of PAL and SECAM Video Signals'. BBC Report, 1974/16, April 1974.

103. GHARAVI, H.:'Bandwidth Compression of Digital Colour Television Signals Using Block Adaptive DPCM'. To be published in the Oct.1980 issue of IEE Proc. Pt.F.

104. WILKINSON, J.H. and LUCAS, K.:'High Quality Transmission of PAL Signals at 34Mbit/s'. IBC 78, IEE Conf. Publications 166, pp.42-45.

105. RATCLIFF, P.A.:'Bit-rate Reduction for High Quality Digital Television Transmission'. IBC-78, IEE Conf. Publication 166, pp.37-41.

106. O'NEAL, Jr., J.B.:'A Bound on Signal-to-Quantizing Noise Ratios for Digital Encoding Systems'. IEEE Proc., Vol.55, March 1967, pp.287-292.

107. TAYLOR, H.J.:'Digital Sub-Nyquist Filters'. IBA Technical Review, Vol.12, Jan.1979, pp.21-26.

108. STENGER, L.:'Digital Comb-Filter Demodulation of PAL Colour Television Signals'. IEEE TRANS on COMMUN., Vol. COM-27, No.10, Oct. 1979, pp.1624-1631.

109. Technical Reference Book, IBA Technical Review,Vol.2, May 1977.

110. CARMEN, P.:'Digital Colour Bar Generation'. IBA Tech. Review, Vol.12, Jan.1979, pp.33-41.